

**STUDIES ON END MILLING OF MARAGING  
STEEL USING CRYOGENIC TREATED AND PVD  
COATED CEMENTED CARBIDE INSERTS  
UNDER DRY, WET AND CRYOGENIC  
ENVIRONMENTS**

Thesis

Submitted in partial fulfilment of the requirements for the degree of

**DOCTOR OF PHILOSOPHY**

by

**VINAY VARGHESE**



DEPARTMENT OF MECHANICAL ENGINEERING

NATIONAL INSTITUTE OF TECHNOLOGY KARNATAKA, SURATHKAL,  
MANGALORE – 575025

OCTOBER, 2019



## **DECLARATION**

I hereby declare that the Research Thesis entitled “Studies on End Milling of Maraging Steel Using Cryogenic Treated and PVD Coated Cemented Carbide Inserts Under Dry, Wet and Cryogenic Environments” which is being submitted to the National Institute of Technology Karnataka, Surathkal in partial fulfilment of the requirements for the award of the Degree of Doctor of Philosophy in Mechanical Engineering is a *bonafide report of the research work carried out by me*. The material contained in this Research Thesis has not been submitted to any other Universities or Institutes for the award of any degree.

Register Number: **158016ME15F27**

Name of the Research Scholar: **VINAY VARGHESE**

Signature of the Research Scholar:

Department of Mechanical Engineering

Place: NITK-Surathkal

Date:



## **CERTIFICATE**

This is to certify that the Research Thesis entitled “**Studies on End Milling of Maraging Steel Using Cryogenic Treated and PVD Coated Cemented Carbide Inserts Under Dry, Wet and Cryogenic Environments**” submitted by **Mr. VINAY VARGHESE (Register Number: 158016ME15F27)** as the record of the research work carried out by him, *is accepted as the Research Thesis submission* in partial fulfilment of the requirements for the award of the degree of **Doctor of Philosophy**.

Research Guides

Dr. M. R. Ramesh

Dr. D. Chakradhar

Research Guide

Research Co-Guide

**Chairman – DRPC**

Date:



## ACKNOWLEDGEMENTS

It is my great pleasure to express my heartfelt gratitude to my research supervisors **Dr. M. R. Ramesh**, Associate Professor, Department of Mechanical Engineering, National Institute of Technology Karnataka, Surathkal, Mangalore and **Dr. D. Chakradhar**, Assistant Professor, Department of Mechanical Engineering, Indian Institute of Technology, Palakkad, for their exemplary guidance and encouragement throughout my research work. Their encouragement and valuable suggestions have increased my knowledge level which led to the completion of my research work and is demonstrated through this thesis. The author wishes to record his deep sense of gratitude to **Prof. Shrikantha S. Rao**, The Head, Department of Mechanical Engineering and all the faculty members, technical and administrative staffs of the Mechanical Engineering, National Institute of Technology Karnataka, Surathkal for their help, as and when needed.

The author is highly thankful to **Prof. Gangadharan K. V.**, **Prof. Narendranath S.**, Department of Mechanical Engineering, **Dr. Udaya Bhat K.**, **Dr. Anandan Sreenivasan**, The Head, Department of Metallurgical, and Materials Engineering. The author wishes to record his deep sense of gratitude to **Mr. Rounak Chandak**, Makrani infrastructures Pvt. Ltd. for his support and interaction in extending cryogenic treatment facility. **Dr. Habibuddin Shaik**, Assistant Professor, Department of Electrical and Electronics Engineering, Nitte Meenakshi Institute of Technology, Bangalore for his help and support in synthesis of PVD coatings using magnetron sputtering. **Mr. Ravindra**, Oerlikon Balzers for synthesis of PVD coatings using cathodic arc deposition. **Dr. Nagahanumaiah**, Director, Central Manufacturing Technology Institute (CMTI) Bangalore for his support and interaction during experimentation. The author wishes to record his deep sense of gratitude to **Dr. N. Balashanmugam**, Joint Director, Central Manufacturing Technology Institute (CMTI) Bangalore, for his support and interaction in extending characterization facility.

The author is highly obliged to **Prof. Katta Venkataramana**, Professor, Dept. of Civil Engineering, National Institute of Technology Karnataka, Surathkal.

The author is highly thankful to RPAC members **Dr. Shivananda Nayaka**, Dept. of Mechanical Engineering and **Dr. Mohammad Rizwannur Rahman**, Dept. of Metallurgical & Materials Engineering and DRPC members **Dr. Gnanasekaran**, **Dr. Sharnappa Joladarashi**, **Dr. Ranjith M.**, **Dr. Jeyaraj P.** and **Dr. S. Kattimani**, Dept. of Mechanical Engineering.

The author wishes to thank his seniors Dr. P. Sivaiah, Dr. G. Venkatesh for their constant help and encouragement during the entire process of this research work. Author also wishes to thank his friends especially to Dr. Nivish George, Dr. Nithin H.S, Dr. Sudheer R., Mr. Sachin B., Dr. Pradeep V Badiger, Dr. Veeresh Nayak, Dr. Hargovind Soni, Mr. Vasu, Mr. Mallikarjun, Dr. Rakesh K. Rajan, Dr. Durgaprasad, Mr. Subba Rao, Mr. Guddala Suresh, Mr. Praveen J. and all the research scholars of Department of Mechanical and Metallurgical and Materials Engineering for their everlasting support.

At this stage of life, I am deeply indebted to my parents Mr. Varghese V.J and Mrs. Regina Jacob who stood by my side all the time. I am also thankful to my family members Varsha Varghese, Jonesh Joseph, Nileena Mariam Jonesh, Nivin George Jonesh without their strong support it would have been difficult for me to transform my dream into reality.

(VINAY VARGHESE)



## ABSTRACT

Maraging steel MDN 250 is an ultra-high strength steel which is developed to meet the large demand for high strength materials. The high strength of maraging steel is due to the precipitation of intermetallics during aging. Maraging steel finds wide applications in tool dies, a piston rod in heavy vehicles, rocket parts etc. The high strength combined with good hardness makes maraging steel difficult to machine material. Excessive tool wear, high heat generation, high power consumption, larger cutting forces, poor surface quality and/or difficulties in chip formation are some of the difficulties faced while machining difficult to cut materials. It is difficult to overcome these difficulties by the use of conventional cutting methods and tool materials. As the conventional cutting tools cannot withstand the high cutting temperature and cutting forces and results in tool wear while machining these difficult to cut materials. This early failure of cutting tools reduce the surface finish, increase the idle time and production cost. Some of the techniques used to overcome these difficulties are cryogenic treatment of cutting tools, coating of cutting tools, using sustainable cutting fluids like cryogenic liquid nitrogen etc.

The cryogenic treatment is a new technique which improves the physical and mechanical properties of existing cutting tool in the most economic and sustainable way. It is reported that cryogenic treatment can improve some of properties of cutting tool like tool life, micro hardness, wear resistance, fatigue life, rupture strength and compressive residual stress. The cryogenic treatment use liquid nitrogen at  $-196^{\circ}\text{C}$  for cooling the samples to cryogenic temperature and generally held for 24 hours to improve the properties of cutting tool. The present study investigates the effect of cryogenic treatment of cemented carbide (WC-Co) inserts at the different soaking period of 18 h (CT-18), 24 h (CT-24) and 32 h (CT-32) at a sub-zero temperature of  $-196^{\circ}\text{C}$ . The cryogenically treated inserts exhibited higher tool life, better surface finish and lower cutting forces during machining at different spindle speeds. The optimum soaking time for cryogenic treatment of WC-Co inserts is found to be 24 h (CT-24) beyond which there is no improvement in microhardness and wear resistance. However, as the spindle speed increased the effect of cryogenic treatment diminished. Hence the machining performance of cryogenic treated WC-Co inserts at a soaking

period of 24 hours under three different environment of dry, wet and cryogenic has been investigated. The machining performance and tool life extended under cooling environments and highest tool life and machining performance is found to be during cryogenic machining.

Coatings on the cutting tools are one of the outstanding strategies developed to avoid the difficulties in machining like rapid tool wear and lower tool life. A large number of PVD coatings are developed for the milling operations to have better performance. Aluminium and silicon based coatings find most promising applications in the end milling. Thus aluminium based coatings like AlTiN and AlCrN coatings synthesized by cathodic arc deposition (CAD) and silicon nitride based coatings like TiSiN and TiAlSiN synthesized by magnetron sputtering were studied for end milling performance. The coated tool along with the use of cutting fluid can minimize the tool wear and extend the life of the cutting tool. Also considering the environmental hazards, operator safety, recycling, and the disposal issues, use of conventional cutting fluids should be minimized. The liquid nitrogen is used in the experiment as nitrogen is abundant in the atmosphere and causes a rapid reduction in cutting temperature and quickly evaporates into the atmosphere. The tool life is maximum using AlCrN coated tool (125 min) compared to cryogenic treated and other coated tools at a spindle speed of 270 rpm under cryogenic environment. AlCrN > TiAlSiN > AlTiN > TiSiN > CT-24 is the order of tool life of cutting tools.

**Keywords:** *Maraging steel; Cryogenic treatment; Cryogenic machining; Magnetron sputtering; Cathodic arc deposition; tool life.*

# CONTENTS

<b>DECLARATION.....</b>	<b>i</b>
<b>CERTIFICATE.....</b>	<b>ii</b>
<b>ACKNOWLEDGEMENTS .....</b>	<b>iii</b>
<b>ABSTRACT.....</b>	<b>v</b>
<b>CONTENTS.....</b>	<b>vii</b>
<b>LIST OF FIGURES .....</b>	<b>xi</b>
<b>LIST OF TABLES .....</b>	<b>xvii</b>
<b>1 INTRODUCTION.....</b>	<b>1</b>
1.1 MACHINING .....	1
1.2 TOOL WEAR .....	3
1.3 CUTTING TOOL .....	6
1.4 COOLING TECHNIQUES FOR REDUCTION OF CUTTING TEMPERATURES .....	7
1.5 NEED FOR THE PRESENT STUDY.....	10
1.6 OUTLINE OF THE THESIS .....	11
<b>2 LITERATURE REVIEW .....</b>	<b>13</b>
2.1 DIFFICULT TO CUT MATERIALS .....	13
2.2 MARAGING STEEL.....	14
2.3 CRYOGENIC TREATMENT .....	14
2.4 PVD COATINGS .....	20
2.4.1 PVD Coating of cutting tools.....	20
2.4.2 Aluminium based coatings for cutting tool.....	21
2.4.3 Cathodic arc deposition.....	22
2.4.4 Magnetron sputtering .....	24
2.4.5 Titanium-based coatings .....	26
2.5 SUSTAINABLE MACHINING .....	27
2.6 SUMMARY OF LITERATURE REVIEW.....	32

2.7	OBJECTIVES OF PROPOSED WORK .....	33
<b>3</b>	<b>EXPERIMENTAL WORK.....</b>	<b>35</b>
3.1	WORK MATERIAL.....	35
3.2	CUTTING TOOL MATERIAL.....	36
3.3	CRYOGENIC TREATMENT OF CUTTING TOOLS .....	38
3.4	PVD COATING OF CUTTING TOOL USING CATHODIC ARC DEPOSITION (CAD) .....	40
3.5	PVD COATING OF CUTTING TOOL USING MAGNETRON SPUTTERING (MS).....	40
3.6	DIFFERENT MACHINING ENVIRONMENTS USED IN THE EXPERIMENTS .....	42
3.6.1	Cryogenic machining .....	42
3.6.2	Dry and wet machining.....	44
3.7	MILLING MACHINE .....	44
3.8	MACHINING PERFORMANCE CHARACTERISTICS .....	45
3.8.1	Cutting Force .....	45
3.8.2	Surface Roughness.....	46
3.8.3	Tool wear .....	47
3.9	CHARACTERISATION OF CUTTING TOOL .....	48
3.9.1	Microstructure and elemental composition analysis (SEM/EDS) .....	48
3.9.2	X-ray diffraction (XRD) analysis .....	48
3.9.3	Raman spectroscopy analysis .....	49
3.9.4	Nano indentation studies.....	49
3.9.5	Microhardness testing .....	50
3.9.6	Calo tester .....	51
3.9.7	Confocal microscope .....	51
3.9.8	Four- probe apparatus .....	52
3.10	METHODOLOGY .....	52
<b>4</b>	<b>RESULTS AND DISCUSSION .....</b>	<b>55</b>
4.1	CHARACTERISATION OF WC-Co INSERTS BEFORE & AFTER CRYOGENIC TREATMENT .....	55

4.1.1	Microstructure & Phase Changes.....	55
4.1.2	Microhardness.....	59
4.1.3	Electrical Resistivity & Conductivity .....	60
4.2	MILLING PERFORMANCE CHARACTERISTICS OF UNTREATED AND CRYOGENIC TREATED TOOL UNDER DRY ENVIRONMENT .....	61
4.2.1	Tool Wear .....	61
4.2.2	Tool Life .....	65
4.2.3	Cutting Force .....	67
4.2.4	Surface Roughness.....	68
4.3	MILLING PERFORMANCE CHARACTERISTICS OF UNTREATED AND CRYOGENIC TREATED TOOL UNDER DIFFERENT ENVIRONMENTS .....	70
4.3.1	Tool wear of Untreated (UT) and Cryogenic treated (CT/CT-24) inserts under dry, wet and cryogenic environments .....	71
4.3.2	Tool life of Untreated (UT) and Cryogenic treated (CT/CT-24) inserts under dry, wet and cryogenic environments .....	74
4.3.3	Cutting force variation during machining using untreated (UT) and cryogenically treated (CT/CT-24) inserts under dry, wet and cryogenic environments .....	78
4.3.4	Surface roughness of workpiece after machining using untreated (UT) and cryogenically treated (CT/CT-24) inserts under dry, wet and cryogenic environments .....	80
4.4	CHARACTERIZATION OF AlCrN & AlTiN COATED TOOLS .....	83
4.4.1	Microstructure & phase changes.....	83
4.4.2	Micromechanical characterisation .....	86
4.5	MILLING PERFORMANCE CHARACTERISTICS OF AlCrN & AlTiN COATED TOOLS UNDER DRY, WET & CRYOGENIC ENVIRONMENTS... ..	87
4.5.1	Tool wear and tool life.....	87
4.5.2	Cutting force .....	94
4.5.3	Surface roughness .....	96
4.6	CHARACTERIZATION OF TiSiN & TiAlSiN COATED TOOLS .....	99
4.6.1	Microstructure and phase changes .....	99

4.6.2	Raman spectroscopy .....	102
4.6.3	Micromechanical characterisation .....	103
4.7	MILLING PERFORMANCE CHARACTERISTICS OF TiSiN & TiAlSiN COATED TOOLS UNDER DRY, WET & CRYOGENIC ENVIRONMENTS.	105
4.7.1	Tool wear and tool life .....	105
4.7.2	Cutting force .....	109
4.7.3	Surface roughness .....	111
<b>5</b>	<b>CONCLUSIONS AND SCOPE FOR FUTURE WORK .....</b>	<b>115</b>
5.1	CONCLUSIONS.....	115
5.2	SCOPE FOR FUTURE WORK .....	117
	<b>REFERENCES.....</b>	<b>119</b>
	<b>LIST OF PUBLICATIONS AND CONFERENCES .....</b>	<b>133</b>
	<b>BIO-DATA.....</b>	<b>135</b>

## LIST OF FIGURES

<b>Figure 1.1</b> Effect of cutting speed on machining cost (Inspektor and Salvador 2014).	2
<b>Figure 1.2</b> Finite element analysis of of Inconel 718 during turning a) stress distribution and b) temperature (Maranhão and Davim 2010).	3
<b>Figure 1.3</b> Tool wear indicating a) Primary wear types and their locations on the cutting edge b) failure mode diagram for a tool material in machining and safe zone (Quint 1996).	4
<b>Figure 1.4</b> Different cutting tools used in machining (Inspektor and Salvador 2014).	6
<b>Figure 1.5</b> Different cooling techniques in machining (Chetan et al. 2015).	7
<b>Figure 1.6</b> Sustainable manufacturing techniques for cleaner production (Chetan et al. 2015).	9
<b>Figure 1.7</b> Characteristics of sustainable machining (Chetan et al. 2015).	9
<b>Figure 2.1</b> Schematic view of a cryogenic treatment process (Akincioglu et al. 2015).	15
<b>Figure 2.2</b> Skeleton of WC-Co structure (Gill et al. 2012a).	18
<b>Figure 2.3</b> Schematic of PVD coating using cathodic arc deposition technique.	23
<b>Figure 2.4</b> Schematic representation of magnetron sputtering (Bosco et al. 2012).	25
<b>Figure 2.5</b> Schematic of cryogenic milling setup (Ravi and Kumar 2012).	31
<b>Figure 3.1</b> EDS analysis of maraging steel.	36
<b>Figure 3.2</b> Cutting tools used for end milling of MDN 250 maraging steel a) tool holder b) H15 uncoated WC-Co inserts.	37
<b>Figure 3.3</b> Microstructure and chemical composition analysis of WC-Co cutting inserts using SEM/EDS a) Microstructure b) EDS analysis.	37
<b>Figure 3.4</b> Schematic of cryogenic treatment (Akincioglu et al. 2016).	39
<b>Figure 3.5</b> Time temperature graph of cryogenic treatment.	39

<b>Figure 3.6</b> Schematic of cathodic arc deposition (courtesy: Bangalore Plasmatek Pvt. Ltd, India). .....	40
<b>Figure 3.7</b> Experimental set up for magnetron sputtering of coatings a) Magnetron sputtering machine b) Sample holder & cutting inserts for coating c) vacuum chamber during the sputtering process. ....	41
<b>Figure 3.8</b> Schematic of Cryogenic machining.....	42
<b>Figure 3.9</b> Modified stainless steel cap for the dewar.....	43
<b>Figure 3.10</b> Experimental setup for cryogenic machining a) Milling machine & cryogenic setup b) Machining zone during cryogenic machining. ....	43
<b>Figure 3.11</b> Experimental setup for a) dry machining b) wet machining. ....	44
<b>Figure 3.12</b> Kistler 9257B dynamometer used for cutting force measurement. ....	46
<b>Figure 3.13</b> Surface roughness tester (Mitutoyo SJ 301) used in the experiment. ....	47
<b>Figure 3.14</b> Optical microscope used in the experiment.....	47
<b>Figure 3.15</b> XRD machine used in the experiment (Courtesy: CeNSE Lab, IISc, Bangalore).....	49
<b>Figure 3.16</b> Nano indenter used in the experiment (Courtesy: NMTC, CMTI, Bangalore).....	50
<b>Figure 3.17</b> Microhardness tester used in the experiment. ....	50
<b>Figure 3.18</b> Calo tester used for coating thickness measurement (Courtesy: Oerlikon Balzers Pvt. Ltd., India). ....	51
<b>Figure 3.19</b> Confocal microscope used for the surface roughness measurement of coatings (Courtesy: NMTC, CMTI, Bangalore).....	52
<b>Figure 3.20</b> Four probe apparatus used in the experiment.....	52
<b>Figure 3.21</b> Flow chart of research work. ....	53
<b>Figure 4.1</b> Microstructure of different cutting tool a) UT b) CT-18 c) CT-24 d) CT-32 .....	57
<b>Figure 4.2</b> Grain size of the different cutting tool.....	58



<b>Figure 4.3</b> XRD analysis of cutting tool under different conditions.....	58
<b>Figure 4.4</b> Microhardness of cryogenic treated and untreated cutting tool. ....	60
<b>Figure 4.5</b> SEM images of rake wear of cutting tool at a cutting speed of 270 rpm. .	62
<b>Figure 4.6</b> EDS analysis of spectrum 1.....	63
<b>Figure 4.7</b> SEM images of flank wear of cutting tool at a cutting speed of 270 rpm.	63
<b>Figure 4.8</b> Progression of maximum flank wear with machining time at a spindle speed of 270 rpm.....	64
<b>Figure 4.9</b> Progression of maximum flank wear with machining time at a spindle speed of 350 rpm.....	65
<b>Figure 4.10</b> Progression of maximum flank wear with machining time at a spindle speed of 540 rpm.....	66
<b>Figure 4.11</b> Tool life of cutting tool at different spindle speed on double logarithmic scale to base 10. ....	67
<b>Figure 4.12</b> Variation of the resultant cutting force during machining using cryogenic treated and untreated cutting tool at different spindle speed. ....	68
<b>Figure 4.13</b> Variation of the surface roughness of maraging steel after machining using cryogenic treated and untreated cutting tool at different spindle speed.....	69
<b>Figure 4.14</b> Progression of flank wear at a spindle speed of 270 rpm using UT & CT cutting tool under different machining environment. ....	72
<b>Figure 4.15</b> Progression of flank wear at a spindle speed of 350 rpm using UT & CT cutting tool under different machining environment. ....	73
<b>Figure 4.16</b> Progression of flank wear at a spindle speed of 350 rpm using UT & CT cutting tool under different machining environment. ....	73
<b>Figure 4.17</b> Variation of tool life with spindle speed. ....	75
<b>Figure 4.18</b> Tool wear of cutting tool at 540 rpm under different environment after machining for 25 minutes a) UT under dry b) CT under dry c) UT under wet d) CT under wet e) UT under cryogenic f) CT under cryogenic.....	77

<b>Figure 4.19</b> Variation of resultant cutting force with spindle speed. ....	79
<b>Figure 4.20</b> Variation of surface roughness with spindle speed. ....	82
<b>Figure 4.21</b> Surface morphology of coatings using SEM a) AlTiN and b) AlCrN. ...	84
<b>Figure 4.22</b> EDS analysis of cutting tool a) Uncoated (UC) b) AlTiN c) AlCrN.....	85
<b>Figure 4.23</b> XRD patterns for Uncoated and Coated tools. ....	85
<b>Figure 4.24</b> Coating thickness measurement using calo-tester a) AlTiN b) AlCrN. ..	87
<b>Figure 4.25</b> SEM images showing flank wear of inserts for a machining time $t = 25$ min, spindle speed- 270 rpm, feed rate- 58 mm/min, depth of cut- 0.3 mm. a) UC - Dry b) AlTiN - Dry c) AlCrN – Dry d) UC – Wet e) AlTiN – Wet f) AlCrN – Wet g) UC- Cryogenic h) AlTiN – Cryogenic i) AlCrN- Cryogenic. ....	89
<b>Figure 4.26</b> SEM images showing crater wear of inserts for a spindle speed- 270 rpm, feed rate- 58 mm/min, depth of cut- 0.3 mm. a) UC - Dry b) AlTiN - Dry c) AlCrN - Dry d) UC – Wet e) AlTiN -Wet f) AlCrN - Wet g) UC- Cryogenic h) AlTiN - Cryogenic i) AlCrN- Cryogenic.....	90
<b>Figure 4.27</b> Progression of flank wear with machining time at a spindle speed of 270 rpm. ....	93
<b>Figure 4.28</b> Progression of flank wear with machining time at a spindle speed of 350 rpm. ....	93
<b>Figure 4.29</b> Progression of flank wear with machining time at a spindle speed of 540 rpm. ....	94
<b>Figure 4.30</b> Variation of cutting force with spindle speed using the coated and uncoated cutting tool under different environment.....	96
<b>Figure 4.31</b> Variation of surface roughness with spindle speed using coated and uncoated cutting tool under different environment.....	98
<b>Figure 4.32</b> Microstructure of coatings a) TiAlSiN at 40 K X b) TiSiN at 40 K X c) TiAlSiN at 100 K X d) TiSiN at 100 K X. ....	101
<b>Figure 4.33</b> EDS analysis of a) TiAlSiN b) TiSiN coatings. ....	101

<b>Figure 4.34</b> XRD patterns of TiAlSiN & TiSiN coated WC-Co inserts.....	102
<b>Figure 4.35</b> Raman spectroscopy of TiAlSiN & TiSiN coatings.....	103
<b>Figure 4.36</b> Flank wear of coated inserts at a spindle speed of 540 rpm a) TiSiN coated inert under dry environment b) TiAlSiN coated insert under dry environment c) TiSiN coated insert under wet environment d) TiAlSiN coated insert under wet environment e) TiSiN coated insert under cryogenic environment f) TiAlSiN coated insert under cryogenic environment.....	106
<b>Figure 4.37</b> Progression of flank wear of different cutting tool at a spindle speed of 270 rpm. ....	108
<b>Figure 4.38</b> Progression of flank wear of different cutting tool at a spindle speed of 350 rpm. ....	108
<b>Figure 4.39</b> Progression of flank wear of different cutting tool at a spindle speed of 540 rpm. ....	109
<b>Figure 4.40</b> Variation of resultant cutting force with spindle speed during dry, wet and cryogenic milling using coated carbide inserts. ....	111
<b>Figure 4.41</b> Variation of surface roughness with spindle speed during dry, wet and cryogenic milling using coated carbide inserts. ....	112



## LIST OF TABLES

<b>Table 1.1</b> Wear mechanism and wear types at cutting edge. ....	5
<b>Table 1.2</b> Cutting fluid consumption in different countries. ....	8
<b>Table 1.3</b> Requirements of metal cutting industry. ....	11
<b>Table 3.1</b> Chemical composition of MDN 250 maraging steel. ....	35
<b>Table 3.2</b> Mechanical properties of MDN 250 maraging steel. ....	36
<b>Table 3.3</b> Specification of the cutting tool used in the experiment. ....	38
<b>Table 3.4</b> Specifications of milling machine. ....	45
<b>Table 3.5</b> Experimental plan for the experiment. ....	53
<b>Table 4.1</b> EDS area analysis of four tool modes depicted in Figure 4.2. ....	57
<b>Table 4.2</b> Electrical resistivity and conductivity of cutting tool. ....	61
<b>Table 4.3</b> Cutting parameters used in the experiments. ....	62
<b>Table 4.4</b> Tool life of cutting tools at different spindle speed. ....	66
<b>Table 4.5</b> Experimental plan for milling characteristics study. ....	71
<b>Table 4.6</b> Percentage improvement in tool life of cryogenic treated cutting tool under different environment. ....	75
<b>Table 4.7</b> Micro mechanical characteristics of AlTiN and AlCrN coatings. ....	87
<b>Table 4.8</b> Tool life for maximum flank wear, $V_b = 0.5$ mm. ....	92
<b>Table 4.9</b> Percentage improvement in tool life of coated tools under different environment and spindle speeds. ....	92
<b>Table 4.10</b> Percentage reduction in surface roughness of machined sample using coated tools. ....	98
<b>Table 4.11</b> Chemical composition of coatings from EDS analysis. ....	101
<b>Table 4.12</b> Micro mechanical characteristics of TiAlSiN and TiSiN coatings. ....	102

**Table 4.13** Tool life of cutting tools at different spindle speed and cutting environments.....109

## CHAPTER 1

### 1 INTRODUCTION

#### 1.1 MACHINING

Machining is a widespread material removal process in the manufacturing industry. It is a process in which a piece of raw material is cut into a desired final shape and size by a controlled material-removal process. The processes that have this common theme of controlled material removal rate are collectively known as subtractive manufacturing, in distinction from processes of controlled material addition, which are known as additive manufacturing. In the traditional or conventional machining processes such as turning, milling, drilling, boring, broaching, sawing, shaping, planing, reaming and tapping, machine tools, such as lathes, milling machines, drill presses, or others, are used with a sharp cutting tool to remove material to achieve a desired geometry.

A large amount of money, approximately US\$ 100 billion is spent worldwide annually for machining processes such as turning, milling, boring and other cutting operations (Ezugwu 2005). The cost of tooling is around 2 to 5% of total manufacturing cost (Inspektor and Salvador 2014). But the actual cost incurred is a lot more than these costs. Figure 1.1 presents the effect of cutting speed on machining cost. The fixed cost in the figure is independent of cutting speed and include the cost of the workpiece material, coolant disposal cost, setting and idle time cost, overhead cost. Line 1 & 2 in the figure is dependent on cutting speed and includes manpower, power cost, tool costs etc. Line 2 mainly shows the cost incurred in the change of tools due to an increase in cutting speed. Tool wears rapidly with an increase in cutting speed and also the idle time to replace the worn tool. High productivity with low manufacturing cost in addition to better surface finish & dimensional accuracy is the main goal for manufacturing industries. But these things are very difficult to achieve especially when machining difficult to cut materials which are more

commonly used in aerospace and aeronautical applications (Devillez et al. 2007). The productivity can be increased only with the increase in cutting speed and this results in high cutting temperature and tool wear. A large mechanical force and the cutting temperature are developed at the point of contact between cutting tool & workpiece material while machining by metal cutting processes like turning, milling, drilling & other methods. These severe service conditions will lead to substantial failure of cutting tool and has to be replaced to produce the desired product at specified tolerance. In order to avoid early failure of cutting tool & to improve tool life, the cutting tool has to be protected, by the coatings that are specially designed to prevent tool damage that occurs for particular applications (Inspektor and Salvador 2014).

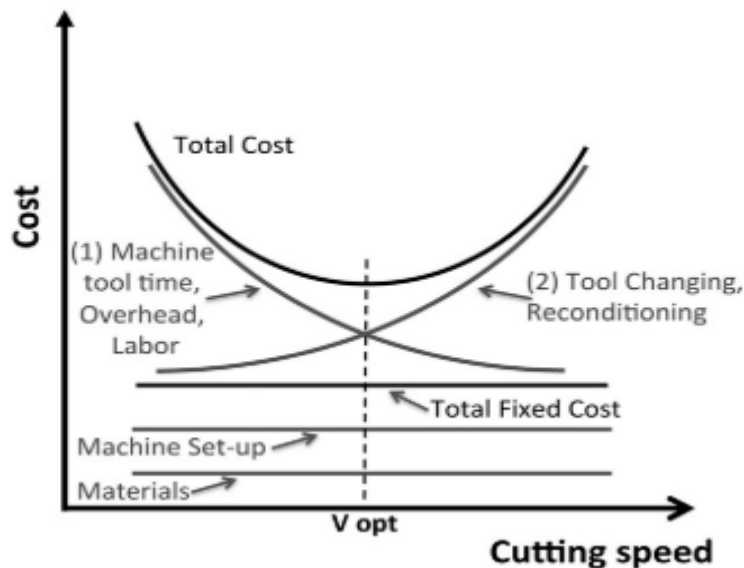


**Figure 1.1** Effect of cutting speed on machining cost (Inspektor and Salvador 2014).

The development of the new and improved cutting tool is the only solution to increasing manufacturing cost problem. The new cutting tool should be capable of withstanding severe cutting conditions at higher cutting speeds by prolonging the tool life. This goal can be only achieved by modifying the cutting tool geometry, the introduction of cutting tool material which has high hardness, toughness, thermal stability and fracture strength, coating of cutting tool to protect the cutting edge.

Machining requires a large amount of energy and consume a lot of power for the removal of material from a workpiece in the form of chips. A machining process like milling consumes more power compared to another process as the cutting tool is



rotated and simultaneously workpiece/ cutting tool moves linearly during the cutting process. The three parameters which influence the cutting operation is mainly cutting speed, feed rate and depth of cut. The high feed rate and cutting speed which is necessary for high productivity and better surface quality results in high temperature and stresses at tool tip. The finite element analysis of temperature gradient and stress during turning of Inconel 718 is presented in Figure 1.2. The highest temperature is developed at the rake face of the tool and temperature at the flank face is comparatively lower to the rake face.

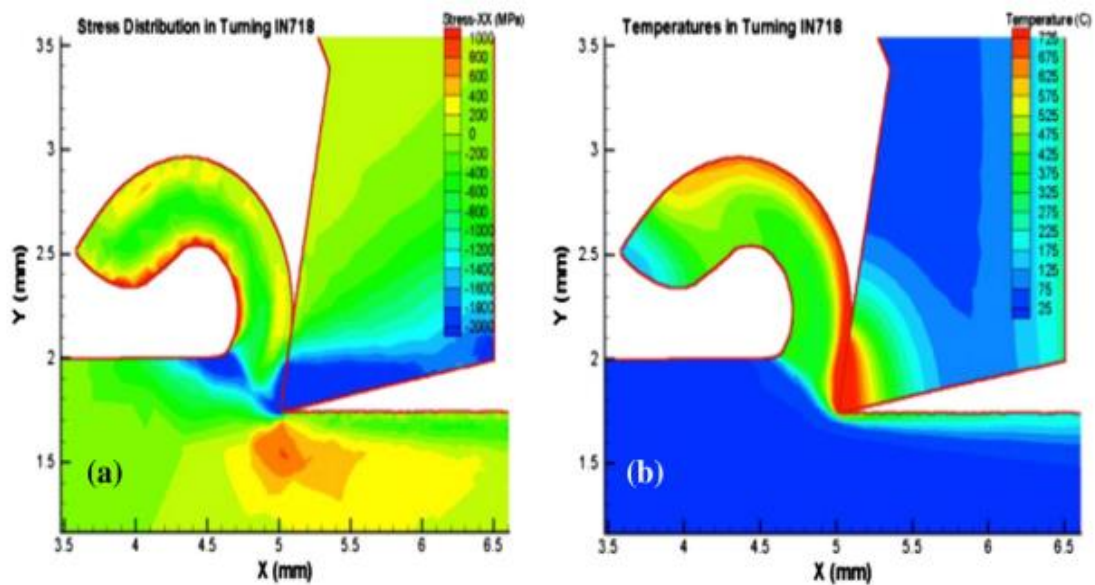


**Figure 1.2** Finite element analysis of of Inconel 718 during turning a) stress distribution and b) temperature (Maranhão and Davim 2010).

## 1.2 TOOL WEAR

The main wear mechanisms during machining are triggered by thermo-mechanical conditions. Figure 1.3 presents the primary wear mechanism during machining and the safe zone for a cutting tool during machining. The crater wear, flank wear, notch wear and chipping are some of the common wear mechanisms during machining. The flank wear is majorly due to abrasion of cutting tool with workpiece material and the crater wear is due to the hot chip flow and interaction with insert. The plastic deformation of tool tip occurs due to insufficient heat dissipation and thermal stresses due to high cutting temperature. The notch wear is mainly observed while machining

materials which show work hardening effect. Quint (1996) developed a typical wear map and is presented in Figure 1.3 (b). The wear map indicates the effect of cutting speed and feed rate on tool wear during machining. As the cutting speed increases the crater wear also increases and results in failure of the cutting tool. Also, the built-up edge formation is seen more during lower spindle speed and feed rate. The increase in feed rate results in the fracture and breakage of the cutting tool.

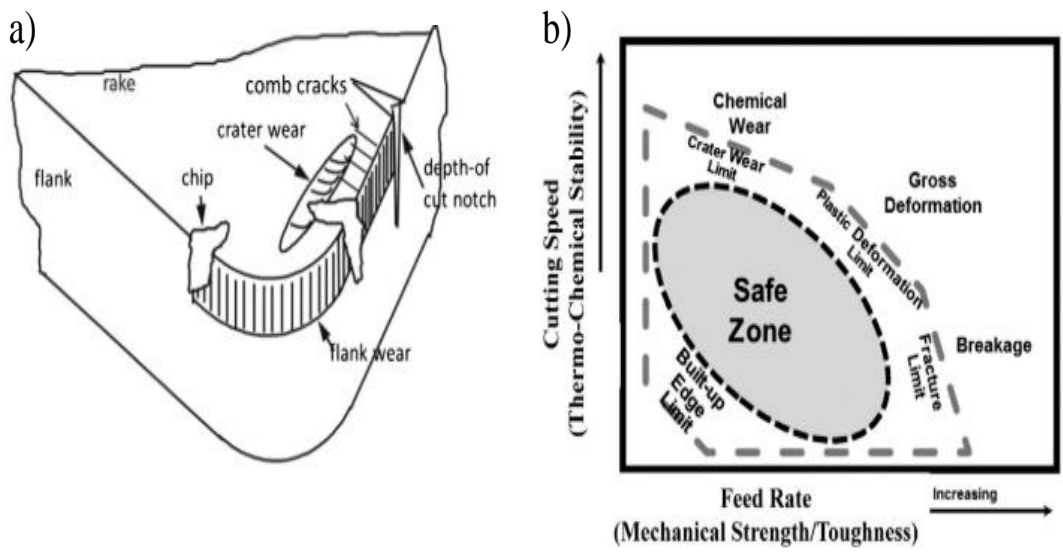


**Figure 1.3** Tool wear indicating a) Primary wear types and their locations on the cutting edge b) failure mode diagram for a tool material in machining and safe zone (Quint 1996).

**Table 1.1** Wear mechanism and wear types at cutting edge.

<b>Wear type</b>	<b>Location on the tool</b>	<b>Typical wear mechanism</b>
<b>Mechanical wear</b>	Nose, flank and clearance face	Abrasive wear: mechanical abrasion between tool and workpiece
<b>Cratering</b>	Top surface (rake face)	Diffusion and chemical wear due to severe friction and chemical interaction between the hot chip and the rake face of the tool
<b>Build-up edge</b>	Nose–rake face	Adhesion of chips due to chemical reaction and solubility with the workpiece, typically at low cutting speed
<b>Depth-of-cut notch</b>	Flank and rake face	Abrasive wear, a deep notch at an approximately depth-of-cut distance for the nose, due to extreme abrasion by the work hardened surface of the workpiece
<b>Thermal cracks</b>	Nose & flank face	Surface and material fatigue due to thermal cycling of the tool
<b>Thermal deformation Flank</b>	Nose	Plastic deformation of the nose due to insufficient thermal strength of the substrate at the specified cutting conditions

### 1.3 CUTTING TOOL

The cutting tool should possess properties like thermal stability, hot hardness, oxidation resistance, fracture toughness, chemical inertness and thermal shock resistance to resist the above-mentioned tool wear. Figure 1.4 presents the different cutting tools used in machining and their hardness/toughness properties. The top left corner represents the super hard materials like cubic boron nitride and diamond which is having higher hardness and thermal deformation resistance but less toughness and is vulnerable to chipping. Super hard materials are mainly used in machining high-temperature alloys, hardened steels, carbon composites and hypereutectic Al–Si alloys. The bottom right corner represents the high-speed steel which is having high toughness but low hardness. It is used in machining at low cutting speeds since high cutting speed softens the cutting tool. They are mainly used in end mills and drills where premature chipping is more. Cemented carbide cutting tools has a balanced combination of hardness, toughness and wear resistance which makes them the most commonly used cutting tool in machining. WC-Co inserts are used for machining a wide variety of materials and grain size of WC can be fine-tuned for a particular application.

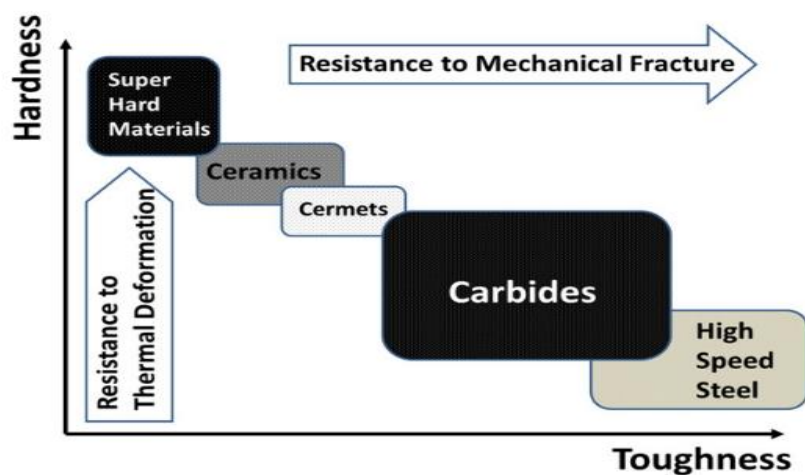


**Figure 1.4** Different cutting tools used in machining (Inspektor and Salvador 2014).

## 1.4 COOLING TECHNIQUES FOR REDUCTION OF CUTTING TEMPERATURES

Reducing the machining zone temperature in a tiny amount will lead to improved tool life. Productivity is one of the deciding factors for the machining cost. When productivity increases the generation of friction and heat at the machining zone also increases, this leads to shortening of tool life hence machining cost increases (Kalyan and Choudhury, 2008). To overcome this problem, many researchers have attempted several cooling techniques to cool the machining zone temperatures as shown in Figure 1.5. For many years, machining industries are using conventional fluid cooling at the machining zone to overcome the temperature raises (Baradie, 1996a). However, it is found that flood cooling technique is not able to reduce the cutting temperature at the tool-chip interface at higher cutting speeds (Shaw et al., 1951; Cassin and Boothroyd, 1965).

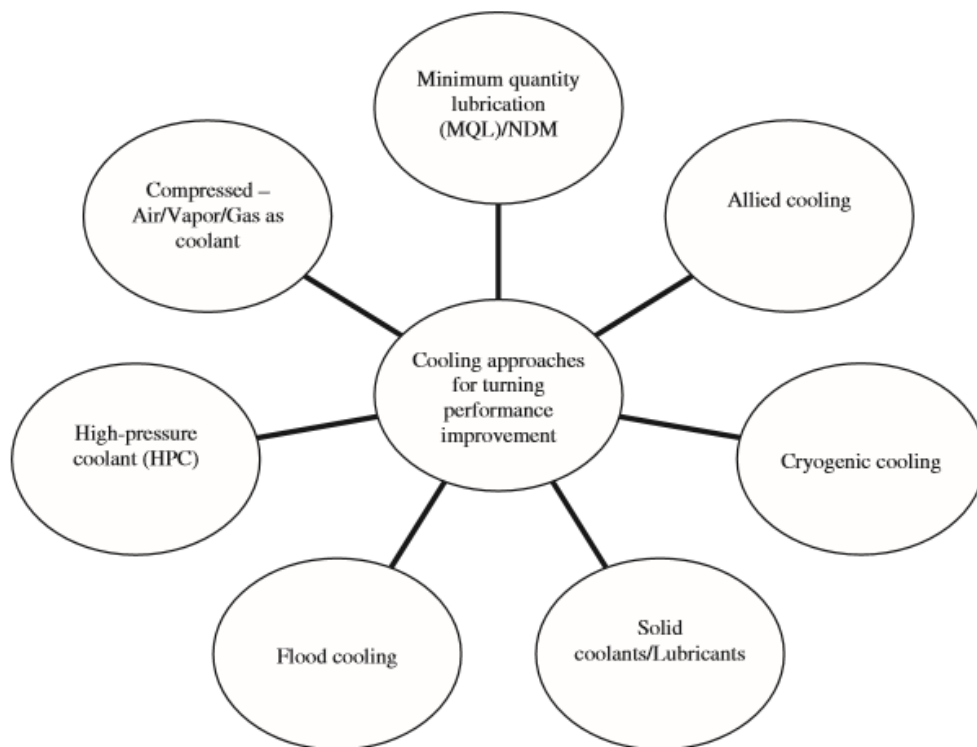


**Figure 1.5** Different cooling techniques in machining (Chetan et al. 2015).

The conventional cutting fluids contain chemical contaminants which cause severe health issues, environmental problems and additional disposal cost (Baradie, 1996b). It has been reported that approximately 1 million workers are exposed to coolant in the U.S (Shaw, 1984; Chetan et al., 2015). Table 1.2 shows the yearly consumption of cutting fluid and their associated costs in various countries and regions.

**Table 1.2** Cutting fluid consumption in different countries.

<b>Country name</b>	<b>Cutting fluid consumption</b>	<b>Purchasing and disposing cost</b>	<b>Reference</b>
<b>United States</b>	100 million gallons per year	48 billion dollars a year	(Feng and Hattori, 2000)
<b>Germany</b>	75,500 tons a year	1 billion German Mark	(Klocke and Eisenblätter, 1998)
<b>Japan</b>	100,000 kilo litres	71 billion Japanese Yen a year (in this 42 billion Yen purchasing cost)	(Feng and Hattori, 2000)
<b>the European Union alone</b>	320,000 tons	60 billion euros	(Lawal et al., 2012)
<b>The Asia-Pacific region</b>	891,330 tons	187 billion USD	(Lahiri N.D.)
<b>Turkey</b>	27,248 kilo litres	1 billion Turkish lira	(Shokrani et al., 2012)
<b>India</b>	1,50,000 tons	1500 billion INR	(Sharma et al. 2015)

It is expected that the annual usage of metal working fluids (MWFs) across the world is a grand total of 640 million gallons (Brockhoff and Walter, 1998). It is predicted that the associated costs related to cutting fluids are in the range of 20-30 % of the total manufacturing costs while machining of hard-to-cut group materials (Pusavec et al., 2010). Usage of cutting fluids additionally includes the maintenance and disposal cost and it can be up to 2 to 4 times their purchase price (Chetan et al., 2015). This issue has been supported through the introduction of environmentally conscious regulations such as the Control of Substances Hazardous to Health (COSHH) in the

U.K and the Technical Code of Practice for Hazardous Substances (TRGS) in Germany (Shokrani et al., 2012), The National Institute for Occupational Safety and Health (NIOSH) and ISO 14001 (Marksberry, 2007), OHSAS 18001 Occupational Health and Safety Assessment Series and many international global standards like ISO 9000,14000,14001 (Rao, 2011) restricted the metal cutting industries in terms of usage and disposal of conventional cutting fluids due to the health hazardous and environmental pollution impact. Because of these drawbacks, recently researchers have concentrated on different sustainable manufacturing processes as shown in Figure 1.6. The characteristics of the sustainable machining process are shown in Figure 1.7.

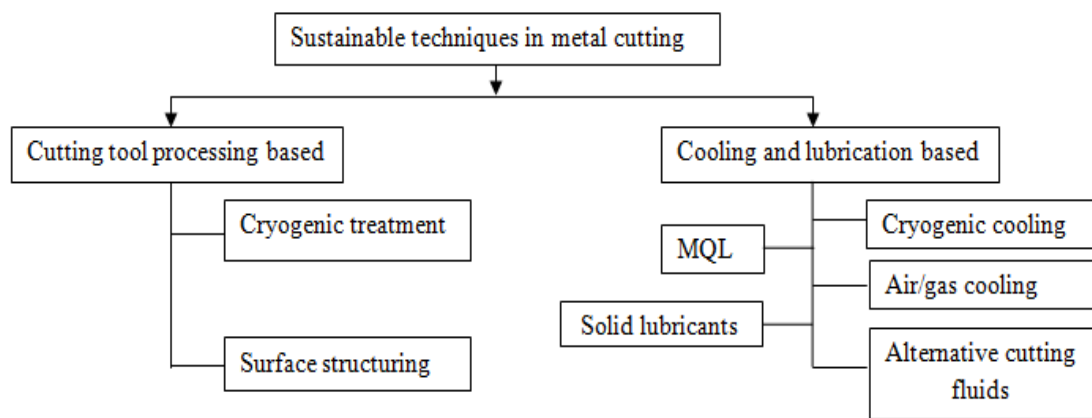


**Figure 1.6** Sustainable manufacturing techniques for cleaner production (Chetan et al. 2015)

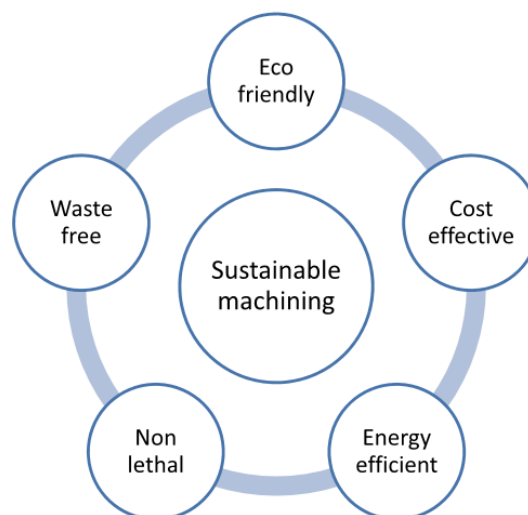


**Figure 1.7** Characteristics of sustainable machining (Chetan et al. 2015).

MQL is one alternative method i.e., supplying the coolant at the tool-chip interface at 50-500 ml/hr. Consumption of cutting fluid in MQL was 10000 times lesser than the conventional cooling method (Dhar et al., 2006). Aoyama et al. (2008) have reported that MQL machining is not feasible for industrial machining conditions because it fails to remove the chips at the cutting zone and creates health problems to the machinist due to the presence of oil mist at the working environment. Chetan et al. (2015) reviewed the different sustainable machining techniques and discussed the advantages and disadvantages of different sustainable machining techniques. It was reported that air/gas cooling technique requires special cooling equipment as well as air/gas coolants inactive in controlling the machining zone temperatures during machining of super alloys. Likewise, solid lubrication cooling technique is costly due to the involvement of more production cost for solid lubricants and requirement of special equipment for supplying the solid lubricants. Alternative coolants like vegetable oil and ionic liquids are biodegradable but these are costly when these applied in flood cooling technique. Also, vegetable fluids have very poor thermal stability results in not able to control the machining zone temperatures.

## **1.5 NEED FOR THE PRESENT STUDY**

Table 1.3 presents the requirements of a metal cutting industry and it is clear from the table, modification of cutting tool and sustainable cooling techniques are required for machining of new workpiece materials. The productivity and surface quality are two factors which cannot be compromised in the manufacturing sector and it cannot be fulfilled without new cutting tools and cooling techniques. The present study concentrates on developing a cutting tool capable of machining the advanced materials with a prolonged tool life under the sustainable cooling environments.



**Table 1.3** Requirements of metal cutting industry.

<b>Improved product quality</b>
• New workpiece materials • Improved machining accuracy and efficiency • Better tolerances and product performance • Improved surface finish
<b>Increased productivity</b>
• Higher output at shorter lead-times • Increased machine tool utilization
<b>Green, eco-friendly manufacturing</b>
• Eliminate the need for metal cutting fluids for cost-saving • Environmental considerations and regulations

## **1.6 OUTLINE OF THE THESIS**

The thesis has been presented in 5 chapters:

**Chapter 1** presents introductory remarks on machining, difficulties in machining, machining cost, tool wear and wear mechanism, different cutting tools, sustainable machining, need for present work and outline of the thesis.

**Chapter 2** Presents a critical review of the published literature relevant to the present study. A literature review is discussed on the difficult to cut materials, maraging steel, cryogenic treatment, characteristics of cryogenic treatment, PVD coatings, aluminium based coatings, cathodic arc deposition, magnetron sputtering, titanium-based coatings, sustainable machining. The broad objectives of the present research work are drawn based on the gaps in the available literature.

**Chapter 3** covers the description of equipment and the various characterization techniques used for the analysis of microstructural features, mechanical properties,

tool wear and machinability characteristics using cryogenic treated and coated inserts under dry, wet and cryogenic environments.

**Chapter 4** explains the results and discussion of experimental investigations. The results of cryogenic treatment, characterisation of cryogenic treated tools and milling performance of cryogenic treated tool under different environments are explained in this chapter. It also contains coating development using cathodic arc deposition and magnetron sputtering technique, characterisation of PVD coated tools, machinability characteristics under different environment.

**Chapter 5** presents the conclusions of the research work and scope for future work.

## CHAPTER 2

### 2 LITERATURE REVIEW

This chapter details the literature on cryogenic treatment of cutting tool inserts, PVD coating of cutting tools and sustainable machining, especially about cryogenic machining.

#### 2.1 DIFFICULT TO CUT MATERIALS

Metal working industry is a sector where worldwide investments keep on increasing even during the recession time. Machining is the most widely used material removal process in the manufacturing industry since the 18th century. Machining is a process in which the raw material is converted into a desired shape and size by removing material at a controlled rate. The operations which have the characteristics of a controlled material removal rate are commonly known as subtractive manufacturing. High productivity with low manufacturing cost in addition to better surface finish & dimensional accuracy is the main goal for manufacturing industries. The introduction of advanced engineering materials and difficult to cut materials caused a threat to existing machining techniques and conventional cutting tools. Super-alloys and refractory metals of nickel, titanium, molybdenum, steel, rhenium, cobalt, tungsten, niobium, tantalum, chromium, etc. are usually considered as difficult to cut materials or hard to cut materials due to their extreme mechanical and metallurgical properties. The superior strength, low thermal conductivity, and tendency to strain harden reduce machinability of these materials. Excessive tool wear, high heat generation, high power consumption, larger cutting forces, poor surface quality and/or difficulties in chip formation are some of the difficulties faced while machining difficult to cut materials. It is difficult to overcome these difficulties in machining by the use of conventional cutting methods and the existing tool materials. The power consumption increases with high cutting forces. The early cutting tool failure reduces the surface finish, increase the idle time and production cost.

## **2.2 MARAGING STEEL**

Maraging steel is a hard material which possesses superior strength and toughness without losing its malleability (Bailey 1977). It belongs to a class of ultra-high strength low carbon steels, which derive their strength from the precipitation of intermetallic compounds and not from carbon (Bhukya et al. 2014). The maraging steel possesses mechanical properties such as high yield strength, ductility and fracture toughness combined with better hardenability (Fortunato et al. 2018). The ultra-high-strength coupled with fracture toughness and minimum weight requirement while ensuring high reliability makes maraging steel ideal candidate for applications in aeronautical and aerospace. These fine properties promoted the use of maraging steel in applications such as dies, piston rods in heavy vehicles, crankshafts, landing gears, fabrication of molds for metal injection molding, gas turbines, jet engines, cryogenic missiles, rocket motor casings, aerospace biomedical applications and military applications where high temperature is encountered (Kosaraju and Chandraker 2015; Li et al. 2018; Nikalje et al. 2013; Viswanathan et al. 1993). The hardness of 50 HRC combined with ultimate strength of 1.84 GPa makes maraging steel a difficult to cut material (Santhanakumar et al. 2017).

## **2.3 CRYOGENIC TREATMENT**

Cryogenic processing or cryogenic treatment is introduced in the late sixteenth century for enhancing mechanical properties of the material. It is in 1937 the cryogenic treatment began to be used in the processing of cutting tools (Amini et al. 2012). The applications of cryogenic treatment include oil drills, musical instruments such as guitar string and piano, dental and surgical instruments, bearings and gears, sports equipment's (Baldissera and Delprete 2008). Another advantage of cryogenic treatment over the coating process is the less expertise of the operator to carry out the process. The cryogenic treatment can improve industrial productivity in terms of improving tool life, reducing downtime, better surface quality and reduced machining cost. The gases used for cryogenic treatment are nitrogen, helium, oxygen and neon which has less environmental effects (Akincioglu et al. 2015). Thus cryogenic treatment is an eco-friendly machining technique which can enhance product quality

at a minimal cost. The cryogenic treatment is used in metal cutting processes like drilling, turning, milling and grinding to enhance mechanical properties of cutting tools (Cicek et al. 2012; Gill et al. 2011b; Thamizhmanii et al. 2011; Yong et al. 2007). The treatment of materials carried out at a temperature of less than zero degree Celsius ( $-196^{\circ}\text{C}/78\text{K}$ ) is known as a cryogenic treatment or deep cryogenic treatment (DCT). The cryogenic treatment can be classified into shallow cryogenic treatment (SCT) and deep cryogenic treatment (DCT), the former which is carried out at temperatures ranging from  $-80^{\circ}\text{C}$  to  $-140^{\circ}\text{C}$  and later at temperatures ranging from  $-140^{\circ}\text{C}$  to  $-196^{\circ}\text{C}$ . It is an extension of standard surface treatment processes, unlike it influences the core of properties (Bensely et al. 2007).

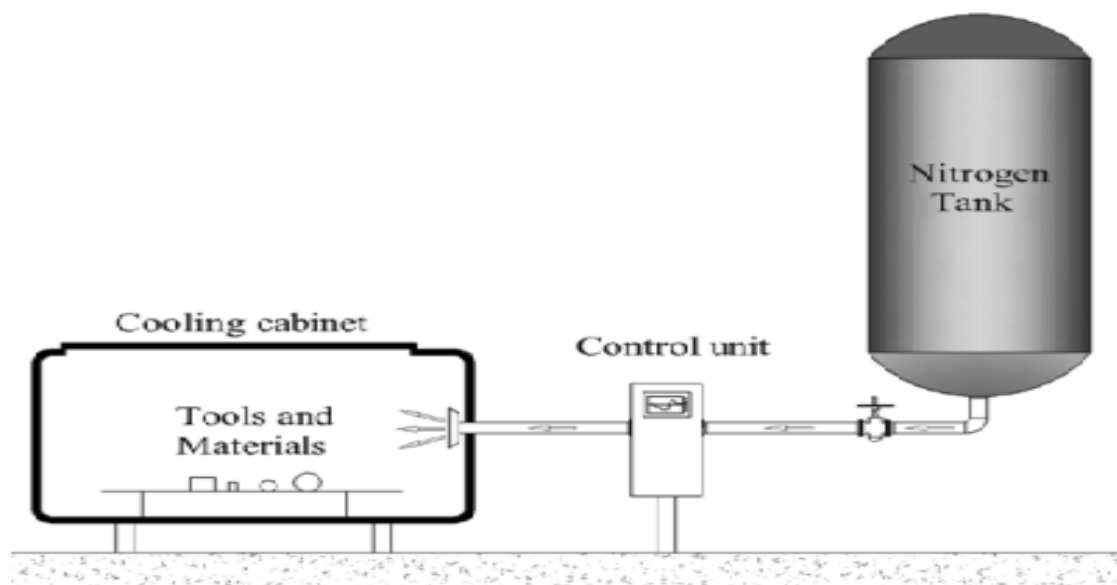


**Figure 2.1** Schematic view of a cryogenic treatment process (Akincioglu et al. 2015).

The changes in mechanical properties and crystal structures are some of the notable effects observed after cryogenic treatment. The DCT process can be explained as a controlled process in which temperature is lowered from room temperature to boiling point of liquid nitrogen ( $-196^{\circ}\text{C}$ ) and then maintaining the temperature for 24 hours or more afterwards raising the temperature gradually to room temperature, accompanied by a tempering process. The schematic of cryogenic treatment is presented in Figure 2.1. The rate of cooling, the soaking period, soaking temperature and tempering process are some of the factors influencing the efficiency of cryogenic treatment. There are chances of thermal shock if we cool the material rapidly to cryogenic

temperature, it may result in microcracking of material. Thus a proper cooling rate is mandatory to avoid thermal shocks according to the studies on cryogenic treatment. Kalinga Simant Bal and Maity (2012) investigated the effect of cooling rate on the cryogenic treatment of tungsten carbide inserts and studied performance during turning of AISI 304. They used a cooling rate of 0.5°C/min and 1°C/min and it is reported that cooling rate of 1°C/min increased hardness and brittleness but decreased toughness as rapid cooling rate decreased percentage of cobalt binder phase while cooling rate of 0.5°C/min is reported with improvement in toughness as well as hardness. The precipitation of fine  $\eta$  phase carbides with WC uniformity in the metal matrix as well as densification of Co binder phase took place as a result of cryogenic treatment at a cooling rate of 0.5°C/min. The results revealed that inserts undergone cryogenic treatment at a cooling rate of 0.5°C/min showed better wear resistance than inserts under a cooling rate of 1°C/min. The soaking period is another most influencing factor in cryogenic treatment, as the literature suggests soaking period is varied from 1 hour to 40 hours by different researchers (Bensely et al. 2007; Das et al. 2009). According to Darwin et al. (2008), the improvement in wear resistance of steel due to cryogenic treatment is most influenced by soaking period by a percentage of 16 to 30 respectively. Mukkoti et al. (2018) studied the effect of cryogenic treatment of tungsten carbide inserts on cutting force and power consumption in CNC milling process and found that cutting force and power consumption minimized after the cryogenic treatment. They used a Box-Behnken design with decision variables such as cutting speed, feed rate, depth of cut and end milling tools to optimise the performance measures such as cutting force and power consumption. It is revealed that cryogenic soaking time is the most significant factor affecting the cutting force and power consumption followed by cutting speed, feed and depth of cut. Dhande et al. (2018) investigated the influence of soaking period (8 hours, 16 hours, 24 hours & 30 hours) in the cryogenic treatment of tungsten carbide inserts and found a significant reduction in a weight loss of 8 hours soaked sample during wear test. The improvement in wear resistance is attributed to the reduction in cobalt percentage in the  $\beta$  phase of WC-Co matrix which resulted in the formation of the  $\eta$  phase. The optimum soaking period reported by researchers mostly varied depending on the material and 24 hours is most reported soaking time by researchers (Shirbhate 2012;

Lal et al. 2001; Ozbek et al. 2014). A finding reported by Das et al. (2007) suggests that soaking period influences wear resistance but does not affect the hardness, as soaking period increases wear resistance also increases. It is Molinari et al. (2001) who suggested soaking period should not exceed 35 hours, as the longer soaking period does not have any impact on the performance while working with M2 high-speed steel and H13 tool steel.

The metal cutting tool insert should possess combined properties of a ceramics such as chemical stability, high hardness and temperature resistance along with properties of metal such as high toughness and good thermal conductivity. Cemented carbides (WC-Co) are commonly used cutting tools which is a composite with cobalt as a soft metal binder and tungsten carbide as hard ceramic phase. Cryogenic treatment of WC-Co inserts is a step to prolong the tool life by constructively altering the morphology of tungsten carbide-cobalt material. Some of the attributes of the cutting tool which can be improved by cryogenic treatment include toughness, hardness, abrasion resistance and electrical conductivity. The early carbide fracture is attributed to the residual stresses developed during sintering and manufacturing process, these micro stresses can be relieved with the help of cryogenic treatment. The precipitation of fine  $\eta$  carbides decreased the amount of cobalt binder  $\beta$ -phase and crystallographic alignment and refinement of the hard  $\alpha$ -phase particle are some of the attributes which improve the wear resistance of cryogenically treated tungsten carbides (Gill et al. 2012a). The cryogenic treatment has resulted in the homogenous distribution of carbides, increase in hardness and toughness, austenite to martensite conversion, austenite transformation at low temperatures in tool steel (Jeleńkowski et al. 2010). According to Gill et al. (2011a), precipitation of  $\eta$ - phase carbides during cryogenic treatment can resist chipping and notch wear of tungsten carbide inserts during turning thereby enhancing tool life. Özbek et al. (2016) studied the effect of deep cryogenic treatment on tungsten carbide inserts in turning of AISI 304 stainless steel and found improvement in wear resistance of treated inserts. The treated inserts had a superior wear performance of 18 % compared to untreated one in terms of flank wear. The wear resistance of treated inserts is attributed to precipitation of newer and finer  $\eta$

phase carbides and their homogeneous distribution in WC-Co matrix. The skeleton of the WC-Co structure is presented in Figure 2.2.

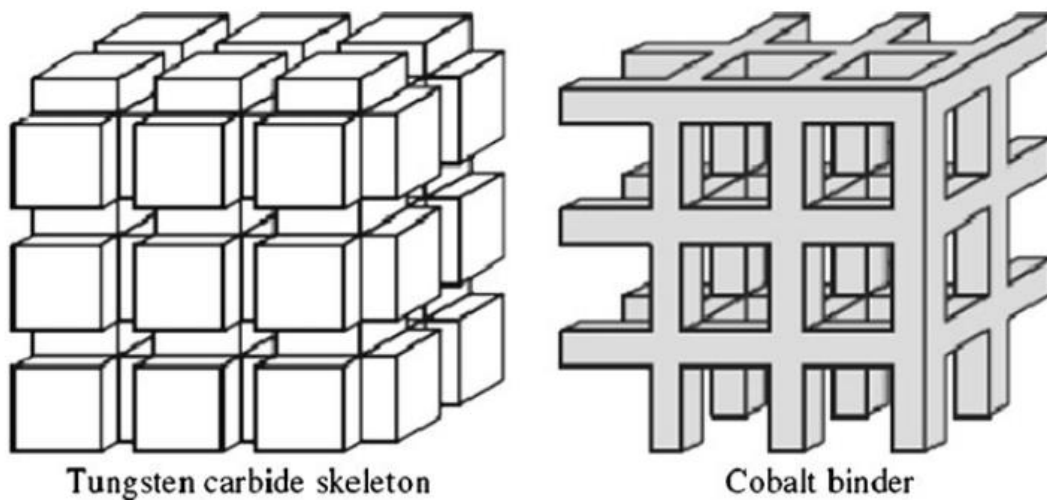


**Figure 2.2** Skeleton of WC-Co structure (Gill et al. 2012a).

Yong et al. (2007) reported improvement in tool life of tungsten carbide inserts after cryogenic treatment. The performance of cryogenically treated inserts depends on machining time and machining conditions. There is a decline in the performance of cryogenically treated inserts after a long time of machining, especially under dry condition. They found that high cutting temperature diminished the effect of cryogenic treatment on inserts and found machining with coolants can reduce this problem. Reddy et al. (2009) reported the turning of AISI 1040 steel using cryogenically treated inserts and found a 27 % improvement in tool life, 11 % reduction in main cutting force, 20 % reduction in surface roughness in a cutting speed range of 200-350 m/min. Further, in another study, they reported that the increase in thermal conductivity and hot hardness of cutting tool after cryogenic treatment is the reason for the improvement in machinability (Reddy et al. 2009). Ozbek et al. (2016) studied the effect of different holding time on the cryogenic treatment of cemented carbide inserts. They used different holding times of 12, 24, 36, 48 and 60 hours for cryogenic treatment and found 24 hours as optimum holding time to give the highest wear resistance. The highest precipitation and homogenization of  $\eta$  phase carbides occurred at 24 hours compared to other holding times. The authors studied the effect of deep cryogenic treatment on cemented



carbides by varying soaking period for 18, 24 & 32 hours and found 24 hours as the optimum soaking period. Beyond 24 hours bigger carbides ( $\alpha$  phase) were produced subsequently instead of finer and more homogeneously distributed ones. This is due to the clusters of carbon atoms becoming bigger in colonies. The further precipitation of  $\eta$  phase carbides is being blocked by the bigger carbides. Also, carbide ( $\eta$  phase) cannot be produced due to the increase in atom concentration near the bigger particle. Thus longer holding duration results in the decrease in carbide percentage. Hence the microhardness and wear resistance no longer increase after 24 hours.

The literature review reveals that the performance of cryogenically treated inserts diminishes during high cutting speeds due to high tool-chip interface temperature and especially during continuous machining (Ozbek et al. 2016). The cryogenic machining is a sustainable cooling approach to reduce tool-chip interface temperature to a large extent, thereby improving tool life and machinability. The spraying of liquid nitrogen at cryogenic temperature ( $-195.8^{\circ}\text{C}$ ) between tool and workpiece is one way of reducing cutting temperature without affecting the environment and operator. Dhar et al. (2001) studied the cryogenic turning of E4340C & AISI 1040 steel and found a 34 % reduction in chip-tool interface temperature. The high reduction in flank wear, better surface finish and improved dimensional accuracy are other significant findings which improved machinability. The cryogenic cooling has been effectively employed in different machining processes like turning, milling, drilling, grinding etc (Ahmed and Kumar 2017; Govindaraju et al. 2014; Kumar. S and Kumar. M 2014; Manivannan and Kumar 2017; Sivaiah and Chakradhar 2017a; b; c). Rahman et al. (2003) investigated the machining performance of ASSAB 718HH mold steel using chilled air. They found that cutting force, surface roughness and tool wear are lower than dry cooling and lower/comparable to conventional flood cooling. Ravi and Kumar (2011) reported a reduction in cutting temperature, cutting forces, surface roughness and tool wear during the machining of AISI H13 tool steel under cryogenic cooling at different cutting speeds. A lubrication layer is produced at cutting tool-chip interface during cryogenic cooling which resulted in a substantial reduction of cutting temperature, the betterment of surface finish and tool life (Ravi and Kumar 2012). Shokrani et al. (2016) studied the effect of cryogenic cooling on surface integrity in

end milling of Ti-6Al-4V alloy and found an exceptional improvement in surface integrity under cryogenic cooling compared to dry and wet cooling.

## **2.4 PVD COATINGS**

Physical vapour deposition (PVD) processes are atomistic deposition processes in which material is vaporized from a solid or liquid source in the form of atoms or molecules, transported in the form of vapour through a vacuum or low pressure gaseous (or plasma) environment to the substrate where it condenses. Typically, PVD processes are used to deposit films with thicknesses in the range of a few nanometers to thousands of nanometers; however, they can also be used to form multilayer coatings, graded composition deposits, very thick deposits and freestanding structures. Material to be deposited is heated and vaporized in a vacuum. The vapours condense on the substrates which are kept at a specified distance from the vapour source. The substrates are cleaned in-situ using glow discharge plasma. This improves the adhesion of the film. Increasing the substrate temperature improves the adhesion further and also helps in getting denser films with fewer voids. Resistive heating, high energy electron beam heating and induction heating are some of the options available for vaporizing the target material. Using different targets and reactive gases it is possible to deposit multi-layer films. Its applications include metallization for packing, decorative coatings, electronic industries, machining tools like inserts, drill bits etc., and coating on wear resistant surfaces.

### **2.4.1 PVD Coating of cutting tools**

The hard and wear resistant properties of cemented carbide make it the most widely used cutting tool in the current market. The coated cemented carbides make the machining of hard & difficult materials easier. It is estimated that 90% of cemented carbide inserts are coated using PVD, CVD or their combination (Inspektor and Salvador 2014). However, it is not easy to select the best insert grade & coatings with the arrival of advanced coating techniques. The selection should begin from workpiece material which is going to be machined, whether coated or uncoated inserts to be used. While machining ferrous materials such as iron, cast iron, steel or stainless

steel, super alloys coating is unavoidable. It is recommended to use coated tools in every application except where the high-pressure coolant is used. The uncoated tools are used for machining non-ferrous materials like aluminium which is soft & lead to the built-up edge. The other materials which do not require coated insert include brass, bronze, wood & many composite materials.

The first commercial coating was a TiN physical vapour deposition (PVD) coating developed for high-speed steel drills in the 1980s and then on carbide inserts used for milling applications. It was followed by monolithic PVD TiN, solid solution strengthened monolithic Ti (CN) coatings. In 1998, the first multilayer coated PVD coatings TiN/Ti (CN) and stoichiometric TiAlN with improved thermal stability and hot hardness was developed. A new era in the manufacture of functional coatings was started in mid-1990 with development of nanostructured coatings that could be designed on atomic level: starting with nano layer coatings, such as TiN/VN, AlN/TiN, AlTiN/TiN, and AlTiSiN/TiN, and followed by nano composite coatings: Ti-Si-N, Al-Ti-Si-N, and Ti-B-N. Most of the commercial coatings available now are thermally stable ternary or quaternary coatings & nano structured compounds made of carbides & nitrides of transition metals like Ti & Zr with other elements such as Al, Cr, Hf, Si, Ta, Nb & V (Inspektor and Salvador 2014). The coatings play a substantial role in high-performance machining of difficult to cut materials. The cutting tool should be protected efficiently at cutting zones as mechanical & thermal loads acting on this area is very high while machining difficult to cut materials. The coating improves the wear resistance of cutting tool thereby increasing tool life & productivity by reducing idle time for a change of tool.

#### **2.4.2 Aluminium based coatings for cutting tool**

The introduction of difficult to cut materials, urge the manufacturing industries to find the excessive application of coatings on the cutting tools. A large number of PVD coatings are developed for the milling operations to have better performance. Al-based coatings find most promising applications in the end milling. Beake et al. (2015) studied about end milling of H 13 tool steel using PVD coated cutting tools. They found that AlCrN and AlTiN coated tools perform well under extreme

conditions because of their good oxidation resistance, hot hardness and wear resistance at elevated temperatures. Mo et al. (2013) reported that AlTiN and AlCrN coating shows much higher impact wear and abrasion resistance at elevated temperature than CrN coatings. The experimental investigation by Nohava et al. (2015) reveals that AlTiN and AlCrN coating shows better wear resistance during room temperature to 600<sup>0</sup>C. Mo and Zhu (2009) investigated the behaviour of AlCrN coating against Si<sub>3</sub>N<sub>4</sub> ball under two sliding conditions. They found out that the AlCrN coating has excellent abrasion resistance on both conditions. They concluded that the formation of wear resistant and thermally stable oxides formed due to tribo-chemical reactions of chromium and aluminium are responsible for imparting abrasion resistance. Endrino et al. (2006) studied the performance of aluminium based PVD coatings AlCrN, AlCrNbN, fine-grained (fg) AlTiN and nano-crystalline (nc) AlTiN for the machining of austenitic steel. The influence of surface post-treatment is investigated by analysing tool wear and surface texture and it was found that nc-AlTiN coating has minimal wear intensity.

### **2.4.3 Cathodic arc deposition**

In the cathodic arc deposition system, thin film development on the surface takes place on the finely finished surfaces. With the ultrasonically cleaned surface and high temperature will increase the adhesion and coating will be denser. Coatings obtained from cathodic arc sources are very dense and adhesion to the substrates is good. The films are free of voids. A reactive deposition is more efficient as the ions are energetic and ionized unlike in magnetron sputtering. The illustration of cathodic arc deposition is described in Figure 2.3.

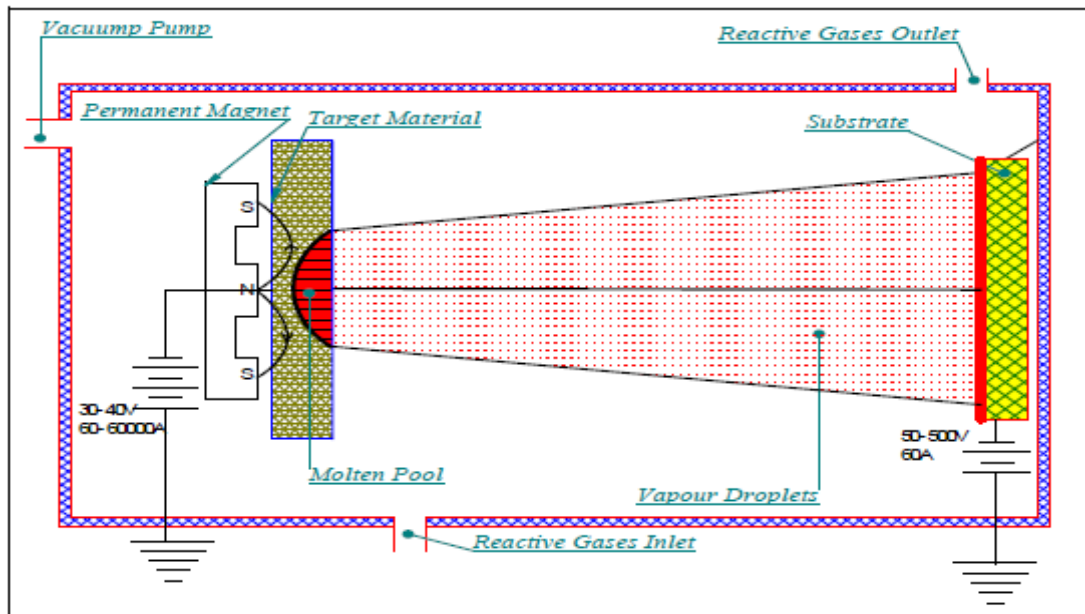


**Figure 2.3** Schematic of PVD coating using cathodic arc deposition technique.

In the development of thin film coatings, three important stages are witnessed namely,

1. Creation of vapour phase.
2. Transport from target to substrate.
3. Film growth on the substrate.

Step1: Creation of vapour phase

An electric arc is generated when the flow of current is suddenly interrupted. During the arc, the electrode material evaporates and reacts with reactive gases in the vacuum and deposited as a compound on the substrate. It is more likely that the reaction takes place on the surface of the substrate. The voltage applied between the cathode and the anode is connected to the wall of the vacuum chamber. The cathode is brought in contact with the anode using the igniter. Withdrawing of igniter creates large current flow, thus the arc is generated on the cathode surface. A few tens of amperes to few kilo amperes of current are maintained in the circuit. The temperature in the cathode arc spot increases so that the region of arc spot starts melting. The corresponding area is called a molten pool of cathode.

Step 2: Transportation of vapours from target to substrate

The produced vapour particles were transported from target to substrate. While transporting some of the atoms can be ionized by creating the plasma in the place. From the molten pool of target, electrons are emitted by the field emission process. The emitted electrons ionize the vapours of a cathode which are coming from the pool. Thus the high-density plasma is created near the cathode this expands towards the substrate which leads to improvement in the adhesion of the coating, film quality improves and crystal orientation also controlled. During the past two decades, non-equilibrium plasmas have revolutionized the surface coating technologies opening up a variety of applications which are otherwise impossible. Some of the ions from the plasma are attracted to the cathode, which leads to the exertion of pressure on the molten pool. The emitted ions are accelerated to energies up to 150 eV. This is more than the cathode voltage of about 25V. Further, the ions are multiplied, these energetic ions are further accelerated at the substrate by the bias voltage. Thus the substrate is attracted by the bias voltage. The substrate is bombarded with high energy ions during the growth of the film. This improves the density of the film. The voids in the film is avoided and the integrity of the film is maintained.

### Step 3: Film Growth on the substrate

In this step condensation of vapour on the substrate and its development of thin film by nucleation and growth process occur. The nucleation and growth process is strongly influenced by the approach of new ions or vapour particles which results in a change in microstructure, composition, impurities and residual stresses. The process utilizes the arc to melt the target; the arc is initiated by breaking a current path.

#### **2.4.4 Magnetron sputtering**

Magnetron sputtering is a plasma vapour deposition process in which a plasma is created and positively charged ions from the plasma are accelerated by an electrical field superimposed on the negatively charged electrode or "target". The positive ions are accelerated by potentials ranging from a few hundred to a few thousand electron volts and strike the negative electrode with sufficient force to dislodge and eject atoms from the target. These atoms will be ejected in a typical line-of-sight cosine distribution from the face of the target and will condense on surfaces that are placed

in proximity to the magnetron sputtering cathode. The targets are fabricated from materials that subsequently deposit on the surface of the component facing the electrode. Conductive materials can be deposited using a direct current (DC) power supply and insulators can be deposited by using a radio frequency (RF) power supply. Magnetron sputtering deposition uses a closed magnetic field to trap electrons, enhancing both the efficiency of the initial ionization process and allowing plasma to be generated at lower pressures which reduces both background gas incorporation in the growing film and energy losses in the sputtered atom through gas collisions. The schematic of RF magnetron sputtering is presented in Figure 2.4.

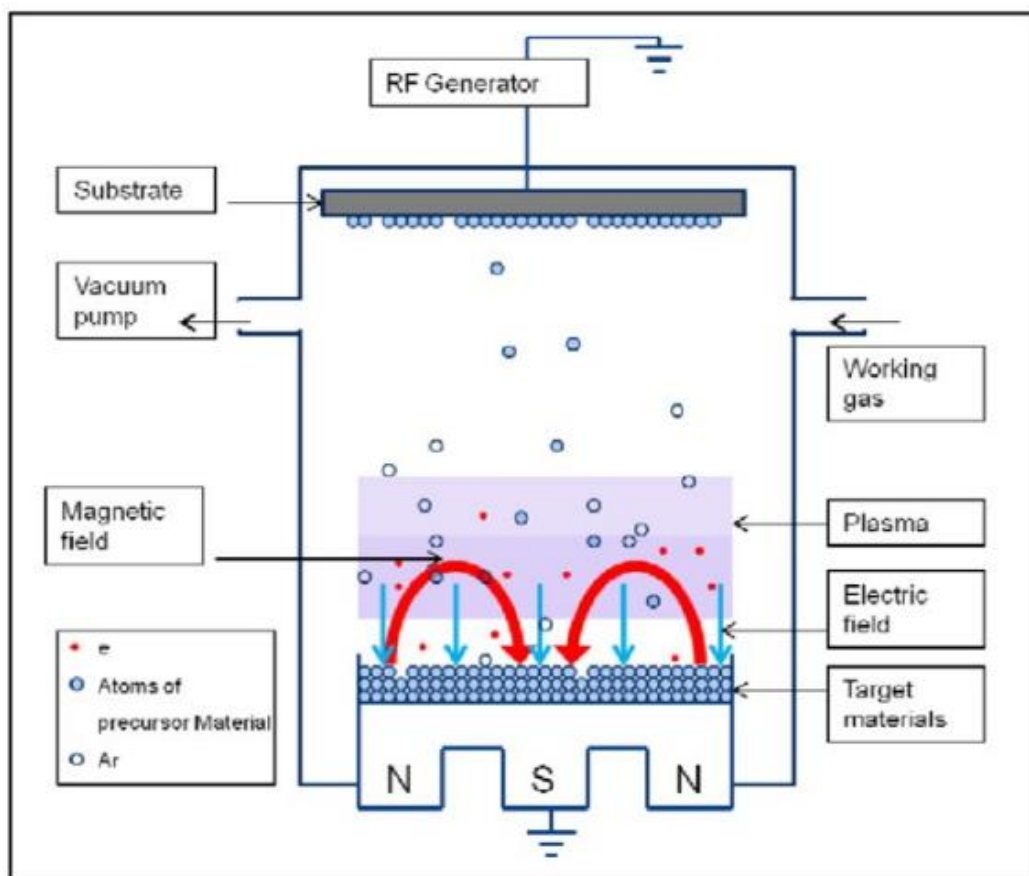


**Figure 2.4** Schematic representation of magnetron sputtering (Bosco et al. 2012).

Magnetron sputtering, cathodic arc, plasma enhanced chemical vapour deposition (PECVD), large area filtered arc deposition (LAFAD) were some of the methods used for coating cutting tools. PVD techniques like magnetron sputtering, cathodic arc and LAFAD were more advantageous over CVD as they avoided precursor gases that are

not suitable with corrosion, fire and environmental hazards (Veprek and Jilek 2002; Veprek and Reiprich 1995). Magnetron sputtering has better adhesion and tribological properties compared to cathodic arc deposition (CAD). The later also forms macro-droplets which increases the surface roughness of coatings (Sanchette et al. 2011). The first commercial coating was a titanium nitride (TiN) based physical vapour deposition (PVD) coating developed for high-speed steel drills (Inspektor and Salvador 2014). The conventional nitride coatings could not meet the demands of dry cutting technology. It is desirable for coatings to have high hardness, low friction and high-temperature oxidation resistance (Ma et al. 2016). Nano composite coatings of MoN/CrN, TiSiN, and TiAlSiN were some of the alternatives due to their extensive mechanical properties. It is found that the addition of Al & Si into TiN coatings can enhance the mechanical properties of titanium nitride coatings (Veprek et al. 2010). TiAlSiN and TiSiN coatings are not only good in mechanical properties but also exhibited low thermal conductivity which is desirable for dry machining.

#### **2.4.5 Titanium-based coatings**

TiAlSiN coatings have drawn attention from many researchers because of their high hardness, adhesion strength and better oxidation resistance at high temperatures (Ma et al. 2017). According to Fuentes et al. (2010), TiAlSiN coating consists of (Ti,Al,Si)N where aluminium and silicon replace titanium atoms in an fcc crystalline lattice, depending on the stoichiometry. It is reported that TiAlSiN coating consisted of nano-crystalline TiAlN phase and amorphous Si<sub>3</sub>N<sub>4</sub> phase, where former is wrapped in later (Veprek and Reiprich 1995). The microstructure of coating is completely dependent on the concentration of each element present and addition of Si to TiAlN has clearly resulted in the refinement of grains and increase in hardness as reported by some of the researchers (She-quan et al. 2011; Wang et al. 2010). The researchers also reported that an increase in Al content decreased grain size and increased thermal stability and oxidation resistance (Chen et al. 2009). The Ti atoms in TiN lattice is replaced by Al atoms and resulted in more lattice distortion and residual stress in the coatings. TiSiN coatings also possess excellent properties as that of TiAlSiN coatings for cutting tool applications. The formation of dense SiO<sub>2</sub> tribo



layer improves the oxidation resistance of TiSiN coatings at high temperature (Cheng et al. 2009). The microstructure of TiSiN is also similar to TiAlSiN coating, consisting of nano-crystalline TiN phase and amorphous Si<sub>3</sub>N<sub>4</sub> phase. TiSiN and TiAlSiN coatings are some of the widely used tribological coatings for cutting tool applications especially high-speed machining under dry environment. Bouzakis et al. (2009) and Chen et al. (2009) reported a decrease in milling performance of TiSiN coating due to high stress and weak adhesive bonding between substrate and coating.

## **2.5 SUSTAINABLE MACHINING**

Sustainability refers to maintaining natural resources and environmental quality for future generations. The production of sustainable products without affecting the environment is defined as sustainable manufacturing (Najiha et al. 2016). The sustainable manufacturing is not only giving importance to occupational safety, personal health issues and environmental problems but also sustainable components such as environment, economy and society are also given prime importance which makes sustainable manufacturing more global and general as compared to green & eco- manufacturing. The products manufactured from sustainable manufacturing shows compatibility with the environment throughout their life cycle.

According to studies, 640 million gallons of metal working fluids is globally consumed per year. It is estimated that cutting fluid cost accounts for 15% of the total manufacturing cost. It is inferred from studies that purchase and recycling of cutting fluids accounts up to two times machining cost and it rises up to 17% of a component cost in the automotive industry (Ezugwu 2005; Xavier and Adithan 2009). According to the reports, more than a million workers worldwide get affected by working with hazardous cutting fluids (Najiha et al. 2016). The employ of cutting fluids in machining processes such as drilling, boring, milling, hoping, and grinding tends to produce hazardous elements such as aerosol particles or mist can risk different human organs such as skin, pancreas, rectum, scrotum, larynx, and bladder. All these necessitated researchers to find ways to reduce total expenditures spent on buying, recycling, and discard of cutting fluids thereby meeting all safety standards. The conventional cutting fluids are also inadequate in reducing the high cutting

temperature by penetrating effectively into tool–chip interface when machining advanced engineering materials. All this paved way for developing advanced cooling techniques which can meet the industry needs as well as the environmental issues. Minimum quantity lubrication is a cooling technique which makes use of mist coolant where compressed air mixed with oil droplets is supplied into tool–chip interface (Liao and Lin 2007; Rahman et al. 2001). But mist cooling also possesses serious threats as similar to as conventional coolants such as respiratory issues, eye irritation, difficulty in breathing, and air contamination (Ravi and Kumar 2011). Thus a need for sustainable and green machining is essential for a great future.

Cryogenics is the study and use of gases at very low temperature, below  $-150^{\circ}\text{C}$ . There are permanent gases like nitrogen, oxygen, neon, hydrogen, helium whose boiling point lies below  $-180^{\circ}\text{C}$ . Aerospace, manufacturing, electronics & Medical are some of the areas which make use of cryogenics mainly for cooling purposes (Yildiz and Nalbant 2008). Liquid nitrogen is the most preferred cryogenic element as nitrogen is the most abundant gas and comprises around 78% of the volume of the atmosphere. It's colourless, odourless & non-toxic properties strengthens its value among other cryogenics. The fractional distillation process is used for commercial production of liquid nitrogen. It was in 1919, the use of cryogen as a cutting fluid is reported in which carbon dioxide is used as a coolant in cutting operations (Jawahir et al. 2016). The introduction of cryogen as a coolant into cutting process to change material properties and to dissipate heat generated at the cutting zone is known as cryogenic machining. The use of liquid nitrogen coolant is one of the emerging sustainable manufacturing processes that utilize the fluids at extremely low temperatures in the machining process (Pusavec et al. 2016).

Cryogenic machining can be classified into four groups according to the application. Cryogenic pre-cooling of the workpiece, indirect cryogenic cooling or cryogenic tool back cooling, cryogenic jet cooling and cryogenic treatment of cutting tools (Yildiz and Nalbant 2008). Cryogenic precooling refers to the cooling of the workpiece before machining to change material properties from ductile to brittle. The breaking of chips become easier during machining when made brittle, thus increasing productivity & performance. The cryogenic enclosed bath was used to freeze

workpiece material by two methods, first by dipping test rod in liquid nitrogen and the second method by pouring liquid nitrogen continuously onto the workpiece. Ding and Hong (1998) reported the significant improvement in chip breaking of AISI 1008 low carbon steel with cryogenic pre-cooling.

The heat produced in the cutting zone is the main reason for major or minor problems encountered in machining. The main objective of using cutting fluid is to increase tool life by reducing tool wear using cooling and lubrication of tool-chip interface. The cutting fluids help in minimizing tool wear by reducing galling, adhesion and welding. It also helps in flushing away chips, debris & residues (Marksberry and Jawahir 2008). But the use of conventional cutting fluids results in environmental hazards, industrial pollution and safety of operators. The cryogenic cooling using liquid nitrogen is one of the eco-friendly and sustainable cooling approaches which improves productivity, surface integrity and tool life, and reduce machining cost to a large extent (Dhananchezian et al. 2011; Yildiz and Nalbant 2008). Most of the researches showed that cryogenic cooling improved machining performance of materials during turning, milling, drilling, and even from non-conventional material removal processes ( Kheireddine et al. 2015; Manivannan and Kumar 2017; Shokrani et al. 2016b; Xia et al. 2016). Dix et al. (2014) found that cryogenic cooling reduce cutting temperature and tool wear compared to dry machining with the help of finite element analysis. Shokrani et al. (2016) performed a feasibility study on cryogenic cooling in the end milling of Ti-6Al-4V alloy and found cryogenic machining as the optimum machining compared to dry and flood cooling. The results showed that cryogenic cooling reduced the surface roughness by 30% and 40% compared to dry and flood cooling. Sivaiah and Chakradhar (2017b) studied the machinability characteristics of 17-4 PH stainless steel under dry, wet, MQL, and cryogenic conditions and reported the maximum flank wear reduction for cryogenic cooling to be 40 %, 31 %, and 23 % compared to dry, wet, and MQL environment respectively. Furthermore, it is found that cryogenic cooling produced favourable chip forms with less residual at all cutting speeds and improved chip breakability compared with other environments. Ravi and Kumar (2012) found the cutting temperature in cryogenic cooling during the end milling of AISI D3 tool steel which reduced by 43–48 % and

26–35 % over dry and wet cooling, respectively. Kalyan and Choudhury (2008) investigated the cutting forces and tool wear developed during cryogenic high-speed machining of stainless steel and found a reduction of 37.39 % in flank wear compared to dry machining. The main findings from recent works show that cryogenic cooling can be effectively used to reduce the cutting temperature at machining zone, improve surface finish, reduce cutting forces, and tool wear without any threat to the operator and environment (Ahmed and Kumar 2016; Ahmed and Kumar 2017; Govindaraju et al. 2014; Sivaiah and Chakradhar 2017a). In contrary to the observations by the researchers suggesting cryogenic cooling improved the machinability, there are few researchers who concluded with no improvement in machinability. A study by Munoz et al. (2014); Nalbant and Yildiz (2011) have suggested that cryogenic machining has no advantage over dry machining of AISI 304. Govindaraju et al. (2014) carried drilling experiments on AISI 1045 steel under liquid nitrogen and reported that at lower feed rates thrust force is found to be increasing by 6–51 % and decreasing at higher feed rates by 4–8 %. Most of studies carried out on cryogenic cooling were on turning or single point cutting, as the cutting under milling varies completely from single point cutting and needs to be studied in detail. There is a strong need to study machinability of maraging steel using sustainable machining techniques such as cryogenic machining in this era of green manufacturing Braham et al. (2015); Dhananchezian et al. (2011). The liquid nitrogen at  $-196^{\circ}\text{C}$  is sprayed in cutting zone which can penetrate into interface between tool-workpiece and tool- chip thereby reducing built-up edge (BUE) formation, adhesion of chip particles and other defects (Dhar et al. 2006a; Huang et al. 2014; Kaynak 2014; Ravi and Kumar 2012; Shokrani et al. 2013).

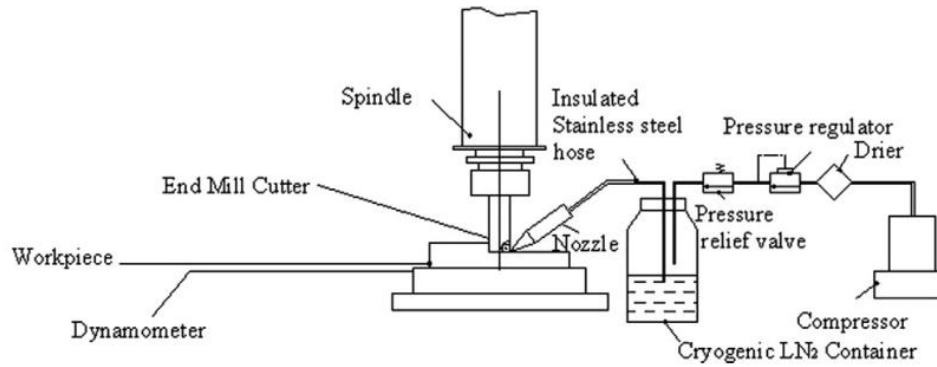


**Figure 2.5** Schematic of cryogenic milling setup (Ravi and Kumar 2012).

The use of cutting fluids in machining is one of the strategies to reduce the heat generated due to friction between tool, chip, and workpiece. Thus coated tool along with the use of cutting fluid can minimize the tool wear and extend the life of the cutting tool. But some of the conventional fluids are not much effective in removing the heat during high-speed machining of advanced engineering materials. Also considering the environmental hazards, operator safety, recycling, and the disposal issues, the use of conventional cutting fluids should be minimized. The cryogenic coolants like liquid nitrogen, helium and carbon dioxide are a good alternative to the conventional cutting fluids in terms of a sustainable future. The liquid nitrogen is most commonly used as nitrogen is abundant in the atmosphere and causes a rapid reduction in cutting temperature and evaporates into the atmosphere within minutes. The cryogenic cooling is well employed in metal cutting processes like turning, milling, drilling, grinding and finishing processes like burnishing,  $\mu$ EDM etc (Govindaraju et al. 2014; Manivannan and Kumar 2017; Sachin et al. 2018; Sivaiah and Chakradhar 2017c). Kalyan Kumar and Choudhury (2008) studied the effect of cryogenic cooling on tool wear and cutting forces generated during high-speed machining of stainless steel under dry and cryogenic environment. It is observed that flank wear reduced up to 37.39% followed by the reduction of cutting temperature and cutting force. Shokrani et al. (2016a) investigated the effect of cryogenic cooling on surface integrity characteristics of Ti-6Al-4V titanium alloy during end milling. They found that cryogenic cooling reduced surface roughness by 39% and 31% compared to dry and flood cooling. The microscopic surface defects reduced and

surface integrity improved under cryogenic cooling. Ravi and Kumar (2012) investigated the influence of cryogenic cooling in the milling of AISI D3 tool steel. They found that cutting force and the cutting temperature reduced under cryogenic cooling compared to dry and wet cooling.

## **2.6 SUMMARY OF LITERATURE REVIEW**

The literature review highlights the importance of cryogenic treatment in improving the life of the cutting tool. However, the effect of soaking period on cryogenic treatment and responses such as tool wear, surface roughness, cutting force and tool life need to be studied (Mukkoti et al. 2018). The soaking period of cryogenic treatment decides the transformation of austenite to martensite, new carbide formation and distribution of carbides (Bensely et al. 2007; Gill et al. 2012b). The optimisation of soaking period and machining parameters is essential to achieve best out of cryogenic treatment (Baldissera and Delprete 2008). The mechanisms which result in the improvement of properties during cryogenic treatment are still not quantified.

Even though the literature review reveals that the performance of cryogenically treated inserts increases after cryogenic treatment. The performance diminishes during high cutting speeds, especially during continuous machining due to high tool-chip interface temperature.

The high wear resistance and thermally stable behaviour of coated tools at high temperatures help to improve the tool life of the cutting tool. The use of coated tools helps in improving the productivity and surface quality during machining of hard materials like maraging steel. The dry and cryogenic machining is considered as the future of the sustainable machining process as the conventional cutting fluids are causing a lot of problems in recycling, disposal, operator safety and environmental pollution. The cutting temperature as a result of dry machining is very high. The need for coatings to withstand the high cutting temperature is a challenge faced by cutting tool manufacturers.

Although mechanical properties and characteristics of coatings are well studied, the wear characteristics are still not clear due to the complex wear behaviour of hard

coatings. An attempt has been made to study the characteristics of TiSiN and TiAlSiN coatings during end milling of maraging steel under dry and wet environments. Milling is a cutting process in which coatings require high adhesive strength and wear resistance as cutting force and thermal stresses are very high. Most of the researchers have studied the microstructure and mechanical properties of the coatings giving less importance to machining aspects. This research not only deals with characteristics of the coatings but also the mechanical behaviour during end milling of maraging steel under dry, wet and cryogenic environment.

Most of the studies carried out on cryogenic cooling were on turning or single point cutting, as the cutting under milling varies completely from single point cutting and needs to be studied in detail. There is a strong need to study machinability of maraging steel using sustainable machining techniques such as cryogenic machining in this era of green manufacturing.

## **2.7 OBJECTIVES OF PROPOSED WORK**

The objectives of the present investigation are:

1. Study the mechanical and metallurgical behaviour of tungsten carbide-cobalt (WC-Co) milling inserts before and after cryogenic treatment.
2. Study the mechanical and metallurgical behaviour of aluminium based PVD coatings on tungsten carbide-cobalt (WC-Co) milling inserts using cathodic arc deposition technique.
3. Study the mechanical and metallurgical behaviour of titanium based PVD coatings on tungsten carbide-cobalt (WC-Co) milling inserts using magnetron sputtering technique.
4. Milling characteristics studies of PVD coated and cryogenic treated carbide tools under different machining environments (dry, wet and cryogenic).





## CHAPTER 3

### 3 EXPERIMENTAL WORK

This chapter gives details about the materials and experimental setups used for the study. In the present work, MDN 250 maraging steel is used as the workpiece material and cemented carbide inserts (WC-Co) as the cutting tool material. The experimental details considered for cryogenic machining, cryogenic treatment, PVD coating, end milling, characterisation and their procedure is included in this chapter. The milling performance characteristics like surface roughness, cutting force, tool flank wear, and tool life was considered for the study.

#### 3.1 WORK MATERIAL

Maraging steel is a hard material which is widely used in piston rods in heavy vehicles, crankshafts, landing gears, tools and dies and gas turbines where high temperature is encountered (Kosaraju and Chandraker 2015). The hardened maraging steel MDN 250 with dimensions 80 x 55 x 30 mm (5 numbers), forged and annealed is used in this study as work material. The material is procured from Mishra Dhatu Nigam Limited, Hyderabad, India. The chemical composition and mechanical properties of MDN 250 as given by the company are presented in Table 3.1 and Table 3.2. The chemical composition of MDN 250 is analysed using EDS analysis and is presented in Figure 3.1.

**Table 3.1** Chemical composition of MDN 250 maraging steel.

Elements	Ni	Co	Al	Mo	Mn	Ti	Si	C	Fe
Chemical composition (Wt. %)	18.32	8.11	0.11	4.87	0.02	0.44	0.01	0.01	Bal

**Table 3.2** Mechanical properties of MDN 250 maraging steel.

Yield tensile strength (GPa)	Ultimate tensile strength (GPa)	Young's modulus (GPa)	Hardness (HRC)	Thermal conductivity (W/mK)	Coefficient of thermal expansion	Melting point (°C)
1.776	1.844	210	50	25.5	$11.3 \times 10^{-6}$	1413

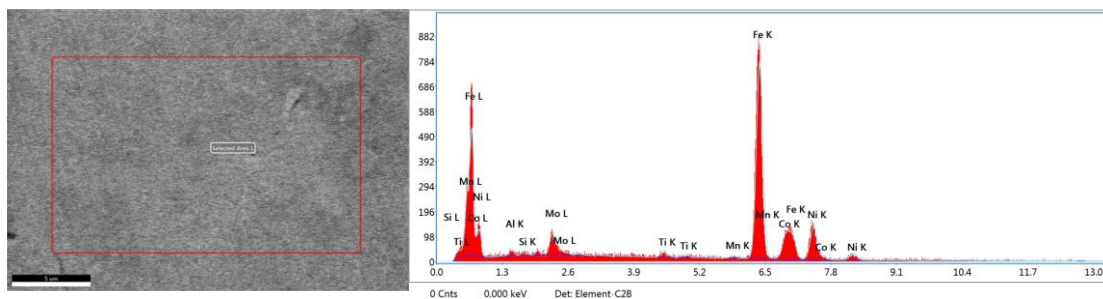


**Figure 3.1** EDS analysis of maraging steel.

### 3.2 CUTTING TOOL MATERIAL

A two flute cutting tool of 20 mm diameter (Seco R217.69-2020.3-10-2A) and uncoated cemented carbide insert ((XOEX10T331FR-E05 H15) supplied by Seco Tools India Pvt. Ltd. is used in the experiment. Figure 3.2 presents the image of a cutting tool used in the experiment. The composition of W, C and Co in WC-Co alloy is found to be 80 %, 10 % and 10 % respectively as obtained from the EDS analysis. Figure 3.3 presents the microstructure and EDS analysis of WC-Co cutting inserts. A detailed specification of the cutting tool used in the experiments is presented in Table 3.3. The H15 uncoated inserts are further used for cryogenic treatment and a PVD coating.

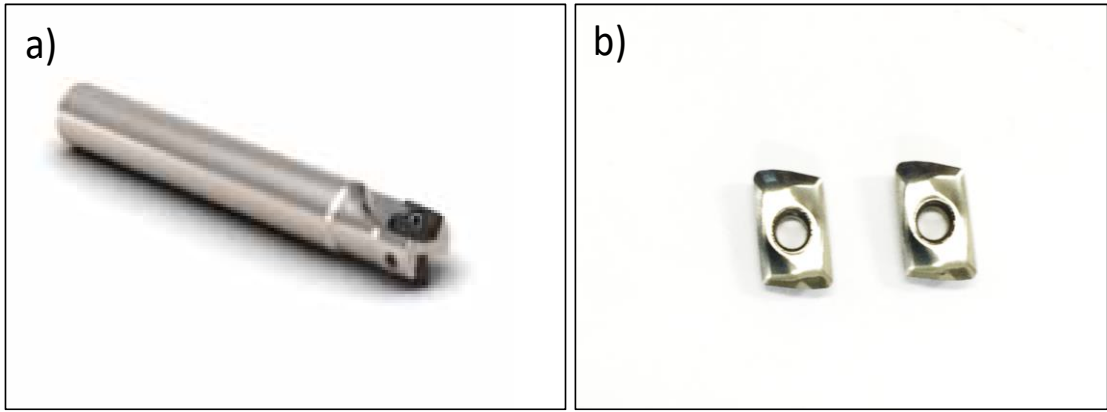


**Figure 3.2** Cutting tools used for end milling of MDN 250 maraging steel a) tool holder b) H15 uncoated WC-Co inserts.

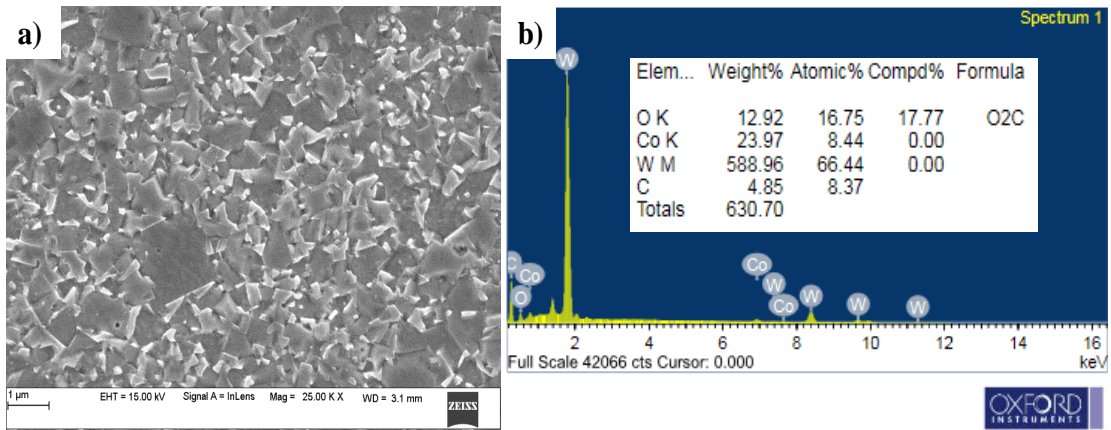


**Figure 3.3** Microstructure and chemical composition analysis of WC-Co cutting inserts using SEM/EDS a) Microstructure b) EDS analysis.

**Table 3.3** Specification of the cutting tool used in the experiment.

<b>Description</b>	<b>Value</b>
Cutting tool	R217.69-2020.3-10-2A
Tool overhang	40 mm
Diameter of cutter	20 mm
Cutting insert	XOEX10T331FR-E05 H15
Cutting edge count	2
Clearance angle	15 degree
Cutting edge effective length	9.7 mm
Corner radius	3.1 mm
Insert thickness	3.8 mm

### **3.3 CRYOGENIC TREATMENT OF CUTTING TOOLS**

The cryogenic treatment of uncoated cemented carbide inserts (WC-Co) is carried out at MIPL cryogenic division Ltd., India. The schematic of cryogenic treatment is presented in Figure 3.4. The cryogenic treatment used is a well monitored and controlled process in which liquid nitrogen is converted into gas using an atomiser and flood into the closed cryogenic chamber. The cryogenic chamber is computer controlled that works in synchronized with an atomiser. The continuous monitoring of inputs and controlled flow of the atomised liquid nitrogen into the chamber regulates the temperature at a specific cooling rate. The precise program control takes the cryogenic cycle through three phases of cooling, soaking and heating. The controlled heating & cooling rate helped to avoid thermal shocks. The temperature of cutting inserts is gradually lowered from room temperature to cryogenic temperature of  $-196$

°C at the rate of 2.5 °C/min and held at  $-196$  °C for 18 hours (CT-18), 24 hours (CT-24) and 32 hours (CT-32) respectively. The temperature is subsequently brought back from the cryogenic temperature of  $-196$  °C to room temperature by controlled heating at a rate of 1.5 °C/min. A tempering process is followed by cryogenic treatment at a temperature of  $150$  °C for 2 h. The time-temperature graph of a cryogenic treatment cycle is demonstrated in Figure 3.5.

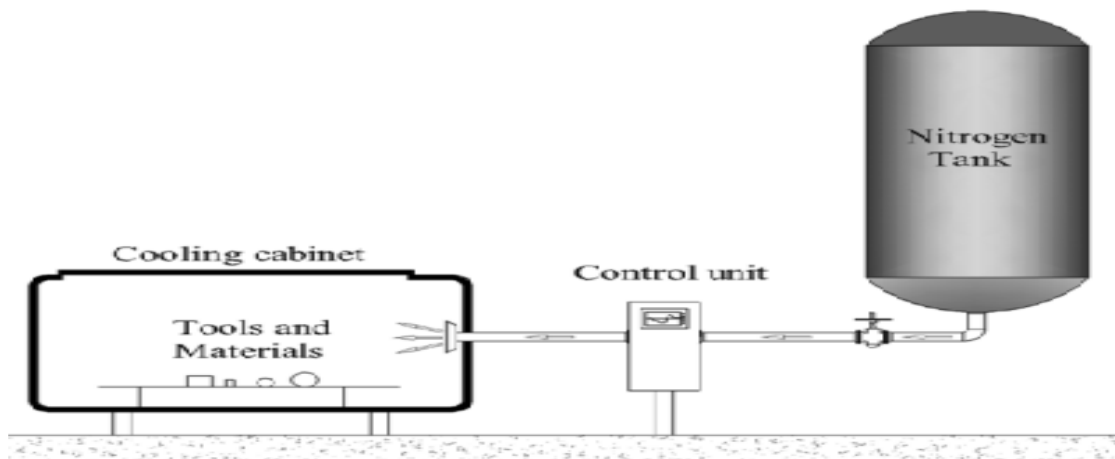


**Figure 3.4** Schematic of cryogenic treatment (Akıncıoğlu et al. 2016).

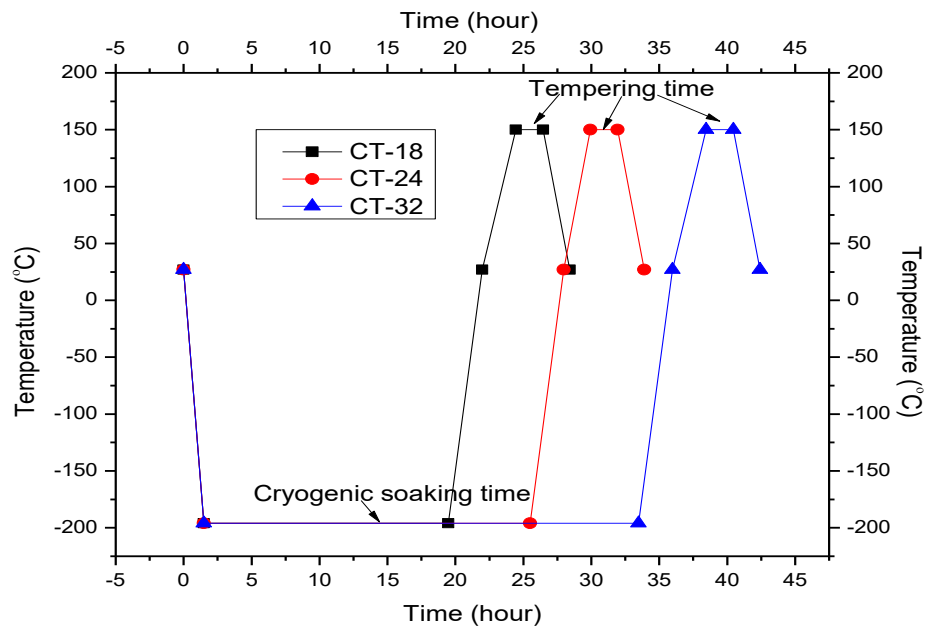


**Figure 3.5** Time temperature graph of cryogenic treatment.

### 3.4 PVD COATING OF CUTTING TOOL USING CATHODIC ARC DEPOSITION (CAD)

The AlCrN and AlTiN coatings were synthesized using cathodic arc deposition technique (CAD) by Oerlikon Balzers, Pvt. Ltd., India. The cutting inserts used for coating is H15 tungsten carbide-cobalt inserts from Seco Tools Pvt. Ltd., India. The schematic of cathodic arc deposition is shown in Figure 3.6. The electric arc generates a molten pool of target which reacts with reactive gases in the vacuum chamber and gets transported to the substrate. While transporting, some of the atoms can be ionized by creating the plasma in the place. This high-density plasma increases the adhesion of the coating and forms a uniform and homogenous coating with fewer voids and defects.

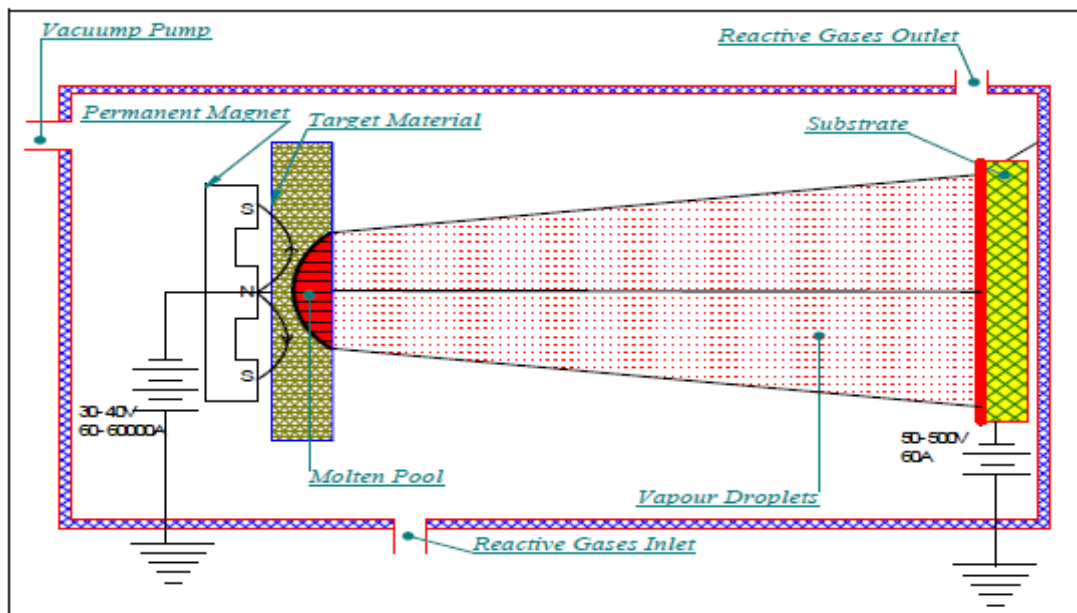


**Figure 3.6** Schematic of cathodic arc deposition (courtesy: Bangalore Plasmatek Pvt. Ltd, India).

### 3.5 PVD COATING OF CUTTING TOOL USING MAGNETRON SPUTTERING (MS)

A commercially available tungsten carbide inserts (H15) purchased from Seco India Ltd is used for the coating process. Samples were ultrasonically cleaned using

isopropyl alcohol (IPA) for 15 minutes at ambient temperature. The sample was placed in the sputtering unit mounted to an aluminium holder rotating at a speed of 20 rpm. The magnetron sputtering unit used is supplied by V.R. Technologies, Bangalore. The chamber was evacuated to a base pressure of about  $1.0 \times 10^{-3}$  Pa. The target alloys of TiSi (80/20 at. %) and TiAlSi (54/36/10 at. %) is procured from Plansee Composite Materials GmbH, Germany. High purity argon gas was supplied to the chamber at a flow rate of 30 sccm to achieve a chamber pressure of 0.6 Pa. The pre-sputtering was carried out for 20 minutes keeping the bias voltage and current at 433V and 0.21 A. The nitrogen partial pressure was subsequently adjusted to 3.35 Pa and a flow rate of 16 sccm. The argon gas pressure was reduced to 20 sccm. The deposition time of TiSiN and TiAlSiN coatings was 120 minutes and 150 minutes. Figure 3.7 shows the experimental setup for magnetron sputtering of coatings.

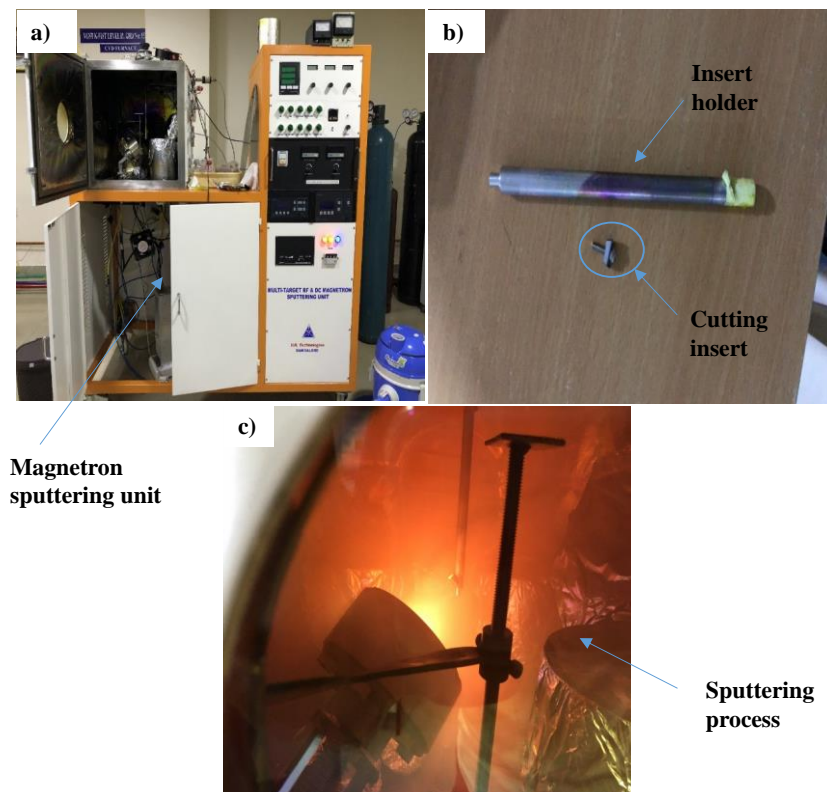


**Figure 3.7** Experimental set up for magnetron sputtering of coatings a) Magnetron sputtering machine b) Sample holder & cutting inserts for coating c) vacuum chamber during the sputtering process.

## 3.6 DIFFERENT MACHINING ENVIRONMENTS USED IN THE EXPERIMENTS

Dry, wet and cryogenic are some of the machining environments used in the experiments.

### 3.6.1 Cryogenic machining

Liquid nitrogen at  $-195.8^{\circ}\text{C}$  is used as the cryogenic coolant for machining. The schematic of the cryogenic machining is shown in Figure 3.8. A 55-litre dewar procured from IOCL, India is used for storing liquid nitrogen ( $\text{LN}_2$ ), a pressure of 2 bar is applied to the dewar using an air compressor and is sprayed into the tool-chip interface. The insulated stainless steel hose and a 1 mm diameter nozzle are used to spray  $\text{LN}_2$  into the cutting zone. A nozzle distance of 30 mm is maintained to avoid the direct contact of  $\text{LN}_2$  and workpiece. The liquid nitrogen is purchased from Mangalore Chemicals and Fertilizers (MCF), Ltd., India.

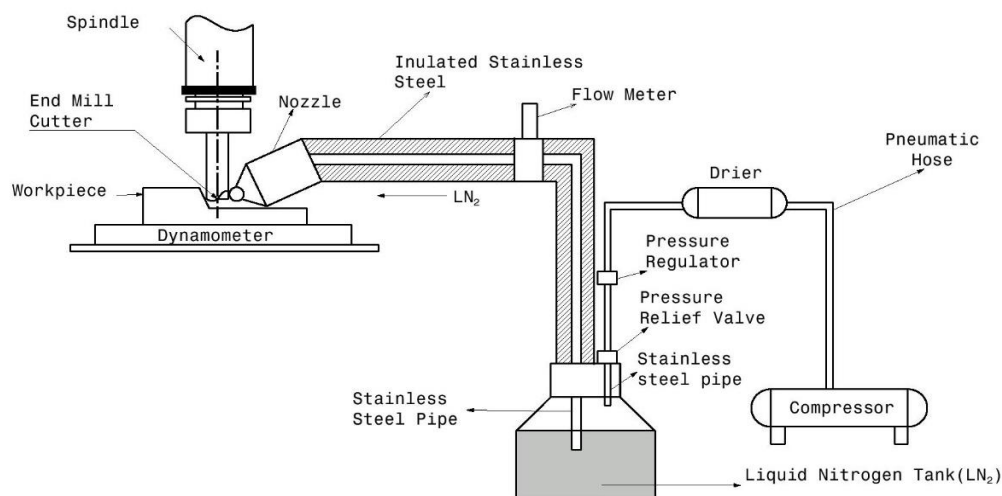


**Figure 3.8** Schematic of Cryogenic machining.

The cryogenic cooling system consists of the following components namely ‘TA55’ model dewar, compressor, modified stainless steel cap, flow regulator, pneumatic hose, pressure relief valve, braided stainless steel hose, and nozzle. Modified stainless steel cap was fabricated to close the dewar at the top as shown in Figure 3.9. The



modified cap design consists of two holes at the top of the cap and inserted two stainless steel pipes of the same diameter of 8 mm in those two holes respectively. Among two stainless steel pipes, one is used to supply the compressed air into the dewar with the help of pneumatic hose and other is for LN<sub>2</sub> outlet. A flexible braided stainless steel was used to transfer the LN<sub>2</sub> from the liquid nitrogen outlet from the dewar to machining zone with the help of a nozzle. A pressure relief valve is connected to the outlet pipe of the dewar, this can avoid the excessive pressure inside the tank. A flow regulator valve is used to control the flow rate. Figure 3.10 presents the experimental setup used for cryogenic machining.

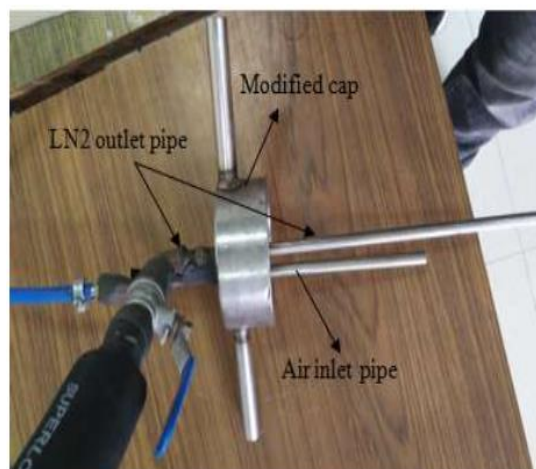


**Figure 3.9** Modified stainless steel cap for the dewar.

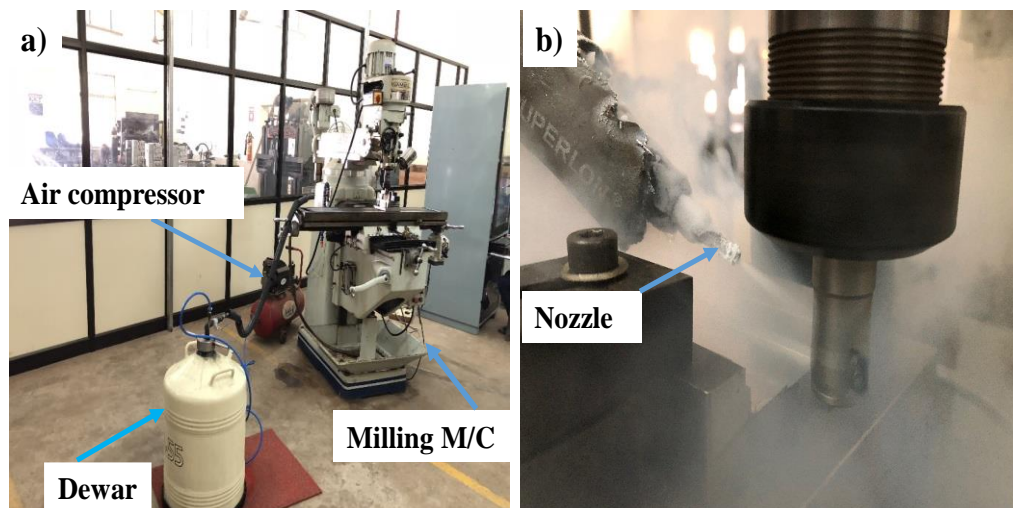


**Figure 3.10** Experimental setup for cryogenic machining a) Milling machine & cryogenic setup b) Machining zone during cryogenic machining.

### 3.6.2 Dry and wet machining

The machining carried out without using any coolant is called dry machining. Figure 3.11 a) presents the experimental setup for dry machining.

An emulsion type cutting fluid obtained by mixing soluble oil with water at a ratio of 1:20 is used as the wet coolant. A predetermined flow rate of 4.2 L/min is used for flooding the machining zone. Figure 3.11 b) presents the wet machining setup used for the machining.

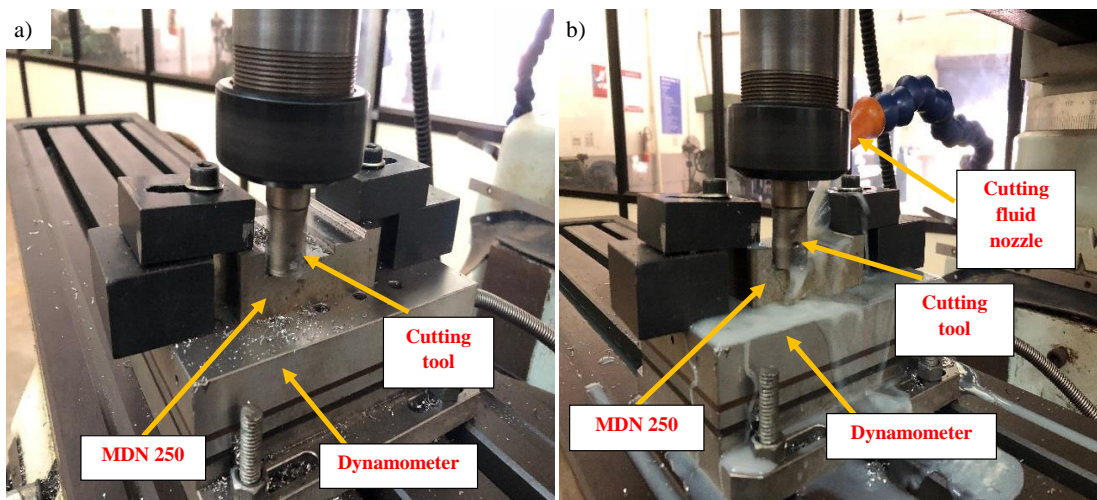


**Figure 3.11** Experimental setup for a) dry machining b) wet machining.

### 3.7 MILLING MACHINE

A conventional three-axis vertical milling machine (Nammill X6325) is used for milling experiments on maraging steel MDN 250. The specifications of the milling machine are presented in Table 3.4. The milling machine used in the experiment is displayed in Figure 3.10 a).

**Table 3.4** Specifications of milling machine.

<b>Description</b>	<b>Specification</b>
Machine	Vertical Milling Machine
Model	NAMMILL XL 6035
Table Area	1320 x 320mm <sup>2</sup>
Feed rate	15-750mm/min
Rapid traverse	2250mm/min
Spindle speed	30-1500 rpm
Spindle power	7.5kW
Spindle taper	ISO 50
Net weight	3200 kg (approx.)

### **3.8 MACHINING PERFORMANCE CHARACTERISTICS**

The performance characteristics during experiments are analysed using different techniques and are as follows:

#### **3.8.1 Cutting Force**

A quartz three component dynamometer Kistler 9257B is used for measuring cutting forces in three different directions. The dynamometer is mounted to machining bed and workpiece is kept on the top of dynamometer as seen in Figure 3.12. The dynamometer is equipped with a 5070A charge amplifier which is connected to the computer with A2D Board and is controlled by Kistler 2825 Dynoware software. The

cutting force along the three cutting directions is obtained. The resultant cutting force is used for the analysis of cutting force results and is expressed as:

$$F_R = \sqrt{F_x^2 + F_y^2 + F_z^2}$$

where  $F_R$  represents resultant cutting force,  $F_x$  is the feed force,  $F_y$  is the normal force and  $F_z$  is the axial force.

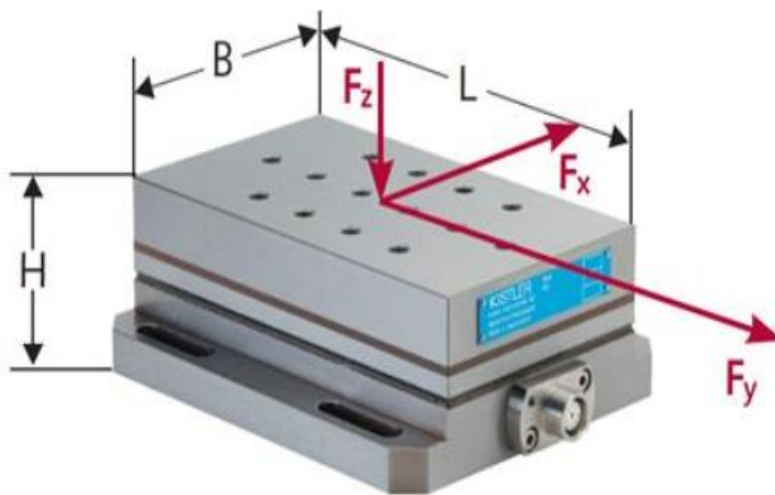


**Figure 3.12** Kistler 9257B dynamometer used for cutting force measurement.

### 3.8.2 Surface Roughness

The Mitutoyo Surftest SJ 301 was employed in measuring the surface roughness of the machined surface. The cut-off length used was 4 mm, and average surface roughness (Ra) was measured at six different locations for each trial. Average surface roughness (Ra) is considered for roughness measurement, other methods are: Rz ten points mean roughness, and Rt is the maximum height of the surface profile measured according to ISO Standard 468:1982. Figure 3.13 presents the surface roughness tester used in the experiments.

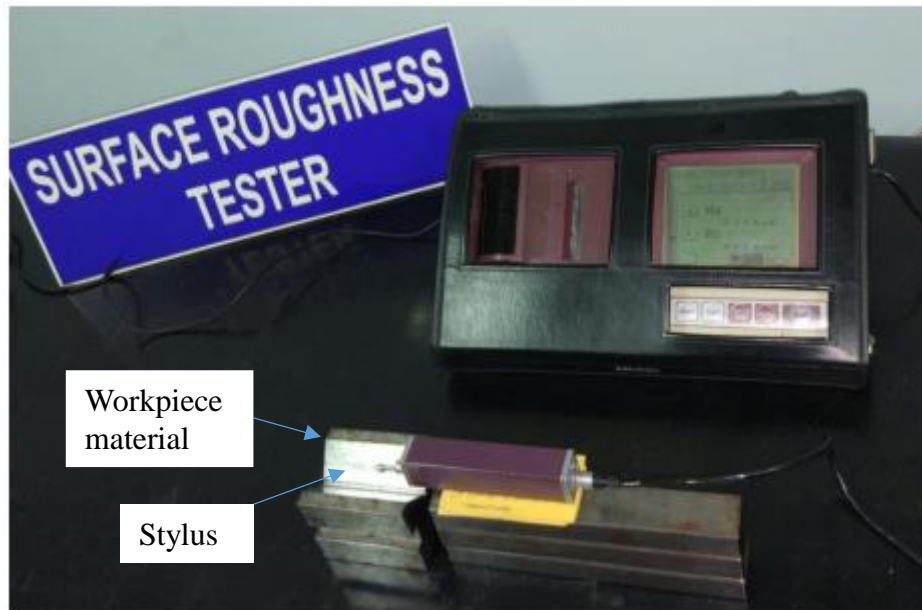


**Figure 3.13** Surface roughness tester (Mitutoyo SJ 301) used in the experiment.

### 3.8.3 Tool wear

The tool wear of cutting insert after machining is observed using a “Zeiss AXIOLAB A1” optical microscope. Figure 3.14 presents the image of an optical microscope used in the experiment. The width of flank wear is measured at an interval of 4 passes (5 min) using the optical microscope.



**Figure 3.14** Optical microscope used in the experiment.

### **3.9 CHARACTERISATION OF CUTTING TOOL**

Characteristics of coatings & cryogenic treated tools are analysed using SEM/EDS, XRD, Nano indentation, microhardness tester, raman spectroscopy etc. The details are as follows.

#### **3.9.1 Microstructure and elemental composition analysis (SEM/EDS)**

A scanning electron microscope is used for analysing the microstructure of coatings and WC-Co inserts. The scanning electron microscope (SEM), JEOL JSM-638OLA is used for the analysis of the microstructure, chemical composition and wear mechanism of the cutting tool. The image analysis software Image J 1.52a is used for measuring the grain size of the cutting tool from SEM images obtained.

The microstructural examination of samples is carried out in accordance with ASTM B 657. The polishing of samples is done using the diamond paste of grade 0.5 $\mu$ m until a mirror finish is obtained. The samples are then dipped in Murakami's reagent for three minutes, flushed in water and dried in acetone. A mixture of 10 g of potassium ferricyanide ( $K_3Fe(CN)_6$ ), 10 g of potassium hydroxide (KOH) and 100 mL of water ( $H_2O$ ) constitute Murakami's reagent. The microstructure is observed both in the optical and scanning electron microscope.

#### **3.9.2 X-ray diffraction (XRD) analysis**

The X-ray diffraction (XRD) is carried out using "Rigaku SmartLab" with Cu  $K\alpha$  ( $\lambda=1.514 \text{ \AA}$ ) radiation at an accelerating voltage of 30 kV and 20 mA for phase changes involved after cryogenic treatment and a PVD coating. The experiments were carried out for  $2\theta$  angle ranging from 20-90°, at a scanning speed of 2°/min. Figure 3.15 shows the image of XRD machine used in the experiment.



**Figure 3.15** XRD machine used in the experiment (Courtesy: CeNSE Lab, IISc, Bangalore).

### **3.9.3 Raman spectroscopy analysis**

RAMAN spectral analysis was carried out on the surface with monochrome laser wavelength 514 nm attached with CCD detector. Raman analysis was carried out for the range of 100-2000 cm. The Raman spectroscopy equipment used in the experiment is LabRam HR.

### **3.9.4 Nano indentation studies**

The Hardness and Young's Modulus of the coatings are measured by using nano-indenter (Microtrac Model: Blue Wave). Figure 3.16 shows the nano-indenter used in the experiment. A peak load of 50 mN is applied for the nanoindentation test to eliminate the effect on measured hardness due to the substrate, by corroborating that resulting pierced depth is within the 10% of coating thickness; around 20 indentations are performed on each sample for ensuring the accuracy of the results. During the nano-indentation, Berkovich indenter is used which is shown in the figure.

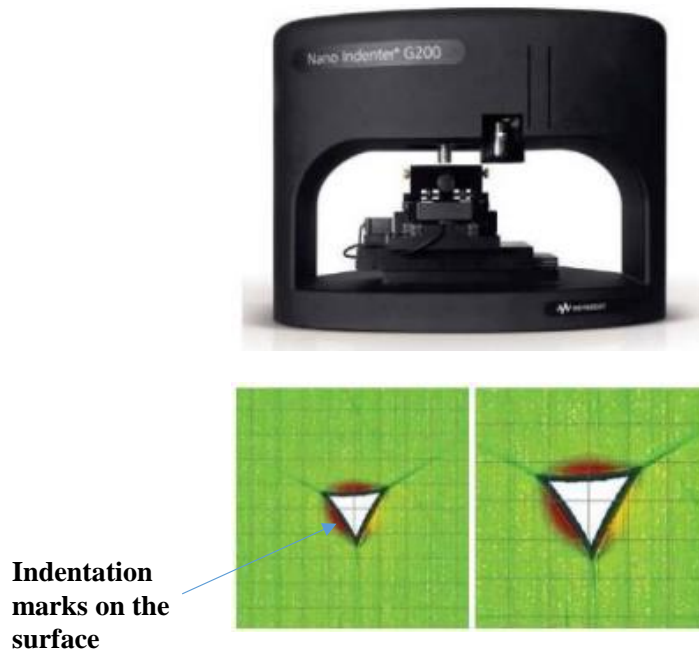


**Figure 3.16** Nano indenter used in the experiment (Courtesy: NMTC, CMTI, Bangalore).

### 3.9.5 Microhardness testing

Vickers microhardness is carried out to find microhardness variation for different cryogenically treated samples and machined samples. A load of 200 g is applied for 20 seconds on each sample and is repeated at 8 different locations for accuracy. Figure 3.17 shows the microhardness tester used in the experiment.



**Figure 3.17** Microhardness tester used in the experiment.



### 3.9.6 Calo tester

Calo tester is used for measuring the coating thickness. The surface was cleaned with IPA solution. Steel ball is run against the surface at 200 rpm for the period of 120-180 seconds with the presence of diamond paste as a lubricant. Wear scar created on the surface after the Calo test is analysed using an optical microscope and coating thickness is calculated with it's in built software. Calo test rig (Figure 3.18) used for the present studies is from Oerlikon Balzers Pvt. Ltd., Bangalore.



**Figure 3.18** Calo tester used for coating thickness measurement (Courtesy: Oerlikon Balzers Pvt. Ltd., India).

### 3.9.7 Confocal microscope

A confocal microscope (Olympus LEXT 4000, Japan) is used for the measurement of surface roughness of the coating. It uses a monochromatic laser to build the 3D profile of the surface. Figure 3.19 shows the confocal microscope used in the experiment.

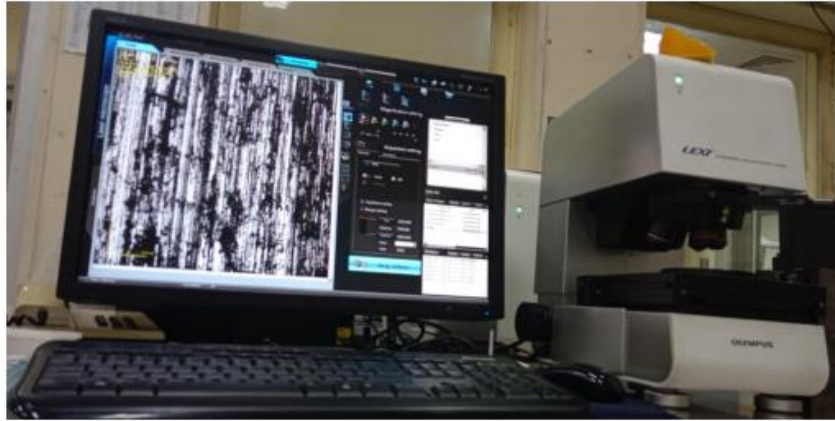


**Figure 3.19** Confocal microscope used for the surface roughness measurement of coatings (Courtesy: NMTC, CMTI, Bangalore).

### **3.9.8 Four- probe apparatus**

A standard four-probe apparatus is used for the measurement of electrical resistivity and conductivity of WC-Co inserts before and after cryogenic treatment. Figure 3.20 presents the four probe apparatus used in the experiment.



**Figure 3.20** Four probe apparatus used in the experiment.

## **3.10 METHODOLOGY**

The methodology followed is shown in Figure 3.21. The experiments have been conducted based on one factor at a time approach (OFATA) approach to know the effect of each process parameter on difference milling performance characteristics. The trial experiments and optimisation results showed spindle speed as the most

influenced parameter. Thus spindle speed is varied keeping feed rate and depth of cut as constant. Table 3.5, presents the experimental design in the experiment.

**Table 3.5** Experimental plan for the experiment.

Expt. No	Spindle speed (rpm)	Feed rate (mm/min)	Depth of cut (mm)
1	540	58	0.3
2	350	58	0.3
3	270	58	0.3

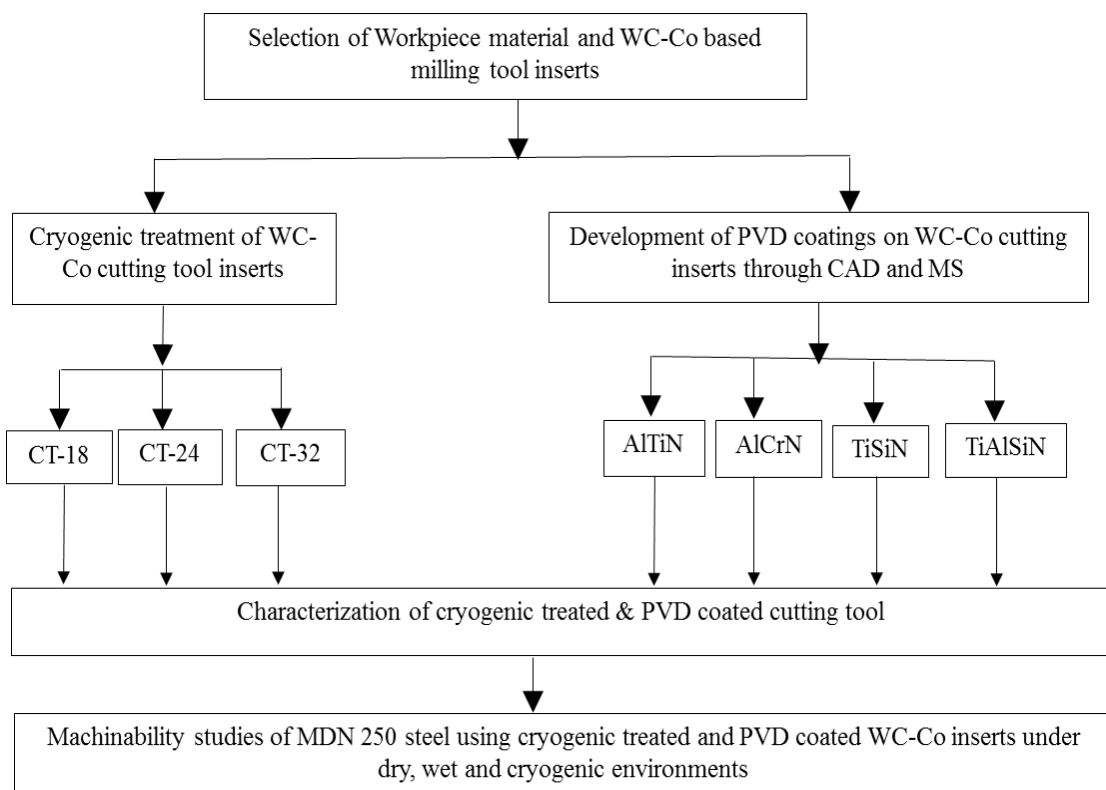


**Figure 3.21** Flow chart of research work.



## CHAPTER 4

### 4 RESULTS AND DISCUSSION

This chapter details about results and discussion during the study. In the present work, MDN 250 maraging steel is used as the workpiece material and cemented carbide inserts (WC-Co) as the cutting tool material. The cryogenic treatment and PVD coating have been carried out on WC-Co inserts. The results and discussion include characterisation of WC-Co inserts before and after cryogenic treatment, characterisation of PVD coatings, analysis of end milling performance like surface roughness, cutting force, tool flank wear, tool life using cryogenic treated & PVD coated tools under dry, wet and cryogenic machining environments.

#### 4.1 CHARACTERISATION OF WC-Co INSERTS BEFORE & AFTER CRYOGENIC TREATMENT

##### 4.1.1 Microstructure & Phase Changes

The SEM images of the cutting tool are shown in Figure 4.1. The microstructure of cemented carbide consists of three phases,  $\alpha$  phase (tungsten carbide) which is called as a ceramic skeleton, soft binder phase  $\beta$  (cobalt), and  $\eta$  phase (multiple carbides of tungsten and at least one metal of the binder). It is seen from microstructure that  $\alpha$  phase forms a continuous structure throughout bulk material. The cryogenic treatment results in the precipitation of fine  $\eta$  carbide particles which act as a filler along with large carbide particle to form a denser, tougher and more coherent structure. The manufacture of cemented carbides involves sintering process which results in the development of residual stress leading to early carbide fracture. The cryogenic treatment relieves these micro stresses permanently which extends the life of the cutting tool. The quantitative EDS area analysis carried out on different cutting tool modes is presented in Table 4.1. Figure 4.2 shows the graph representing the grain size of the different cutting tool. The results reveal that the grain size of inserts reduced as a result of cryogenic treatment. The CT-24 showed a reduction in grain size up to 22 % followed by CT-18 (18.1 %) and CT-32 (9.18 %). The grain size

refinement of  $\alpha$  phase resulted in a more stable form due to the phenomenon of spheroidization (Gill et al. 2012a). The stable form of  $\alpha$  phase has induced a stress-free configuration to the structure thereby improving the wear resistance of the material. The EDS results show that there is carbide precipitation after cryogenic treatment which is inferred from Table 4.1. The cryogenic treatment decrease the formation and size of  $\beta$  phase (Co) particle which is evident from the EDS results. The  $\eta$  phase particle has occupied the voids left by the  $\beta$  phase particle. Bolognini (Polytechnique and Lausanne 2000) proposed deformation behaviour of  $\alpha$  phase and  $\beta$  phase at elevated temperature. Since machining takes place at a higher temperature, it is important to understand the behaviour at high cutting temperature. The  $\beta$  phase (Co binder) content is the determining factor for the deformation behaviour of a different domain. While the  $\beta$  phase content reduces, the chance of failure due to plastic deformation is quite less as WC-Co material is enabled to resist higher cutting temperature. The precipitation of fine  $\eta$  carbide particle and grain size reduction attribute to the increase in microhardness. The toughness of cemented carbide inserts remains unchanged due to tempering followed by cryogenic treatment. The XRD analysis of different cutting tool is represented in Figure 4.3 and if u observe peak between the diffraction angle (two theta)  $30^\circ$  and  $40^\circ$ , we can observe the intensity of  $\eta$  phase ( $\text{Co}_3\text{W}_3\text{C}$  &  $\text{Co}_6\text{W}_6\text{C}$ ) has increased after cryogenic treatment. It is inferred from XRD results that precipitation of  $\eta$  phase in the cryogenically treated inserts would have improved the mechanical properties such as hardness and wear resistance. It is also seen from the plot that the intensity of  $\beta$  phase ( $\text{Co}_2\text{C}$  &  $\text{Co}_3\text{C}$ ) in the cryogenically treated tool has reduced compared to the untreated tool in between the peaks  $60^\circ$  and  $70^\circ$ .

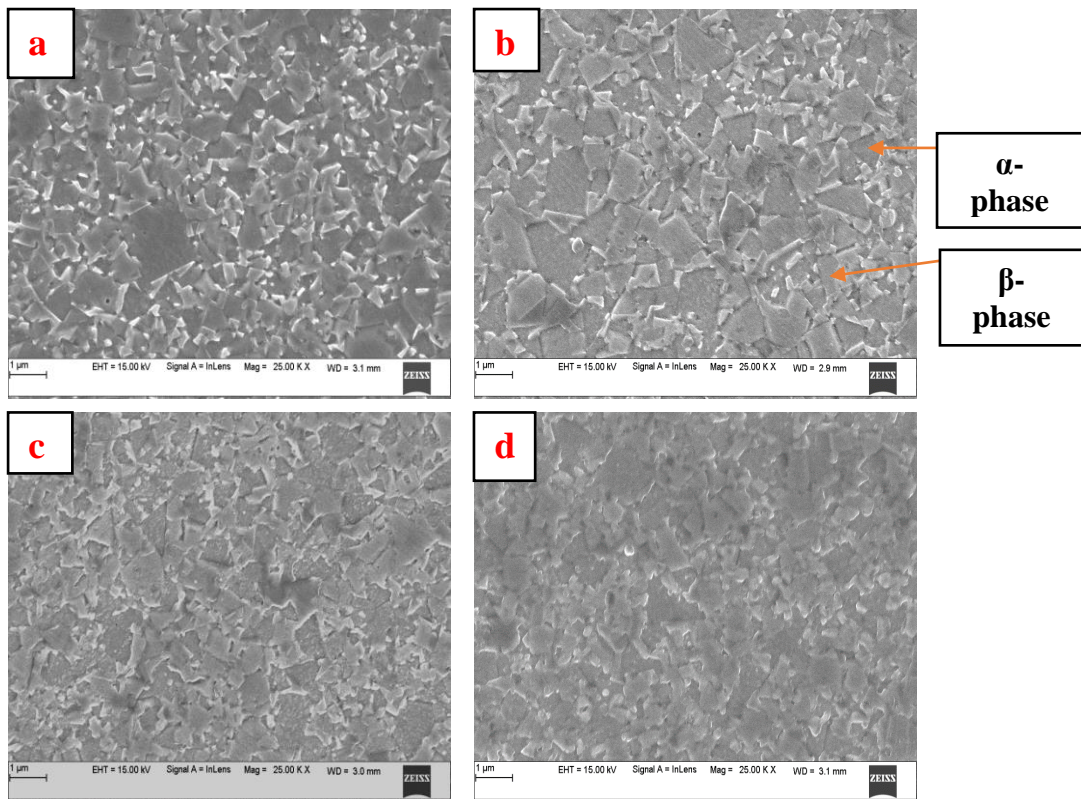


**Figure 4.1** Microstructure of different cutting tool a) UT b) CT-18 c) CT-24 d) CT-32

**Table 4.1** EDS area analysis of four tool modes depicted in Figure 4.2.

<b>Designation</b>	<b>W (At. %)</b>	<b>C (At. %)</b>	<b>Co (At. %)</b>
UT	79.98	9.94	10.07
CT-18	72.25	20.37	7.38
CT-24	67.65	24.61	7.75
CT-32	76.41	14.56	9.03

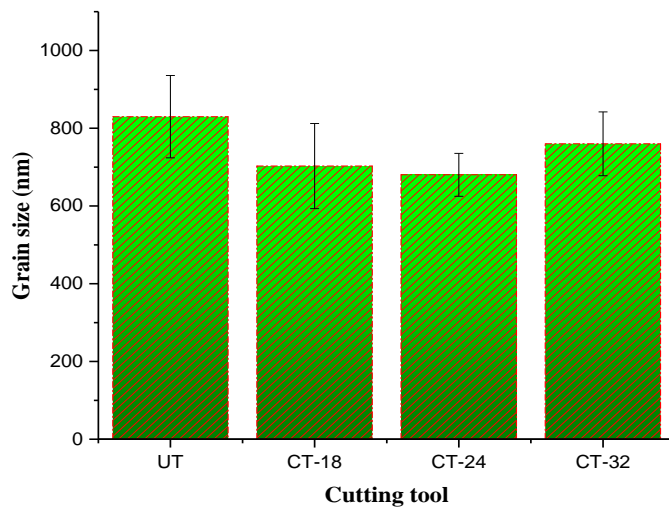


**Figure 4.2** Grain size of the different cutting tool.

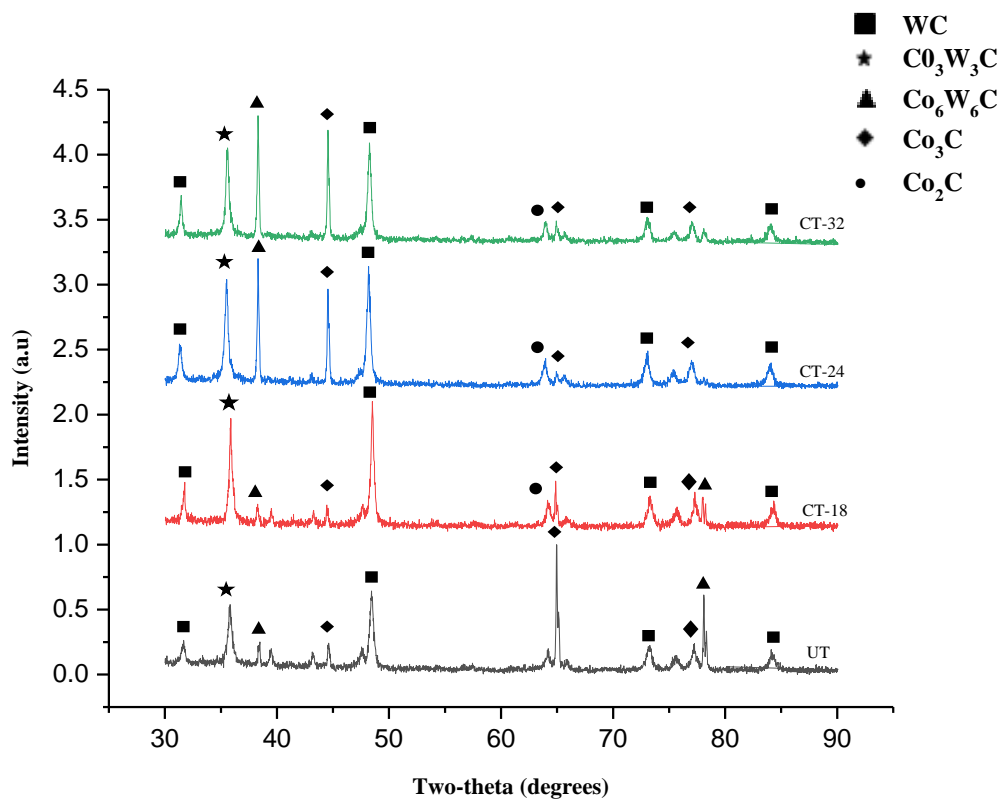


**Figure 4.3** XRD analysis of cutting tool under different conditions.



### 4.1.2 Microhardness

Figure 4.4 represents the microhardness of different cutting tools. The microhardness results reveal that the cryogenic treatment increased the hardness of the cutting tool. The cemented carbide structure is subjected to compressive ( $\alpha$  phase) and tensile stresses ( $\beta$  phase). The decrease in cobalt binder ( $\beta$  phase) increases stress and results in compression of hard  $\alpha$  phase (Kalinga Simant Bal and Maity 2012). This increase in compressive stress is the reason for the increase in microhardness. It is seen that the CT-24, cryogenically treated tool for a soaking period of 24 hours had the highest hardness followed by CT-18 and CT-32. The reduction in microhardness after 24 hours of cryogenic treatment is due to a reduction in precipitation of  $\eta$  phase and an increase in the  $\beta$  phase. The CT-24 showed an improvement of 14 % compared to the untreated one. Özbek et al. (2014) found that microhardness of tungsten carbide insert after undergoing cryogenic treatment for a soaking period of 24 hours is 6 % higher than the untreated insert. The maximum microhardness is found to be at a soaking period of 24 hours and the microhardness decreased after 24 hours. Beyond 24 hours, the carbon atom clusters become bigger in colonies and subsequently produce bigger carbides ( $\alpha$  phase) instead of finer and more homogeneously distributed ones. These bigger carbides prohibit  $\eta$  phase carbides from being produced due to the lack of the carbon concentration near the big colonies. It is completely common that the atom concentration changes between the two particles. Near the bigger particle, the atoms concentration increases and subsequently some nearby carbides ( $\eta$  phase) cannot be produced. This behavior leads to a decrease in the carbide percentage in the longer holding duration. Hence grain size increases and microhardness reduces after 24 hours of the soaking period (Akhbarizadeh et al. 2013; Amini et al. 2014). Gill et al. (2012) investigated the effect of cryogenic treatment on tungsten carbide inserts and found a 5 % improvement on microhardness of cryogenically treated samples compared to untreated inserts. Kalinga Simant Bal and Maity (2012), Yong and Ding (2011) and several other researchers also reported the improvement in microhardness of tungsten carbide inserts after cryogenic treatment.

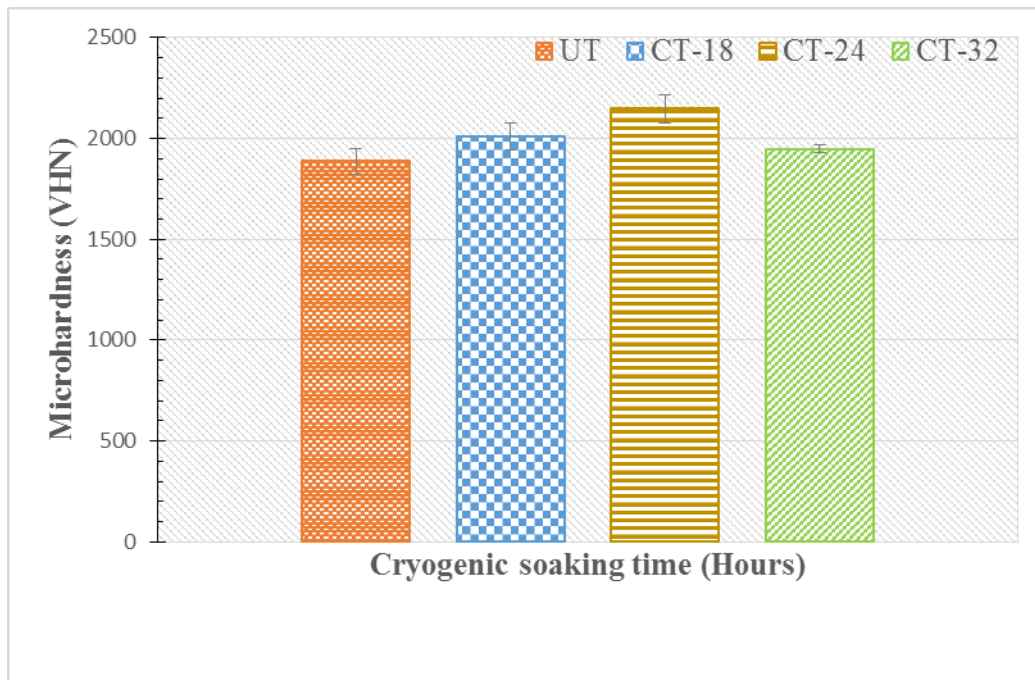


**Figure 4.4** Microhardness of cryogenic treated and untreated cutting tool.

### 4.1.3 Electrical Resistivity & Conductivity

The electrical resistivity and conductivity of untreated and cryogenic treated samples are presented in Table 4.2. It is observed from the table that the electrical conductivity of the cutting tool increased after cryogenic treatment. The CT-24 showed highest electrical conductivity compared to other cryogenic treated samples. The improvement in electrical conductivity for CT-24 sample is 16.76 % compared to the untreated sample. The free electrons are primarily responsible for the electrical and thermal conductivity of metals and alloys. The lower binder contents (Co) in the CT inserts increased the overall electrical conductivity of the cryogenically treated inserts. The increase in carbide grain size due to cryogenic treatment also increased the thermal conductivity of inserts. This is due to the role of the carbide phase and carbide grain contiguity in the thermal conduction of tungsten carbide inserts (Ozbek et al. 2016; SreeramaReddy et al. 2009). The electrical conductivity is directly proportional to thermal conductivity according to Wiedemann-Franz-Lorenz Law. This increase in electrical conductivity increases the thermal conductivity of cutting tool thereby improving heat dissipation capacity of cutting tool and hence reducing

the cutting temperature. Sreeramareddy et al. (2008, 2009) studied the electrical conductivity of tungsten carbide inserts and reported an increase in electrical conductivity after cryogenic treatment. The results were in agreement with other researchers who also reported the improvement in electrical and thermal conductivity after the cryogenic treatment of tungsten carbide inserts (Gill et al. 2011a, 2012a).

**Table 4.2** Electrical resistivity and conductivity of cutting tool.

<b>Cutting tool</b>	<b>Electrical resistivity (ohm-m)</b>	<b>Electrical conductivity (ohm-m)<sup>-1</sup></b>
UT	0.0018	541
CT-18	0.0015	629
CT-24	0.0015	650
CT-32	0.0016	597

## **4.2 MILLING PERFORMANCE CHARACTERISTICS OF UNTREATED AND CRYOGENIC TREATED TOOL UNDER DRY ENVIRONMENT**

### **4.2.1 Tool Wear**

The milling experiments were planned as per Table 4.3 under dry environment. The tool rake wear is measured using SEM after machining for 5 minutes at a spindle speed of 270 rpm and is depicted in Figure 4.5. SEM images show that crater wear, notch wear and built up edge formation were the wear mechanisms observed in the rake face of the untreated cutting tool as shown in Figure 4.5 a). The cryogenically treated inserts were not found with crater wear rather notch wear and built up edge as seen in Figure 4.5 d). The abrasion marks are evident from cryogenically treated inserts at the nose of the tool as seen from Figure 4.5 b). The EDS analysis of tool wear area as presented in Figure 4.6 is taken to find built-up edge formation and untreated inserts, UT is seen with foreign particles from workpiece stick to cutting tool justifying built-up edge formation. The plastic deformation resulted in the microchipping and fracture of untreated cutting inserts. The cryogenic treatment

resisted plastic deformation of WC-Co material by a reduction in  $\beta$  phase particle which is the reason for deformation at the elevated temperature. Figure 4.7 represents the SEM images of the flank wear of different cutting tool at 270 rpm. The maximum flank wear is reported with untreated cutting tool followed by CT-32, CT-18 and CT-24. It is evident from tool wear results that cryogenic treatment improved the wear resistance of the cutting tool.

**Table 4.3** Cutting parameters used in the experiments.

Expt. No	Spindle speed (rpm)	Feed rate (mm/min)	Depth of cut (mm)
1	540	58	0.15
2	350	58	0.15
3	270	58	0.15

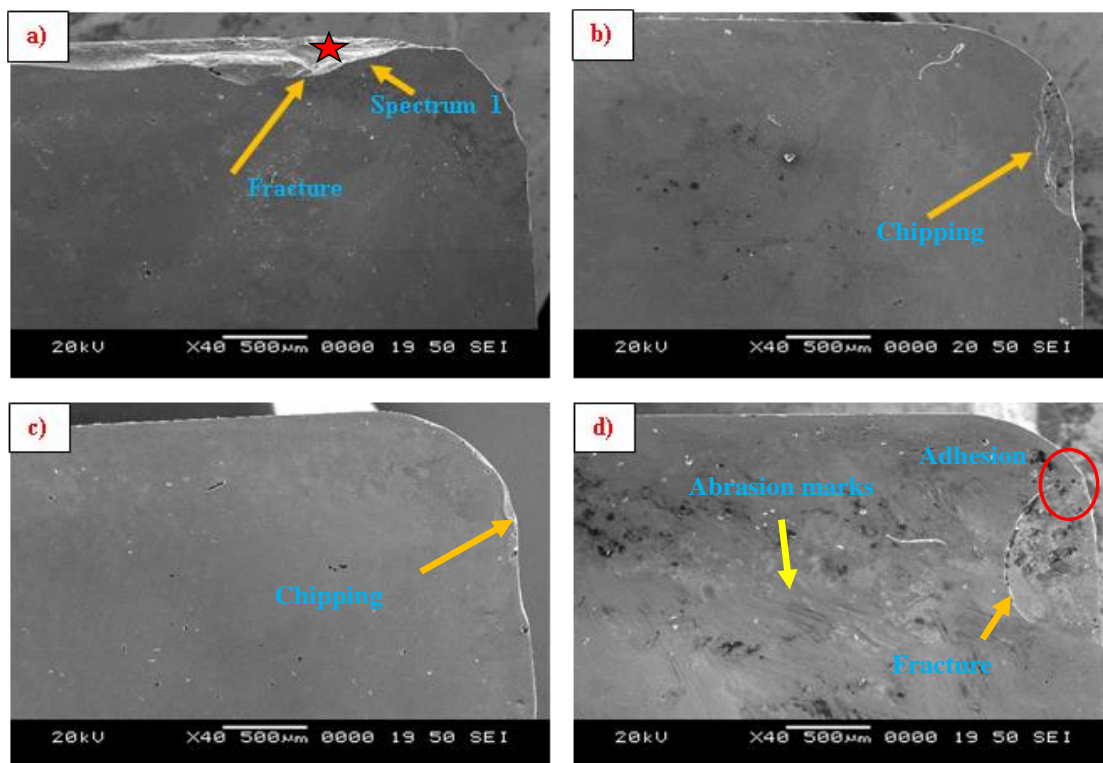


**Figure 4.5** SEM images of rake wear of cutting tool at a cutting speed of 270 rpm.

a) UT b) CT- 18 c) CT-24 d) CT-32.

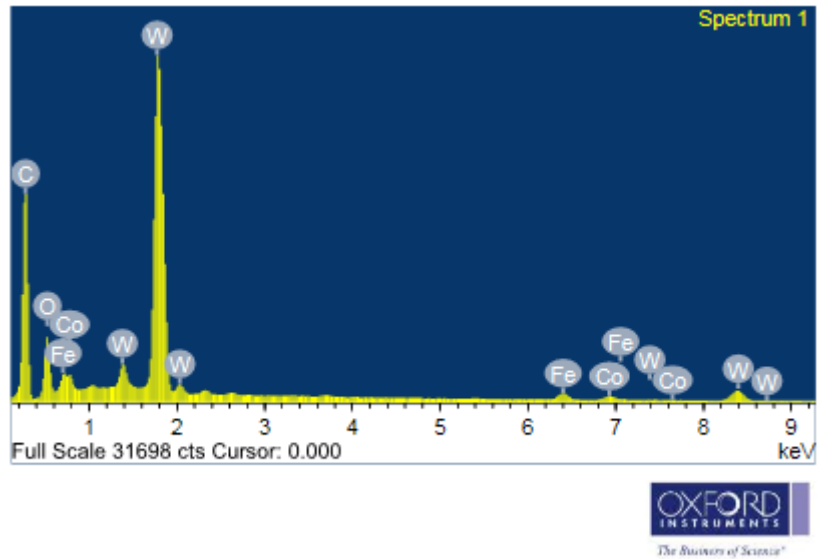


Figure 4.6 EDS analysis of spectrum 1.

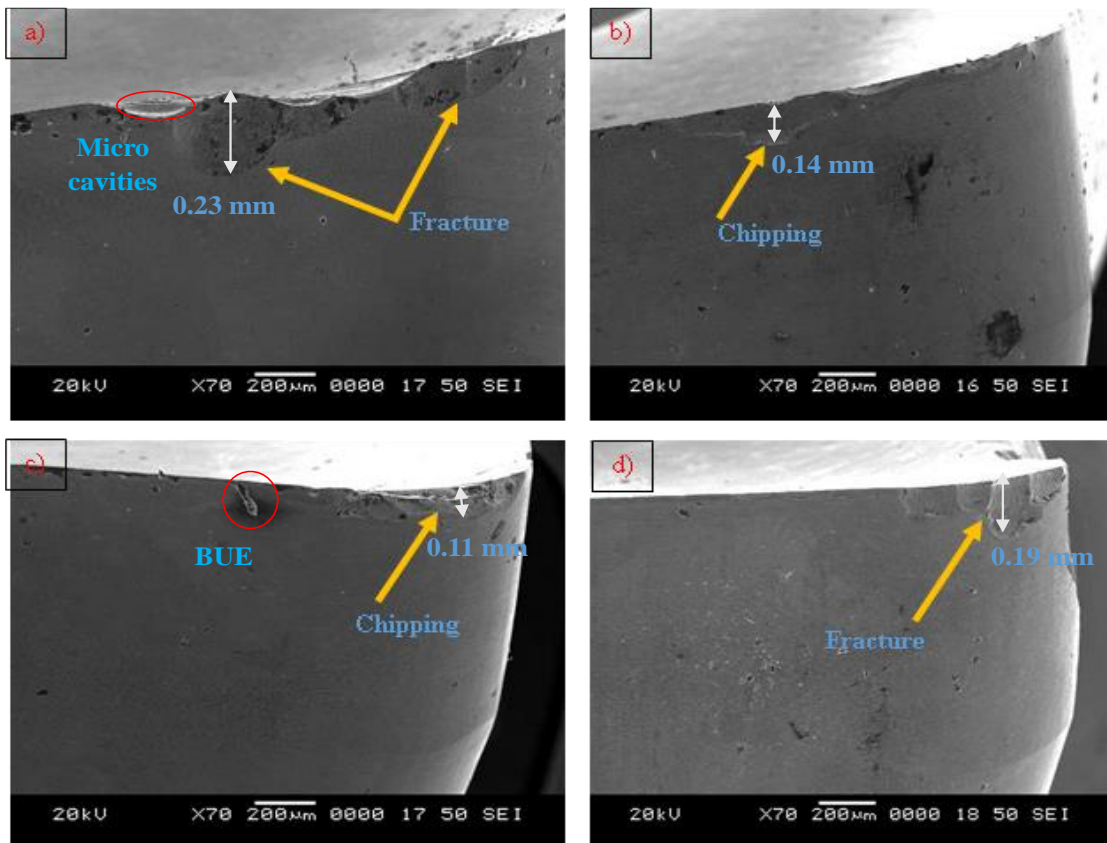
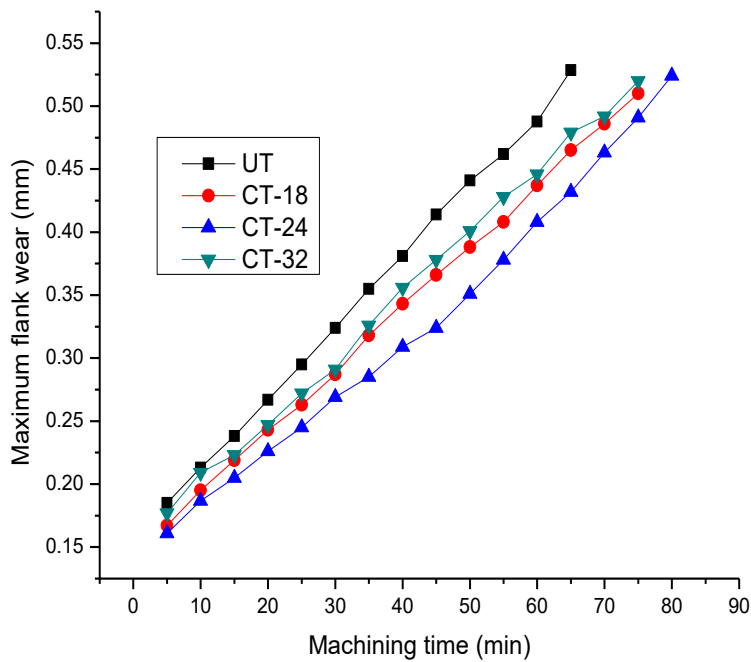


Figure 4.7 SEM images of flank wear of cutting tool at a cutting speed of 270 rpm.

a) UT b) CT- 18 c) CT-24 d) CT-32

Figure 4.8, Figure 4.9 & Figure 4.10 indicates the progression of flank wear at an interval of 5 minutes. As seen in the graph cryogenic treatment improved wear resistance of the cutting tool. The CT-24 showed maximum wear resistance followed by CT-18 and CT-32. The flank wear of untreated inserts is close to cryogenically treated inserts during the initial 20 minutes of machining. But cryogenically treated inserts showed effective wear resistance as the time progressed, even when cutting temperature is high. This repeated even at a high spindle speed of 540 rpm where untreated inserts showed a poor tool life. Thus it is inferred that cryogenic treatment is effective in altering metallurgy of cutting inserts and improving the wear resistance of cutting inserts as reported by others (Gill et al. 2011a; Mohan Lal et al. 2001).



**Figure 4.8** Progression of maximum flank wear with machining time at a spindle speed of 270 rpm.

## 4.2.2 Tool Life

The tool life of cryogenic treated and untreated cutting tool at different spindle speed is given in Table 4.4. It is clear from the table that tool life improved after cryogenic treatment. The tool life reduced as the spindle speed increased because of an increase in cutting temperature and tool wear. But cryogenic treatment is much effective in resisting tool wear even at high spindle speeds. The high thermal conductivity of cryogenically treated tool helped to uniformly distribute cutting temperatures during high-speed cutting thereby reducing tool wear and hence a higher tool life. The CT-24 showed maximum tool life followed by CT-18 and CT-32. The percentage improvement in tool life is maximum for CT-24 (39.84%) during machining at a spindle speed of 350 rpm.

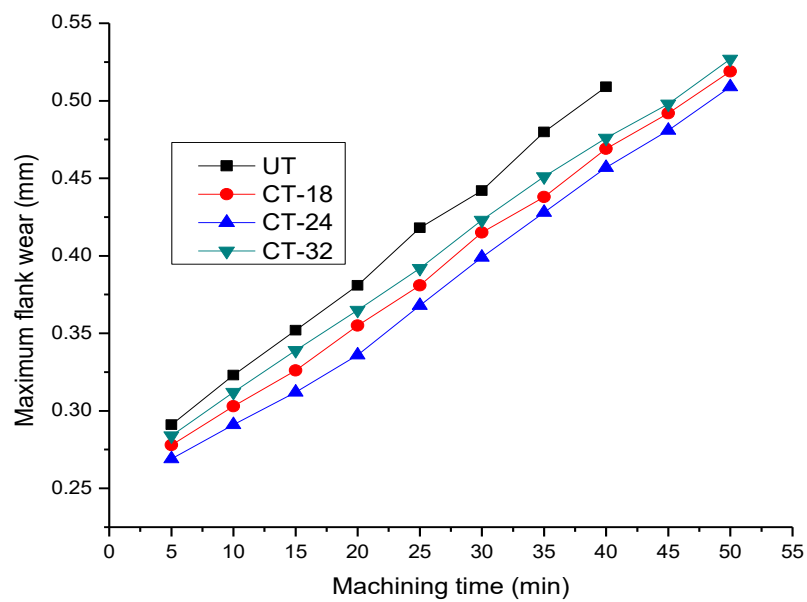


**Figure 4.9** Progression of maximum flank wear with machining time at a spindle speed of 350 rpm.

**Table 4.4** Tool life of cutting tools at different spindle speed.

Cutting speed (rpm)	Tool life (min)				% improvement		
	UT	CT-18	CT-24	CT-32	CT-18	CT-24	CT-32
270	61.50	74.76	76.20	73.44	21.56	23.90	19.41
350	39.20	47.13	48.60	46.50	20.22	23.98	18.62
540	26.70	31.00	32.67	29.86	16.10	22.36	11.84

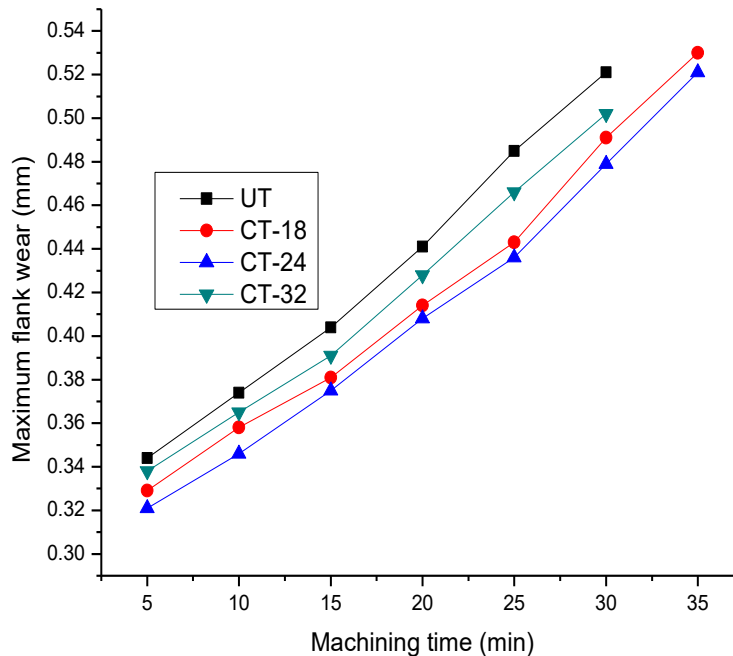


**Figure 4.10** Progression of maximum flank wear with machining time at a spindle speed of 540 rpm.

The tool life for different spindle speed is found using criteria of maximum flank wear of 0.5 mm. Figure 4.11 indicates the plot of spindle speed and tool life of cutting tool on a double logarithmic scale of base 10. It is analyzed from the graph that cryogenically treated cutting tool has a higher tool life even at higher spindle speed. The CT-24 showed a linear regression line with a coefficient of determination value ( $R^2 = 0.987$ ) higher than CT-18 ( $R^2 = 0.982$ ) and CT-32 ( $R^2 = 0.971$ ). The untreated



inserts showed a least linear fit with a regression value ( $R^2 = 0.969$ ). This indicates the inconsistent tool life of the untreated cutting tool. The high surface roughness and cutting forces during machining using untreated cutting tool is due to lower and inconsistent tool life (Gill et al. 2011a).

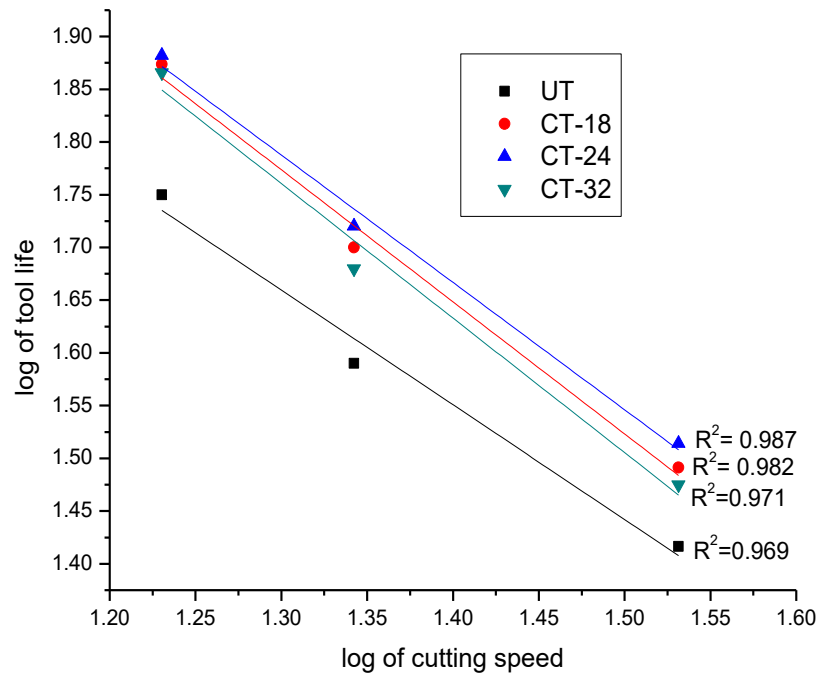


**Figure 4.11** Tool life of cutting tool at different spindle speed on double logarithmic scale to base 10.

### 4.2.3 Cutting Force

The resultant cutting force during machining at various spindle speed is shown in Figure 4.12. The results reveal that cryogenic treatment reduced cutting force during machining. The wear resistance of cryogenically treated inserts reduced the distortion and resulted in a reduced cutting force (Gill et al. 2011a, 2012b). The improvement in thermal conductivity after cryogenic treatment helped to dispense heat at the cutting edge and reduce cutting temperature and tool wear. It is also seen that cutting force decreased as the spindle speed increased for cryogenic treated and untreated cutting inserts. This is due to thermal softening of the workpiece due to the increase in cutting temperature at higher spindle speeds (Ravi and Pradeep Kumar 2011). Mukkoti et al.

(2018) studied the effect of cryogenic treatment of tungsten carbide inserts on cutting force and power consumption while CNC milling of P20 mold steel. They found that cutting force decreased with cryogenically treated tungsten carbide inserts compared to untreated inserts. It is found that inserts treated for a soaking period of 36 hours have the lowest cutting force compared to 24 hours and untreated inserts. Several other researchers also reported the reduction in cutting force with the cryogenically treated cutting tool (Gill et al. 2011a, 2012a).

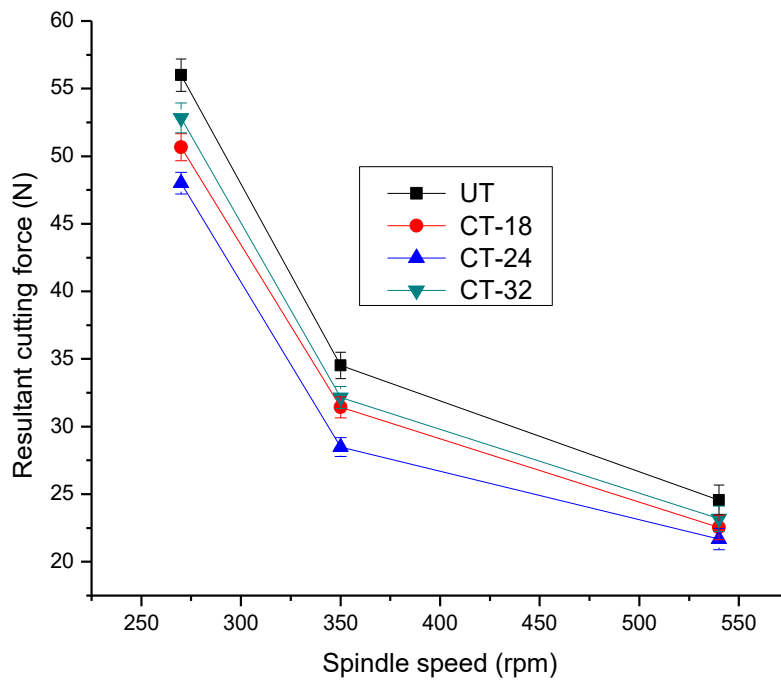


**Figure 4.12** Variation of the resultant cutting force during machining using cryogenic treated and untreated cutting tool at different spindle speed.

#### 4.2.4 Surface Roughness

The surface roughness of workpiece after machining using the different cutting tool at different spindle speed is measured and illustrated in Figure 4.13. The surface roughness decrease as spindle speed increase and CT-24 showed the least surface roughness followed by CT-18, CT-32 and UT. The surface roughness depends on tool wear, fracture, chipping, irregular deformation, built up edge and vibration of the cutting tool. The cryogenic treatment results in grain size refinement, precipitation of

$\eta$  phase and reduction of  $\beta$  phase particle which results in microhardness improvement and wear resistance. As the spindle speed increase cutting force decreases thus reducing the vibration and chatter and results in a better surface finish as reported in previous works (Gill et al. 2011a; Kalsi et al. 2010).

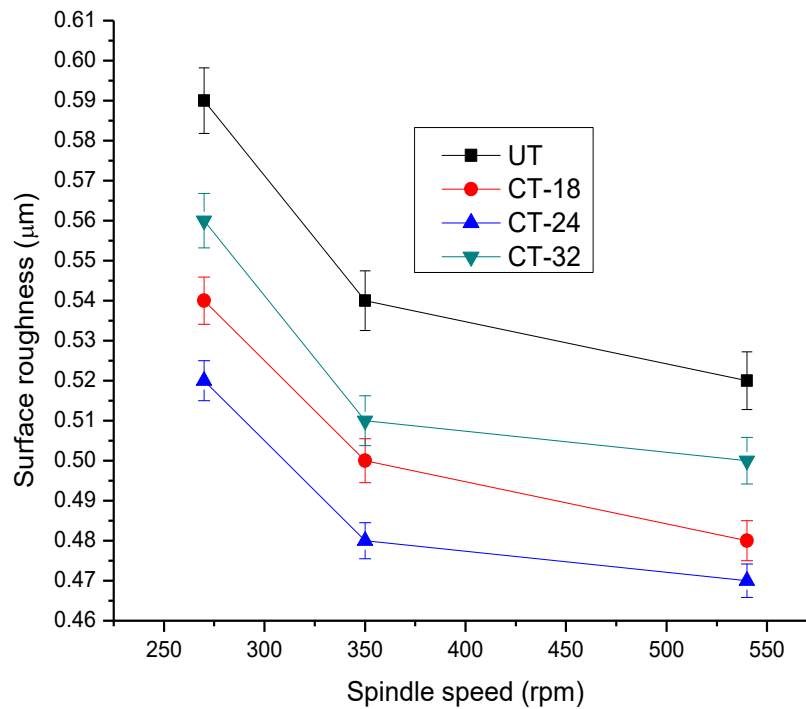


**Figure 4.13** Variation of the surface roughness of maraging steel after machining using cryogenic treated and untreated cutting tool at different spindle speed.

## SUMMARY

- The cryogenic treatment can significantly enhance the machinability by extending tool life, better surface quality and the reduced cutting force resulting in reduced power consumption.
- The optimum soaking period of cryogenic treatment for better machinability is found to be 24 hours (CT-24). The wear resistance and machining performance of tungsten carbide insert reduced after subjecting to the cryogenic treatment of 32 hours (CT-32).

- The microhardness of tungsten carbide inserts improved up to 14 % after carrying out cryogenic treatment for a period of 24 hours (CT-24).
- The electrical conductivity of cutting tool improved after cryogenic treatment and CT-24 showed maximum improvement of 16.76 % compared to the untreated cutting tool.
- The cryogenically treated inserts showed wear resistance even at high spindle speed, chipping, crater wear and built up edge is reduced. The tool life of cutting tool improved up to 29 % during high-speed cutting using CT-24 cutting tool.
- The resultant cutting force reduced significantly using cryogenically treated inserts. The wear resistant and better tool life of cutting tool reduced chatter and vibration of the cutting tool which resulted in lesser cutting forces during machining.
- The surface roughness of workpiece reduced significantly using cryogenically treated inserts. The reduction in tool wear and cutting temperature resulted in a better surface finish.
- The improvement in wear resistance, microhardness and thermal conductivity is due to precipitation of  $\eta$  phase carbides, the increase in grain size of WC, decrease in  $\beta$  phase (Co) and grain refinement. The grain size of cryogenically treated samples reduced up to 22 % for CT-24.

### **4.3 MILLING PERFORMANCE CHARACTERISTICS OF UNTREATED AND CRYOGENIC TREATED TOOL UNDER DIFFERENT ENVIRONMENTS**

The characterisation and machining performance of cryogenically treated tool showed CT-24 had higher wear resistance and tool life compared to other cryogenic treated tools. However, the effect of cryogenic treatment diminished at higher speeds due to high cutting temperature. This is a continuation of previous work with a higher depth of cut (0.3 mm) to analyse milling performance of cryogenic treated (CT-24/CT) tool

and untreated tool under dry, wet and cryogenic machining environments. The experimental plan for the machining studies is presented in Table 4.5.

**Table 4.5** Experimental plan for milling characteristics study.

<b>Expt. No</b>	<b>Spindle speed (rpm)</b>	<b>Feed rate (mm/min)</b>	<b>Depth of cut (mm)</b>	<b>Cutting environment</b>
1	540	58	0.3	Dry, wet & cryogenic
2	350	58	0.3	Dry, wet & cryogenic
3	270	58	0.3	Dry, wet & cryogenic

#### **4.3.1 Tool wear of Untreated (UT) and Cryogenic treated (CT/CT-24) inserts under dry, wet and cryogenic environments**

The maximum flank wear during machining using CT and UT cutting tool at different spindle speed under different environment is measured at an interval of 5 minutes and presented in Figure 4.14, Figure 4.15 & Figure 4.16. As observed from the graph, the CT tool resists flank wear more effectively than UT cutting tool at three different spindle speeds and all the three environments. The cryogenic treatment enhanced the wear resistance of CT tool and reduced the flank wear compared to UT tool. The increase in thermal conductivity of CT tool helped to dissipate the heat from the tool tip to the surrounding atmosphere. The metallurgy of CT tool is altered such a way that it can withstand wear resistance at high speed (Gill et al. 2011a). But the extent of wear resistance reduces at higher spindle speeds. The cutting tool under cryogenic environment is reported with least flank wear compared to conventional wet and dry environments. Figure 4.14 shows the variation of flank wear of cutting tool at 270 rpm under dry, wet and cryogenic environments. The flank wear is almost same for CT and UT cutting tool during the first 20 minutes of machining. The cutting temperature during dry machining at lower spindle speed is not sufficient in diminishing the wear resistance properties of cryogenic treatment. The CT cutting tool resisted the flank wear as the time progressed compared to UT cutting tool. But at high spindle speeds, the high temperature at tool tip diminishes the wear resistance of CT tool. As we can observe from Figure 4.15, the resistance of CT and UT cutting tool towards flank wear reduced as the spindle speed increased from 270 rpm to 350

rpm. The variation of flank wear for CT and UT is similar during the first 5-10 minutes of machining under dry and wet environment. The cryogenic environment showed an exceptional reduction in flank wear compared to dry and wet environment. Figure 4.16 indicates the progression of flank wear at a spindle speed of 540 rpm, where flank wear is maximum compared to other spindle speeds. The CT cutting tool had higher wear resistance compared to UT, the dry and wet environments were poor in resisting tool wear compared to cryogenic environments. The cryogenic cooling proves to be an effective method in reducing flank wear even at high spindle speed.

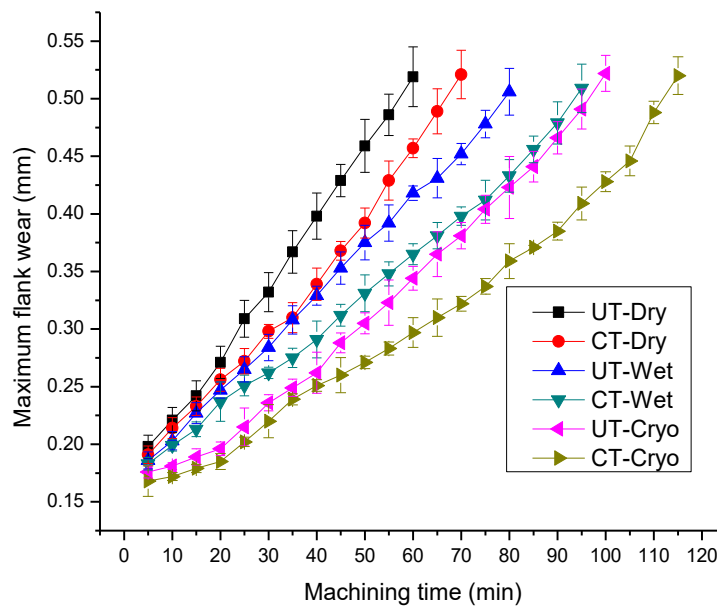


**Figure 4.14** Progression of flank wear at a spindle speed of 270 rpm using UT & CT cutting tool under different machining environment.

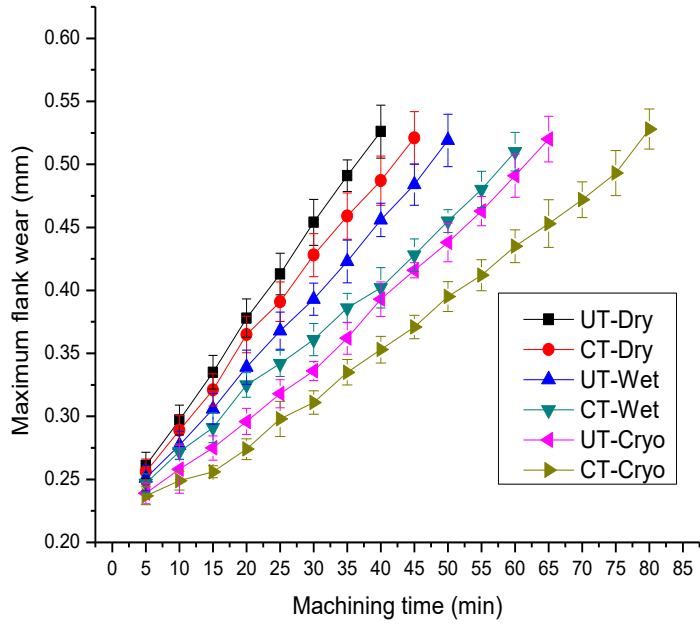


**Figure 4.15** Progression of flank wear at a spindle speed of 350 rpm using UT & CT cutting tool under different machining environment.

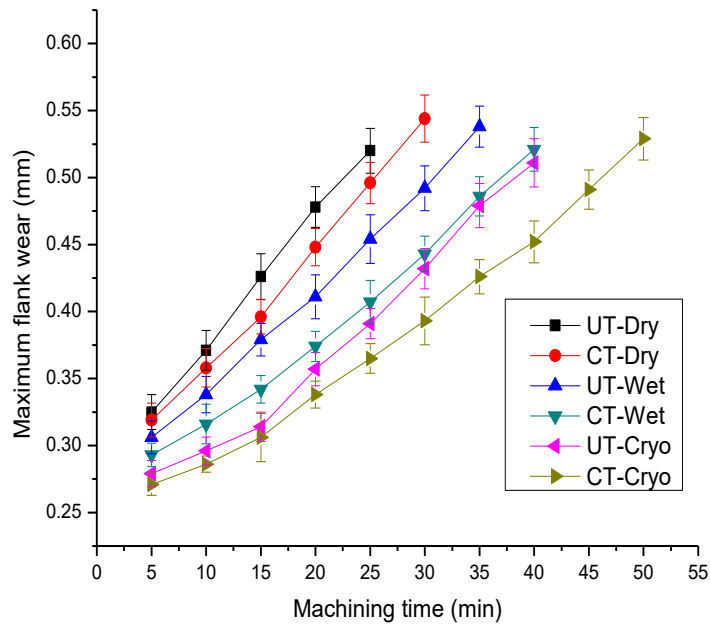


**Figure 4.16** Progression of flank wear at a spindle speed of 350 rpm using UT & CT cutting tool under different machining environment.

### **4.3.2 Tool life of Untreated (UT) and Cryogenic treated (CT/CT-24) inserts under dry, wet and cryogenic environments**

The tool life of UT and CT cutting tool along with percentage improvement in tool life of CT tool under dry, wet and cryogenic environment is presented in Table 4.6. Figure 4.17 shows the graphical presentation of the variation of tool life during machining at different spindle speed and environment. At 270 rpm, the percentage improvement in tool life of CT tool under dry, wet and cryogenic environments are 17 %, 23 %, and 24 % respectively. The CT tool showed better tool life under cryogenic environment compared to a wet and dry environment. But as the spindle speed increased from 270 rpm to 540 rpm, percentage improvement in tool life of CT cutting tool under dry, wet and cryogenic environment reduced to 13 %, 18 %, and 20 % respectively. The performance of CT tool decreased as the spindle speed increased, the high cutting temperature generated during machining diminished wear resistance of CT tool which resulted in lower tool life. The high lubrication and cooling ability of cryogenic cooling helped in reducing the cutting temperature and to withhold wear resistance of CT tool even at high spindle speeds. The tool life of UT cutting tool also increased under cryogenic cooling. The highest improvement in tool life of CT tool is 24 % under a cryogenic environment at 270 rpm. During cryogenic cooling, the tool life of UT tool improved by 63-72 % and 21-29 % compared to dry and wet cooling. Similarly tool life of CT tool under cryogenic cooling improved by 73-84 % and 22-30 % respectively compared to dry and wet cooling.



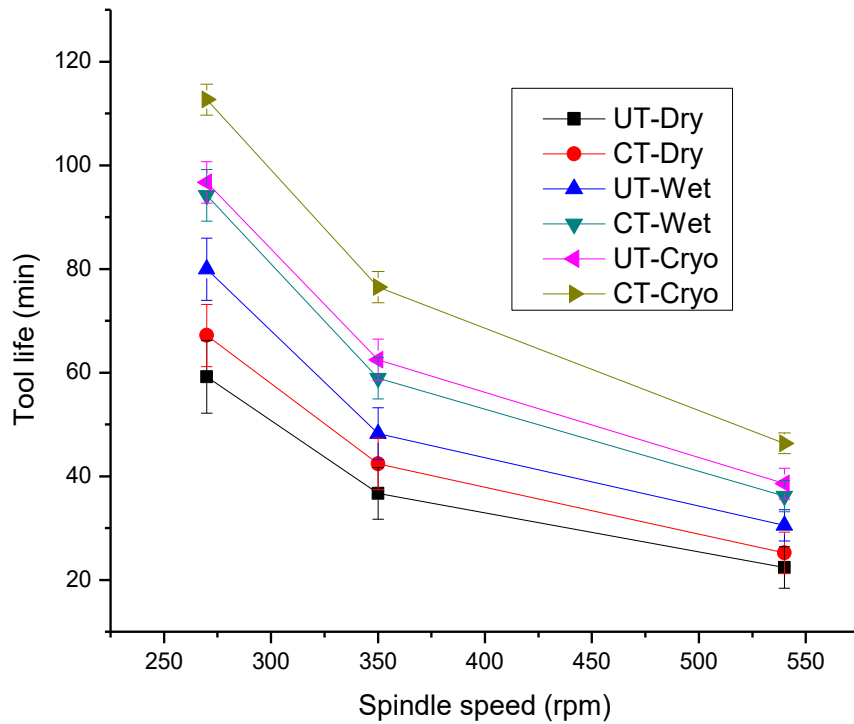


**Figure 4.17** Variation of tool life with spindle speed.

**Table 4.6** Percentage improvement in tool life of cryogenic treated cutting tool under different environment.

Spindle speed (rpm)	Dry environment			Wet environment			Cryogenic environment		
	Tool life (min)		% improvement $((T_{CT} - T_{UT}) / T_{UT} * 100)$	Tool life (min)		% improvement $((T_{CT} - T_{UT}) / T_{UT} * 100)$	Tool life (min)		% improvement $((T_{CT} - T_{UT}) / T_{UT} * 100)$
	UT	CT		UT	CT		UT	CT	
270	59	69	16.86	80	98	22.82	97	120	23.73
350	37	42	15.53	48	59	22.17	62	77	22.49
540	22	25	12.57	30.5	36	18.46	39	46	20.17

The SEM images of tool flank wear of UT and CT cutting tool after machining about 25 minutes, at a spindle speed of 540 rpm under dry, wet and cryogenic environment is presented in Figure 4.18. The flank wear mechanism is studied extensively because it majorly affects the cutting force and other problems. The figure shows that flank

wear is minimum for CT cutting tool compared to UT cutting tool under dry, wet and cryogenic environments. The results also reveal that flank wear of the UT and CT cutting tool is minimum under cryogenic cooling compared to dry and wet environments. The fracture and chipping are prominent during dry machining due to severe abrasion. The substantial plastic deformation accompanied by multiple thermal cracks were formed in UT tool under dry environment. The deformation of tool tip is more during dry machining as evident from the figure. The intermittent cuts during milling results in cyclic thermal stresses leading to irregular deformation of tool tip. The built-up edge (BUE) formation and adhesion of workpiece material also accompanied. The CT cutting tool showed better wear resistance compared to UT cutting tool. The enhanced thermal conductivity of CT tool enabled heat dissipation at the tool tip more rapidly and reduced thermal cracks due to severe plastic deformation (Gill et al. 2011a). The chipping and fracture are also observed during machining under a wet environment but less compared to a dry environment. The CT tool under a wet environment performed better than UT tool under a wet environment and CT tool dry environment. But the results show that the use of conventional cutting fluids is also not effective in reducing the extent of tool wear. The notch wear is observed during dry and wet cooling. The wet cooling cause's faster corrosion and oxidation of tool surfaces and accelerates micro fracture of tool tips. The reduction in adhesion and diffusion wear by wet cooling is surpassed by micro fracture. This is the result of thermo-mechanical shocks due to fluctuating temperatures and stresses while machining under a wet environment (Dhar et al. 2006a). The micro-chipping is the mechanism observed under cryogenic environment. The cryogenic cooling is observed with the minimum wear compared with the dry and wet environment. This is mainly because of the inert atmosphere created by liquid nitrogen which protects the tool from adhesion and diffusion. The thermal conductivity of the cutting tool is increased and disperse heat to surrounding and avoids thermo-mechanical shocks. The flank wear is reduced drastically under cryogenic cooling due to the enhanced hardness and stability of the cutting tool. The high-temperature oxidation and corrosion are less during cryogenic cooling compared to dry and wet cooling. The built-up edge formation is less in cryogenic cooling which is the root cause of crater wear. The improved microhardness and toughness as a result of cryogenic treatment

and tempering process helped to reduce the tool wear of CT cutting tool. The reduced cutting temperature, low chemical affinity, increased thermal conductivity, high heat dissipation capacity, better lubrication are some of the reasons which reduced the tool wear under cryogenic environment compared to the dry and wet environment (Ravi and Kumar 2011).

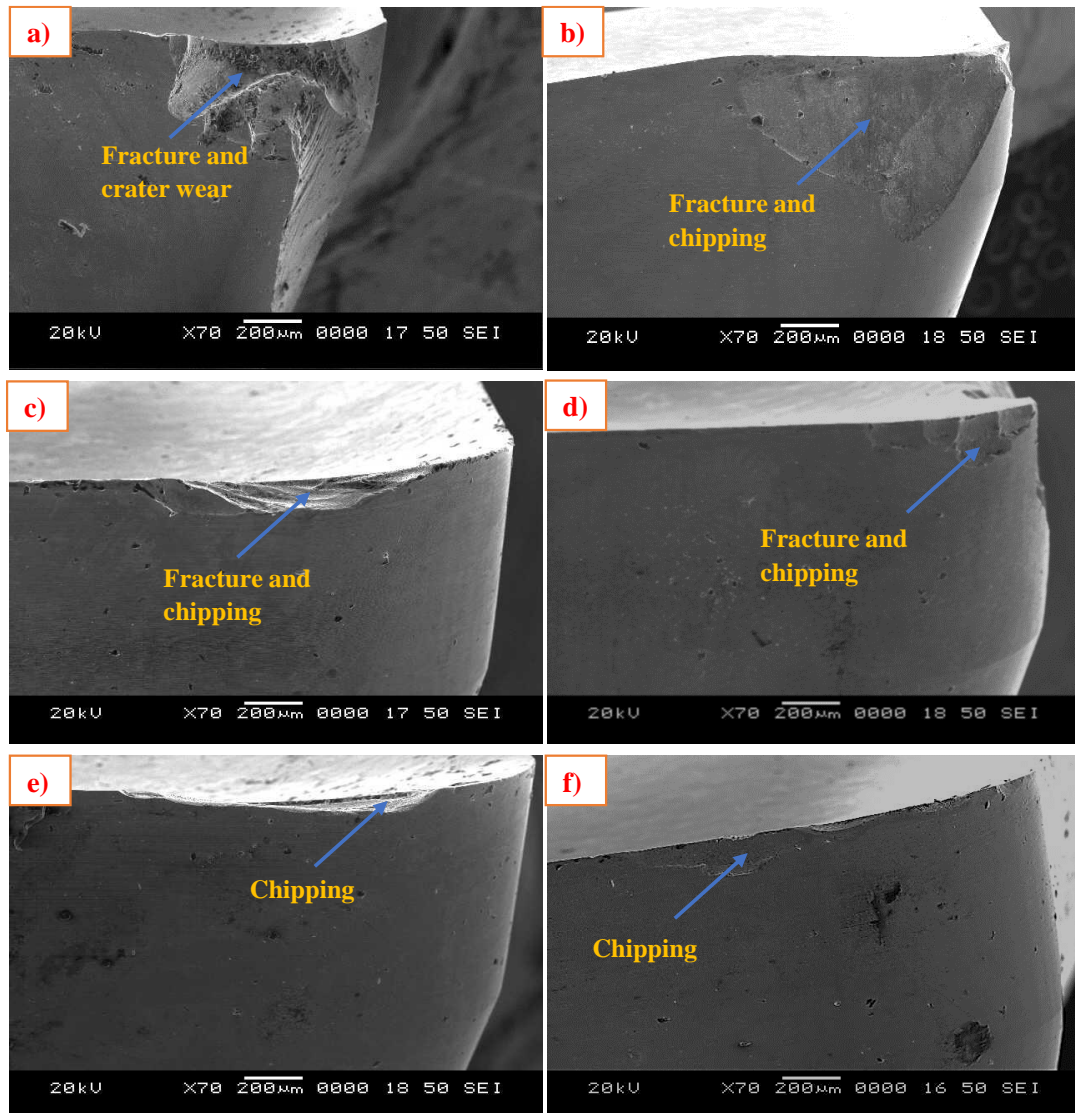


**Figure 4.18** Tool wear of cutting tool at 540 rpm under different environment after machining for 25 minutes a) UT under dry b) CT under dry c) UT under wet d) CT under wet e) UT under cryogenic f) CT under cryogenic.

### **4.3.3 Cutting force variation during machining using untreated (UT) and cryogenically treated (CT/CT-24) inserts under dry, wet and cryogenic environments**

The cutting force is an important performance characteristic in machining as the power consumption is directly related to cutting force which decides the machining cost. Figure 4.19 shows the variation of resultant cutting force with spindle speeds using CT and UT cutting tool under dry, wet and cryogenic environment. The results reveal that cutting force decrease with an increase in spindle speed. The chatter and vibration are more during lower spindle speeds which increases the cutting force. At high spindle speed, the cutting force reduces due to excess heat generation which results in thermal softening of the workpiece (Ravi and Kumar 2012). The cutting force for CT tool is less than the UT tool at all the spindle speeds and the machining environments. Also, the cutting force is minimum during cryogenic machining followed by wet and dry machining. During dry machining, at a spindle speed of 270 rpm, the cryogenic treated tool showed a 9 % reduction in cutting force compared to the untreated tool. The percentage reduction in cutting force of CT tool further reduced to 7 % with an increase in spindle speed from 270 rpm to 540 rpm. The heat generated at high spindle speed diminishes wear resistance of CT tool. This results in adhesion and built up edge formation (BUE) of the cutting tool. Thus leading to a loss of stability of the cutting tool and irregular deformation of the tool tip. Hence the percentage reduction of cutting force drops with an increase in spindle speed. The percentage reduction in cutting force of CT tool increased from 9 % to 10 % when compared to UT tool under wet machining. The wet machining provides better cooling and lubrication than dry machining which is the reason for the better performance of CT tool. It further increased to 11 % when spindle speed increased from 270 rpm to 350 rpm. At 540 rpm, during wet machining, the percentage reduction in cutting force of CT tool reduced to 8 %. The percentage reduction in cutting force of CT tool at 270, 350 and 540 rpm is 11 %, 10 %, and 8 % respectively. During cryogenic machining even at high spindle speed, the percentage reduction in cutting force of CT tool showed maximum when compared to wet and dry machining. The reduction in cutting force during cryogenic cooling using UT tool is 28-39 % and

15-24 % compared to dry and wet cooling. Similarly cutting force reduction during cryogenic cooling for CT tool is 31-43 % and 17-24 % compared to dry and wet cooling. The increase in heat transfer coefficient during cryogenic machining reduces the heat generated at the tool-chip interface. Thus welding and adhesion of chips are less in cryogenic machining which results in a stable machining condition and a reduced cutting force. The boiling of liquid nitrogen results in a cushion formation between tool and workpiece which improves lubrication of cutting tool during machining (Ravi and Kumar 2011). This reduces the chatter and vibration of the cutting tool to a large extent, further contributing to a reduction in cutting force. The results are in accordance with the study by Ravi and Kumar (2011), which also indicated the reduction in cutting force with cryogenic cooling. A previous study by Sivalingam et al. (2018) on cryogenic treatment also indicated the reduction in cutting force using CT tool compared to UT tool.

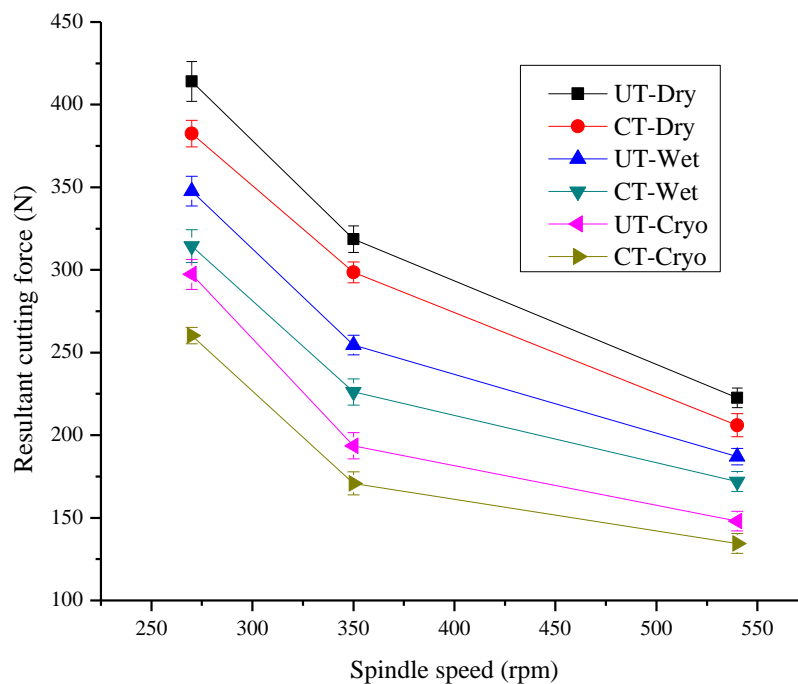


**Figure 4.19** Variation of resultant cutting force with spindle speed.

#### **4.3.4 Surface roughness of workpiece after machining using untreated (UT) and cryogenically treated (CT/CT-24) inserts under dry, wet and cryogenic environments**

The surface roughness of workpiece is an important factor which decides product quality, fatigue behaviour, creep life, corrosion resistance etc. The surface finish of finished product effects the functional attributes like friction, wear, heat transmission, lubrication, light reflection etc. The reasons for poor surface finish of workpiece are tool marks during machining, built-up edge (BUE), chatter & vibration from machining system, deformation of tool tip due to chipping, fracture and wear (Gill et al. 2011a). The choice of the cutting tool, speed, feed rate, and machining environment are cutting parameters influencing surface finish (SreeramaReddy et al. 2009).

Figure 4.20 presents the variation in surface roughness of workpiece at different spindle speeds using UT and CT cutting tool under dry, wet and cryogenic environments. The surface roughness of workpiece decreases with an increase in spindle speed (Ravi and Kumar 2011). The CT cutting tool has a better surface finish than UT cutting tool under dry, wet and cryogenic environment. The improved wear resistance of CT tool and stable cutting edge are reasons for better surface finish. The UT & CT cutting tool showed better surface finish under cryogenic environment followed by the wet and dry environment. The results show that in a dry environment when spindle speed is 270 rpm CT cutting tool showed an 8 % reduction in surface roughness. The percentage reduction in surface roughness decreased from 8 % to 6 % while increasing spindle speed from 270 rpm to 540 rpm respectively. The CT tool showed better resistance to tool wear at higher spindle speeds. The high cutting temperature developed during high spindle speed caused thermal softening of the workpiece. The cutting force reduced due to thermal softening and there are less vibration and chatter leading to a better surface finish. When spindle speed is 540 rpm, the surface roughness of the CT tool under wet machining showed a percentage reduction of 10 % compared to UT tool. There is an increase in the percentage reduction of surface roughness from 6 % to 10 % under wet machining at a spindle

speed of 270 rpm compared to dry machining. This is due to better cooling & lubrication provided by wet machining. The wet machining reduced cutting temperature which helped CT tool to prolong the tool from chipping and fracture. Thus reducing the surface roughness of workpiece using CT tool under wet machining. The surface roughness of workpiece reduced from 0.65  $\mu\text{m}$  to 0.55  $\mu\text{m}$  and 0.47  $\mu\text{m}$  when increasing spindle speed from 270 rpm to 350 rpm and 540 rpm respectively. The decrease in surface roughness is due to chipping and fracture of a tool tip with the increase in spindle speed. It is evident from results that wet machining is not sufficient to resist high cutting temperature generated at high spindle speed. The wear resistance of cryogenic cutting tool tends to decrease at high spindle speed. The surface roughness during cryogenic machining showed a percentage reduction of 18 %, 17 % and 12 % at spindle speeds of 270 rpm, 350 rpm, and 540 rpm. The reduction in surface roughness of workpiece using CT cutting tool at 540 rpm increased from 10 % to 12 % during cryogenic machining compared to wet machining. Thus cryogenic machining promise to be better machining than dry and wet machining even at high speeds. During cryogenic cooling the surface roughness of workpiece using UT tool reduced by 44-54 % and 27-37 % compared to dry and wet cooling. Similarly using CT tool the reduction in surface roughness under cryogenic cooling is 51-57 % and 31-38 % respectively. The better lubrication and cooling reduced the chemical affinity of tool and workpiece and reduced tool-chip interface temperature during cryogenic machining helps to improve the surface finish of workpiece (Ravi and Kumar 2012; Ravi and Kumar 2011). Similar results have been observed in the previous study by Shokrani et al. (2016) indicate surface roughness while machining Ti-6Al-4V titanium alloy is minimum under cryogenic environment compared to dry and wet environment. Another study by authors (Varghese et al. 2019) shows the reduction in surface roughness while machining maraging steel using CT tool.

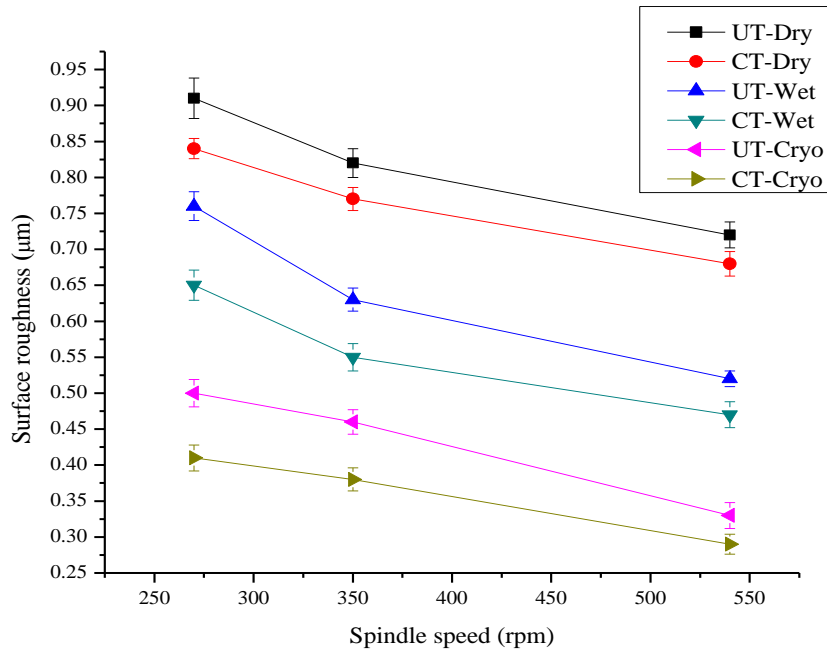


**Figure 4.20** Variation of surface roughness with spindle speed.

## SUMMARY

An experimental investigation is carried out to determine the influence of cryogenic treatment of cutting tools at varying spindle speeds under different machining environment (dry, wet and cryogenic) on the machinability of maraging steel. The characterization of the cryogenically treated tool is carried out to determine changes in microstructure, phase, and microhardness. The machinability studies like tool life, cutting force, surface roughness and microhardness using cryogenic treated (CT) and untreated (UT) cutting tool are analyzed under different spindle speed and environment. The major findings are summarized below.

- The tool life of CT cutting tool improved up to 17 %, 23 %, and 24 % compared to UT cutting tool under dry, wet and cryogenic environments.
- The tool life of UT and CT cutting tool under cryogenic environment improved up to 72 % and 29 %, 83 % and 30 % compared to dry and wet environment.
- The SEM images showed that tool wear is maximum for UT cutting tool compared to CT cutting tool under dry, wet and cryogenic environments. The



fracture and chipping of the cutting tool are more under dry and wet environments compared to cryogenic environments.

- The grain refinement, precipitation of  $\eta$  phase carbides, more stable structure of  $\alpha$  phase, a decrease in  $\beta$  phase which resulted in an increase in compressive stress on tungsten carbide are some of the reasons to enhance the tool life after cryogenic treatment.
- The cutting force reduced using CT compared to UT cutting tool. The percentage reduction in cutting force using CT cutting tool is 9 %, 10 %, and 11 % compared to UT cutting tool under dry, wet and cryogenic environments.
- The cutting force of UT and CT cutting tool under cryogenic environment reduced to 39 % and 23 %, 42 % and 24 % compared to dry and wet environment.
- The surface roughness also reduced using CT compared to UT cutting tool. The percentage reduction in surface roughness using CT cutting tool at a spindle speed of 540 rpm is 6 %, 10 %, and 12 % compared to UT cutting tool under dry, wet and cryogenic environments.
- The surface roughness of cutting tool under cryogenic environment reduced to 44-54 % & 27-37 % (UT) and 51-57 % & 31-38 % (CT) compared to the dry and wet environment.

## **4.4 CHARACTERIZATION OF AlCrN & AlTiN COATED TOOLS**

### **4.4.1 Microstructure & phase changes**

Before carrying out the machining tests it is necessary to find out physical, metallurgical (microstructure), mechanical and chemical properties. The surface morphology of coated inserts using SEM is shown in Figure 4.21. The coatings are found to be homogenous, dense and defect free. The SEM images reveal that the AlCrN coating is much more uniform than AlTiN coatings. Large numbers of macroparticles are visible on the surface of the AlTiN coating. The macro particles are clusters of titanium and nitrogen atoms formed during coating deposition. This

macro particles on the surface of the coating have important effects on tribological properties. Smoother and uniform surface provides good tribological properties. During machining, non-uniform coatings provide a high coefficient of friction which in turn results in reduced tool life, higher cutting forces & power consumption, and poor surface finish. Figure 4.22 shows the EDS spectra of uncoated, AlTiN and AlCrN coated inserts. The chemical composition (at. %) of AlTiN coating is found to be aluminium (32%), titanium (18%) and nitrogen (40%) respectively. Similarly, the chemical composition of AlCrN is aluminium (32%), chromium (20%) and nitrogen (46%) respectively. Figure 4.23 shows the XRD pattern of coated and uncoated tools. Both AlCrN and AlTiN coated tools show the presence of AlN. The presence of CrN is evident from the XRD of AlCrN coating.

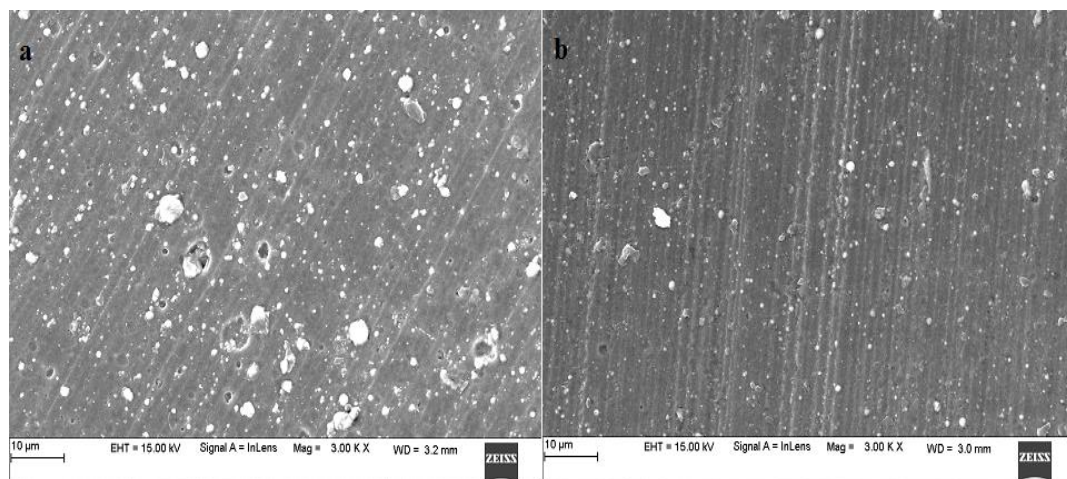


**Figure 4.21** Surface morphology of coatings using SEM a) AlTiN and b) AlCrN.

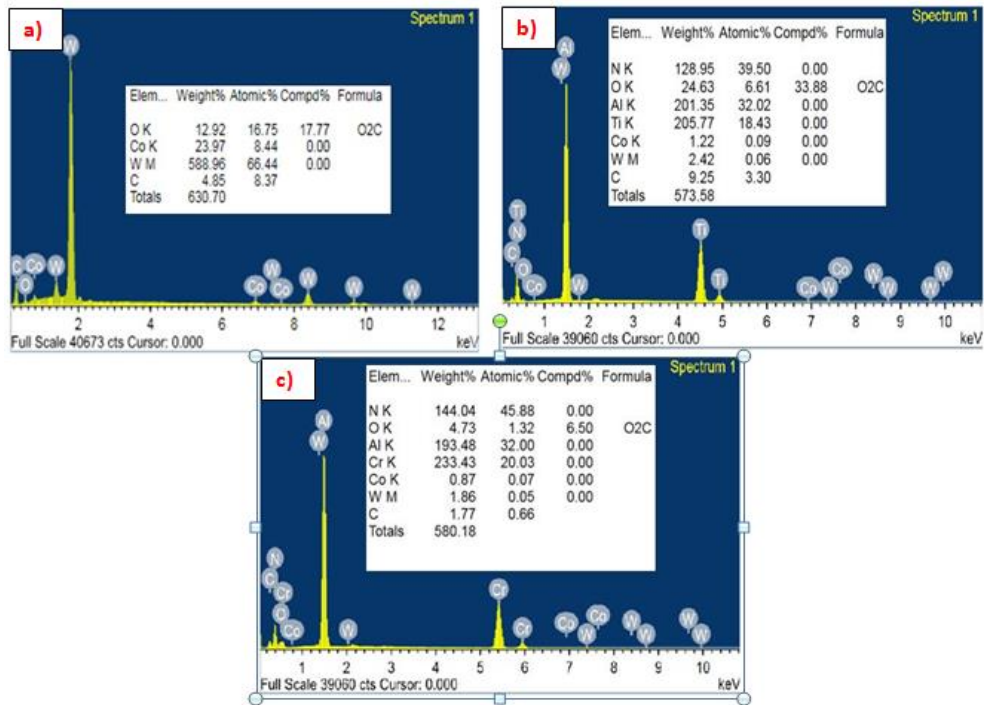


Figure 4.22 EDS analysis of cutting tool a) Uncoated (UC) b) AlTiN c) AlCrN.

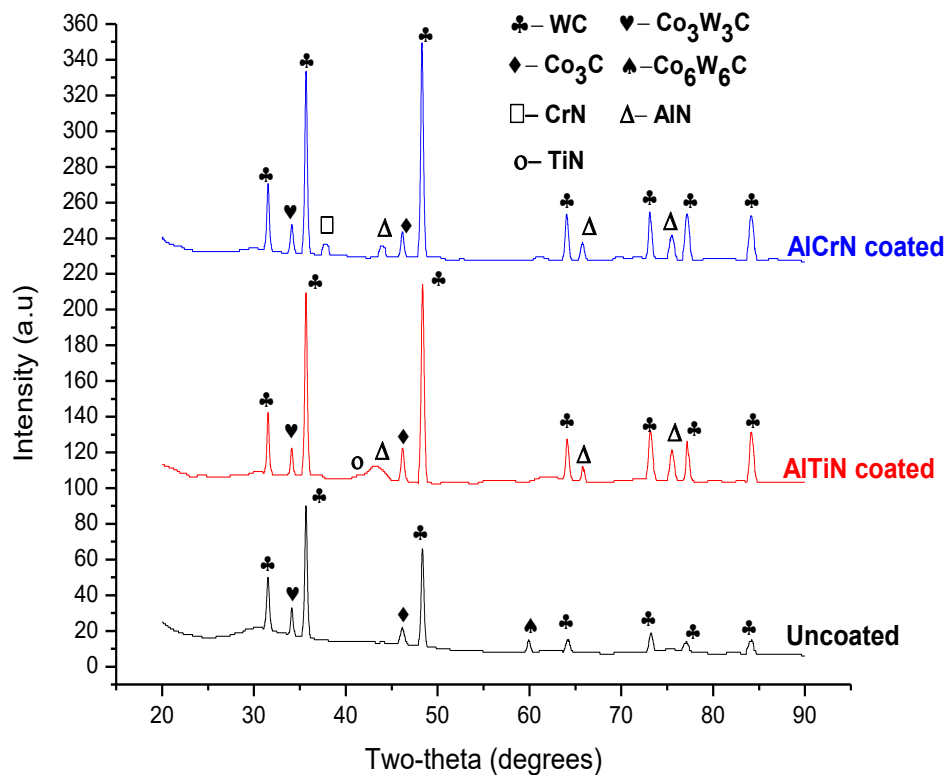


Figure 4.23 XRD patterns for Uncoated and Coated tools.

#### 4.4.2 Micromechanical characterisation

The thickness of the coating is determined by calo tester using a ball indenter rotated at 120 rpm which wears out the coating. The worn out coating is observed using an optical microscope to determine the coating thickness. The images of coating thickness obtained from Calo tester are presented in Figure 4.24. The thickness and mechanical properties of the coatings are given in Table 4.7. The thickness of AlTiN and AlCrN coatings are 3.654  $\mu\text{m}$  and 1.972  $\mu\text{m}$  respectively. The thickness of AlTiN coated samples are around 1.85 times that of AlCrN coated inserts. The mechanical properties of the coatings like hardness, Young's modulus, load-bearing capacity, and plasticity index is determined by nanoindentation. The plasticity index is nothing but a measure of toughness. The hardness and toughness are two important properties affecting the life and performance of the cutting tool (Varghese et al. 2018a). The hardness and Young's modulus of AlCrN coatings are much higher than AlTiN coatings. Generally cutting tools requires higher values of hardness in order to avoid the drastic tool wear. Higher H/E values are obtained for AlTiN coatings which are a measure of plasticity. The load-bearing capacity ( $H^3/E^2$ ) of both coatings is found to be quite similar. In general tribological conditions, the higher H/E value results in lower wear. But the hardness and H/E ratio are inadequate to evaluate the performance of the coating in the severe cutting conditions like high-speed machining (Beake et al. 2009). The plasticity index is more reliable to evaluate the actual cutting conditions. The plasticity index (PI) of the coating is the plastic work done during indentation ( $W_p$ ) divided by the total elastic work ( $W_e$ ) and plastic work ( $W_p$ ) done (Cheng et al. 2008). The plasticity index of the coating is expressed as:

$$PI = W_p / (W_p + W_e) = 1 - x (H/E) \dots \dots \dots (1)$$

Where x is a constant, H- Hardness of the coating and E is Young's modulus of the coating. The x value is approximated as 5 by a suggestion from the finite element analysis (FEA) (Cheng et al. 2008). The PI of AlCrN coating is higher compared to the AlTiN coating. The plasticity index of the coating is correlated with the tool life in end milling of hardened steel (Beake et al. 2009). It can be seen that AlCrN coatings showed improved mechanical properties in comparison with AlTiN coated inserts.

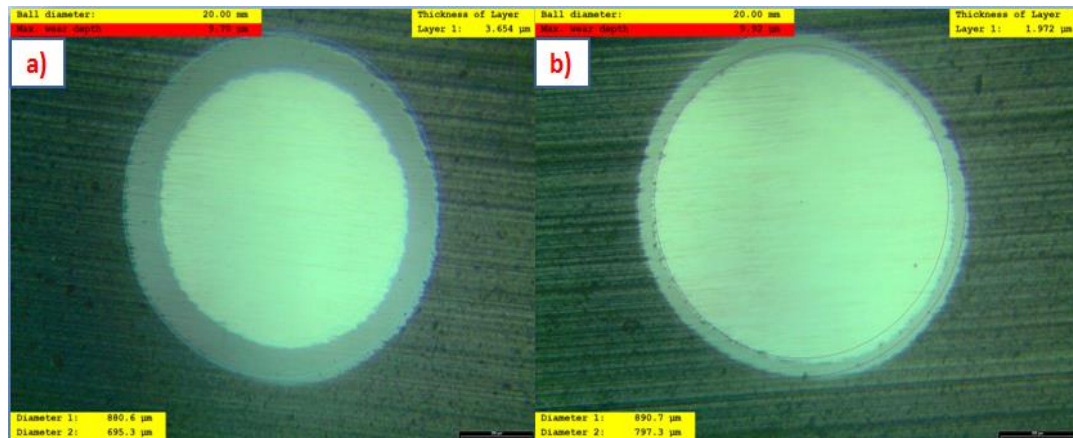


**Figure 4.24** Coating thickness measurement using calo-tester a) AlTiN b) AlCrN.

**Table 4.7** Micro mechanical characteristics of AlTiN and AlCrN coatings..

Coatings	Thickness	Surface roughness	Hardness (H)	Young's modulus (E)	H/E Ratio	H <sup>3</sup> /E <sup>2</sup> Ratio	Plasticity index, [1-x(H/E)]
	μm			GPa		GPa	
AlTiN	3.654	0.651	28.94±6.44	376.7±59.3	0.076	0.17	0.468
AlCrN	1.972	0.547	44.31±12.02	727.5±118.6	0.06	0.16	0.58

## 4.5 MILLING PERFORMANCE CHARACTERISTICS OF AlCrN & AlTiN COATED TOOLS UNDER DRY, WET & CRYOGENIC ENVIRONMENTS

### 4.5.1 Tool wear and tool life

Tool life and tool wear are critical aspects of machining studies since they are evaluated as a measure of machinability. The tool wear has a direct influence on the surface roughness of components. The surface roughness critically affects the service life of the components. The rapid tool wear increases the idle time during machining, which increases the production cost. Reduced tool wear shows an improvement in tool life. The SEM images of the crater wear and flank wear of the cutting tool have

been presented in Figure 4.25 and Figure 4.26. The coated tool reduced the tool wear compared to the uncoated tool. The crater wear is observed more on the uncoated tool. Microchipping, adhesion of particles and fracture is more dominant in the uncoated tool. The coated tools are also observed with microchipping but comparatively less with respect to the uncoated tool. The fracture due to thermal fatigue is a wear mechanism observed in the cutting tool during machining under dry environment. The built-up edge (BUE) formation is seen more during lower spindle speeds under dry environment. Built up edge is mainly the welding of work material on to the tool edge due to the cutting pressure. The flow of chips removes BUE while some part of coating and cutting tool is also taken off leading to crater wear. The crater wear leads to chipping and notch wear resulting in exposure of substrate and acceleration of flank wear (Shokrani et al. 2019). The adhesion and chipping are observed during machining under a wet environment. In wet machining, cutting fluid failed to penetrate into the tool-chip interface. The chipping and adhesion of chips are comparatively less in cryogenic machining as LN<sub>2</sub> penetrated into the tool-chip interface and reduced the cutting temperature. The cryogenic machining reduced the tool wear of coated and uncoated tool to maximum compared to dry and wet machining. The crater wear is seen in the uncoated tool from. The temperature on the rake face is more compared to the flank face. The tribo-oxidation is another important feature of a coated tool like micromechanical characteristics which determines the tool life. Tribo-oxidation is more dominant on the rake face as reported by the investigations on similar coatings. There is a formation of tribo films on the coatings as part of the tribo oxidation. The AlTiN and AlCrN coatings result in the formation of tribo oxide films like alumina, chromium oxides, titania and complex alumina–chromium oxides. The alumina–chromium oxides (Al, Cr)<sub>2</sub>O<sub>3</sub> which forms on the AlCrN coating is more useful in protecting the surface of coatings compared to AlOx which forms in AlTiN coating (Beake et al. 2007; Endrino et al. 2006). The chromium oxide (CrOx) tribo film formed in AlCrN coating is a high-temperature lubricant while titanium oxide films (TiOx) is not a lubricant or protective during high-temperature cutting. The complex alumina- chromium oxide films formed in the AlCrN coating has low thermal conductivity than AlOx films formed (Rabinovich et al. 2009).

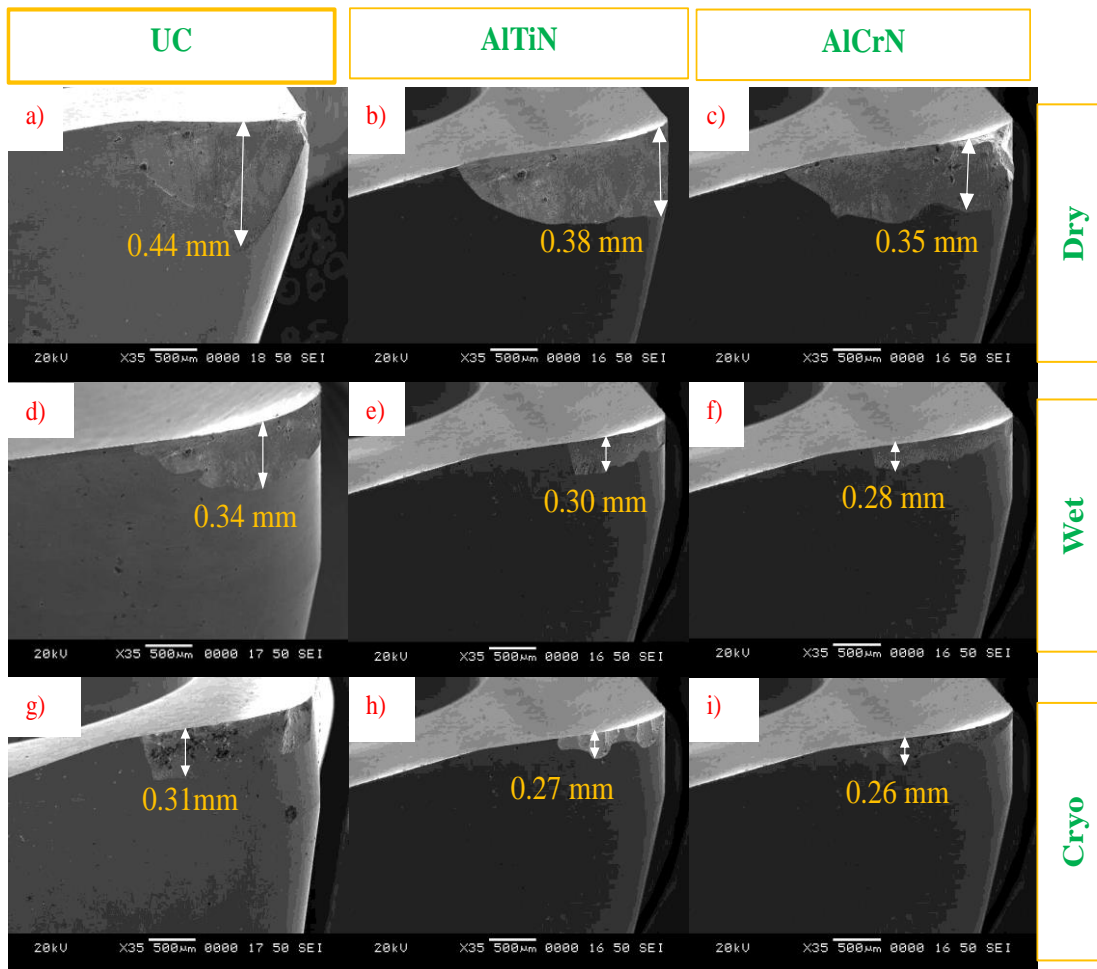


**Figure 4.25** SEM images showing flank wear of inserts for a machining time  $t = 25$  min, spindle speed- 270 rpm, feed rate- 58 mm/min, depth of cut- 0.3 mm. a) UC - Dry b) AlTiN - Dry c) AlCrN – Dry d) UC – Wet e) AlTiN – Wet f) AlCrN – Wet g) UC- Cryogenic h) AlTiN – Cryogenic i) AlCrN- Cryogenic.

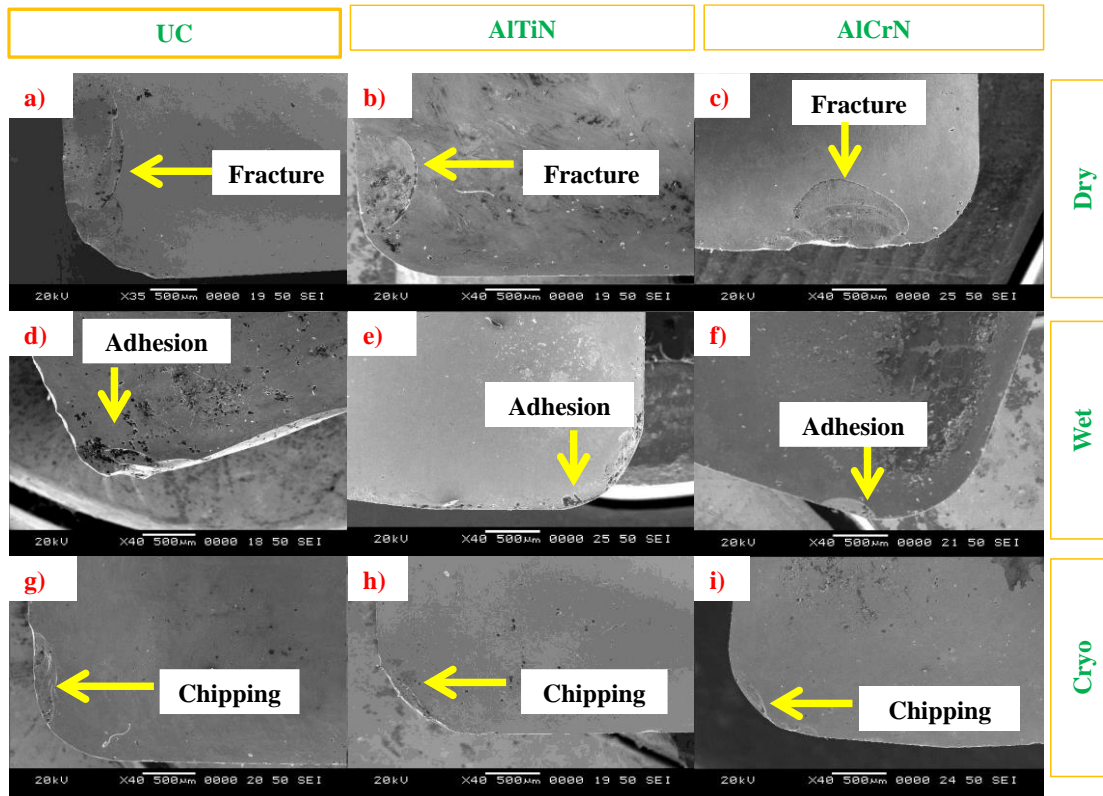


**Figure 4.26** SEM images showing crater wear of inserts for a spindle speed- 270 rpm, feed rate- 58 mm/min, depth of cut- 0.3 mm. a) UC - Dry b) AlTiN - Dry c) AlCrN - Dry d) UC – Wet e) AlTiN -Wet f) AlCrN - Wet g) UC- Cryogenic h) AlTiN - Cryogenic i) AlCrN- Cryogenic.

The environment has a predominant role in cutting temperature developed in the machining zone. The larger values of cutting temperature in the workpiece-tool interface cause the thermal fatigue of the tool and thereby increased tool wear, which leads to premature failure of the tool. The use of cutting fluids in the machining zone helps to remove the temperature generated which reduces the thermal fatigue and thereby tool wear. The percentage change in tool life from dry to wet environment is in the range of 30-38 %. It can be seen that the cryogenic environment performs superior over the other environments. This is due to the increased capacity of LN<sub>2</sub> to remove heat generated compared to normal cutting fluids. Excess of chipping and crater wear have occurred during dry machining and resulted in the fracture of the tool. Tool wear of cutting tool has been observed less for wet machining compared to dry machining, the adhesion of particles is quite common for dry and wet



environments. The high thermal stress and cutting temperature associated with milling due to cyclic heating and cooling is the reason for edge chipping and cracking of cutting tool. The wet machining is not effective in heat removal and thermal crack which lead to chipping and fracture of cutting edge. The cryogenic cooling improved the wear resistance and microhardness of the cutting tool by the precipitation of  $\eta$  carbides in the cemented carbide microstructure (Varghese et al. 2019). It can be seen from Table 4.8 that there is an improvement in tool life from dry to wet and wet to the cryogenic environment for both coated and uncoated tools for all spindle speeds. The increase in tool life for the cryogenic environment is found to be in the range of 65-75% for all types of inserts with respect to the dry environment. The wear rate of the cutting tool is higher in wet machining than cryogenic machining because the soluble oil supplied at low pressure is not able to dispense the heat at the tool-chip interface. The liquid nitrogen had a higher cooling effect than soluble oil and reduce the friction between tool and workpiece to a minimum. The cryogenic liquid nitrogen applied in the cutting zone developed a chemically inert atmosphere which reduced cutting temperature to a minimum and protected cutting insert from cracking. The adhesion of particles on the tool is more in wet and dry machining due to strong affinity which exists between carbon particles in tungsten carbide inserts and maraging steel.

The maximum flank wear values of uncoated and coated inserts are measured using an optical microscope at an interval of 5 minutes for all milling experiments. The curves have been plotted for maximum flank wear ( $V_b$ ) at 270, 350 & 540 rpm in all environments and shown in Figure 4.27, Figure 4.28 & Figure 4.29. The graph reveals that coated tools show improved wear resistance compared to uncoated inserts in all environments. The AlCrN coated tools performed well rather than the AlTiN tools. The presence of chromium in the AlCrN coating starts reacting with atmospheric oxygen during the machining and forms  $CrO_2$  tribological layer which is highly worn resistant and reduces the wear rate. Thus AlCrN coating gives better wear resistance compared to AlTiN coated tools.

Table 4.8 shows the tool life for uncoated and coated inserts. By ISO 8688-1 the allowable flank wear for optimum tool life is  $V_b = 0.5$  mm. Based on these criteria, tool life is measured and tabulated. From the table, it can be seen that coated inserts

possess higher tool life than uncoated inserts. This is due to improved tribological properties of coated tools. Higher tool life indicates improved wear resistance capacity. Among the coated tools the AlCrN coated inserts gave better tool life than AlTiN. AlCrN exhibits 3-8 % higher tool life in comparison with AlTiN coated inserts under all the environments. This is due to the higher values of hardness possessed by the AlCrN inserts. Generally, the presence of chromium in coatings shows improved wear resistance due to the formation of chromium oxide tribo-film. Table 4.9 indicates the percentage improvement in tool life of coated tools compared to uncoated tools under different machining environments. The percentage improvement in tool life is calculated using expression  $((T_C - T_{UC}) / T_{UC} * 100)$ , where  $T_C$  is the tool life of coated tools and  $T_{UC}$  is the tool life of uncoated tools. The percentage improvement is highest (28.87 %) during cryogenic machining using AlCrN coated tools at a spindle speed of 270 rpm.

**Table 4.8** Tool life for maximum flank wear,  $V_b = 0.5$  mm.

Spindle speed	Tool life (min)								
	UC	AlTiN	AlCrN	UC	AlTiN	AlCrN	UC	AlTiN	AlCrN
(rpm)	Dry	Dry	Dry	Wet	Wet	Wet	Cryo	Cryo	Cryo
270	59	71	72	80	97	101	97	120	125
350	37	44	45	48	58	61	63	77	81
540	22	26	27	30	36	38	39	47	50

**Table 4.9** Percentage improvement in tool life of coated tools under different environment and spindle speeds.

Spindle speed	% improvement in tool life $((T_C - T_{UC}) / T_{UC} * 100)$					
	AlTiN	AlCrN	AlTiN	AlCrN	AlTiN	AlCrN
(rpm)	Dry	Dry	Wet	Wet	Cryo	Cryo
270	20.34	22.03	21.25	26.25	23.71	28.87
350	18.92	21.62	20.83	27.08	22.22	28.57
540	18.18	22.73	20.00	26.67	20.51	28.21

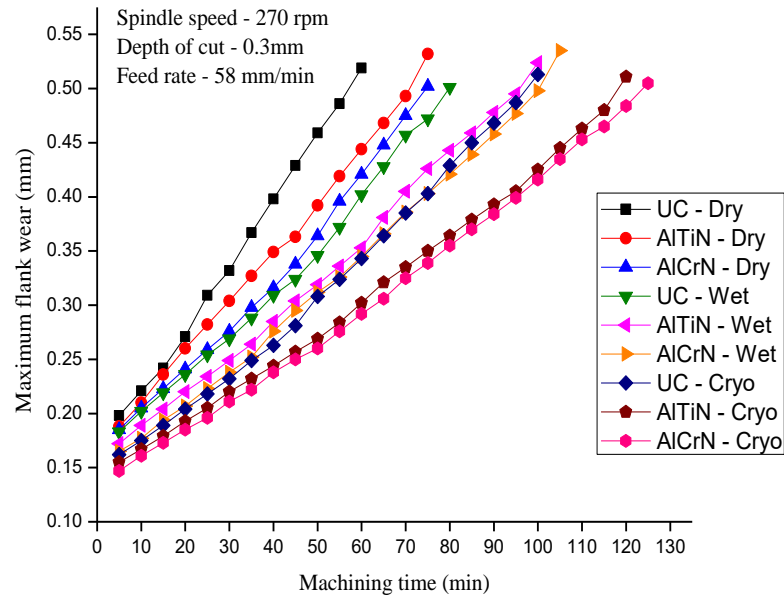


**Figure 4.27** Progression of flank wear with machining time at a spindle speed of 270 rpm.

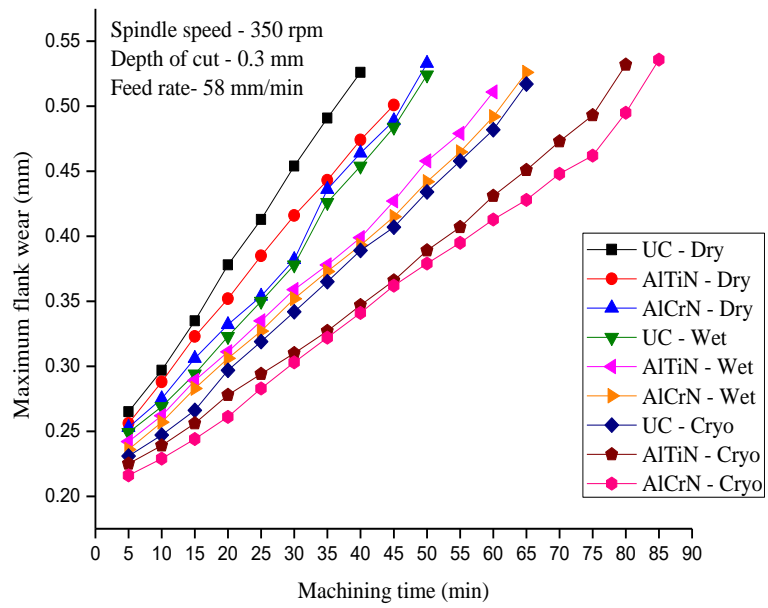


**Figure 4.28** Progression of flank wear with machining time at a spindle speed of 350 rpm.

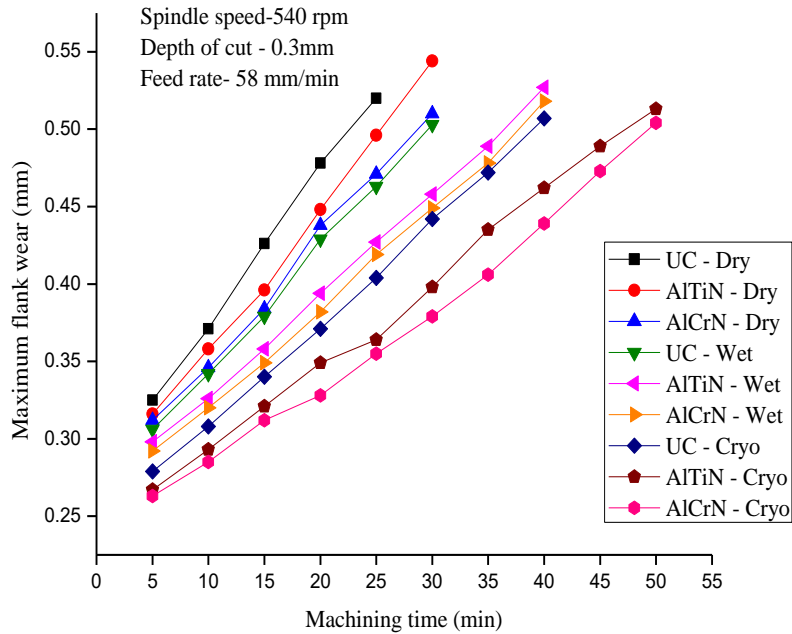


**Figure 4.29** Progression of flank wear with machining time at a spindle speed of 540 rpm.

#### 4.5.2 Cutting force

Cutting force is regarded as the measure of power consumption during the machining. Cutting force developed during machining is mainly affected by tool geometry, tool material, work material properties, cooling methods and machining parameters (speed, feed, and depth of cut). Generally, it is desired to have reduced values of cutting forces since it has a direct influence on the tool wear, tool life, and surface roughness. The experimental results show that cutting forces are reduced while using coated tools in comparison with uncoated tools.

Figure 4.30 depicts the variation of cutting force against spindle speed under various environments. It can be seen that the coated tools reduce the cutting forces by 8 -14 % compared to uncoated tools. This is mainly due to the high wear resistance characteristics of coated tools. The good mechanical properties of coatings like high hardness and plasticity index combined with the tribo-film protection helped the substrate from thermal stresses and softening (Thakur et al. 2016). The uncoated tool is subjected to cyclic stresses and fatigue due to the increasing cutting temperature

and wear progress quickly resulting in fracture of tool tip and cutting edge. The fracture and deformations in the tool tips of uncoated inserts lead to high cutting force. The high oxidation resistance and hot hardness of coatings reduce abrasive wear due to high cutting temperature (Devillez et al. 2007). The minimum friction developed between the applied coatings to the flowing chip also helped in lowering the magnitude of force components. It can be seen that AlCrN exhibits a 2-5 % reduction in cutting force compared to AlTiN coated tools. AlCrN coatings had a balanced hardness and toughness (PI) compared to AlTiN coating. The tribo-films of alumina ( $\text{Al}_2\text{O}_3$ ) and chromium oxides in AlCrN coating had better wear protection than titania ( $\text{TiO}_2$ ) and alumina in AlTiN coating. The better wear resistance combined with balanced hardness and toughness of AlCrN coating helped in protecting substrate and fracture of tool tip leading to a lower cutting force. These results hold good for the dry, wet and cryogenic environment.

It is found that as spindle speed increases the cutting force decreases in all environments. The localization of heat in the shearing zone at higher speeds makes cutting much easier. Larger friction present in the lower spindle speed makes machining and formation of chips difficult and thereby increases the cutting force (Ravi and Kumar 2011). It can be observed from Figure 4.30, that cutting forces are reducing from dry to wet and wet to the cryogenic environment. The use of coolants in machining reduces the temperature in the cutting zone. The reduced cutting temperature helps the tools to maintain their hardness. Thus wet and cryogenic environments result in reduced tool wear and cutting force in comparison with the dry environment. The cryogenic environment shows a higher cooling rate and increased lubrication effect by developing small lubrication layer in the machining zone. There is precipitation of  $\eta$  phase carbides and grain refinement occurring in the cutting tool during the cryogenic cooling which increases the wear resistance of cutting tool material (Gill et al. 2012a). There is 28-42 % reduction in cutting forces with the use of cryogenic cooling in comparison with dry conditions. Ravi and Kumar (2011) also reported a reduction in cutting force with cryogenic cooling compared to conventional dry and wet cooling.

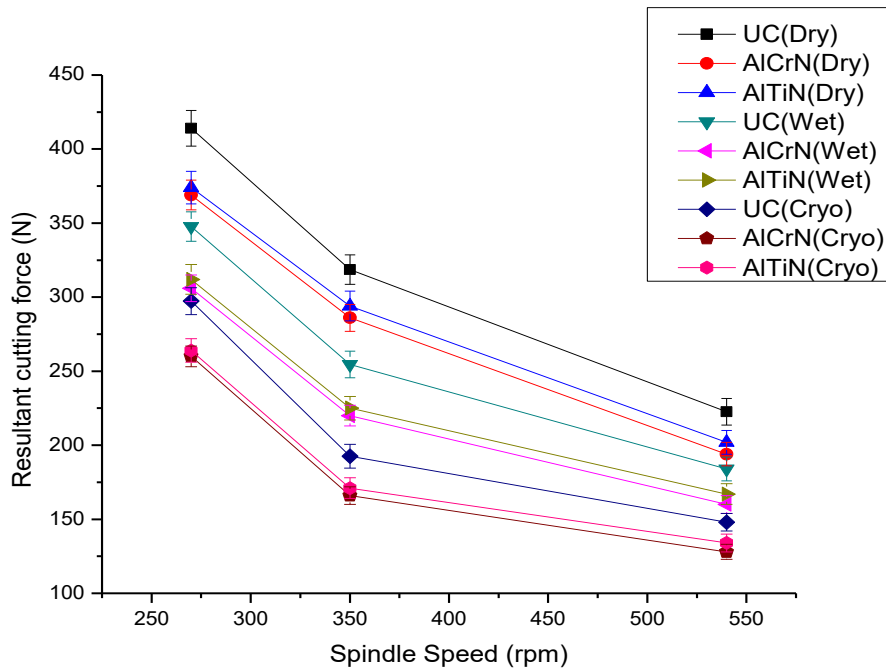


**Figure 4.30** Variation of cutting force with spindle speed using the coated and uncoated cutting tool under different environment.

### 4.5.3 Surface roughness

The surface roughness of the machined component has a critical effect on the performance and service life of components, especially the components fatigue life. So the manufacturer always desired to have low values of surface roughness. The average values of surface roughness of maraging steel after machining at a spindle speed of 270, 350 & 540 rpm under various environments are shown in Figure 4.31. The results revealed that coated tools provide a better surface finish than uncoated tools. The range of reduction in surface roughness for coated tools in comparison with uncoated ones is found to be 8-18% respectively. Tool wear is an important factor which affects the surface finish during machining. The high hardness and toughness (PI) of coated tools reduced the tool wear which in turn lead to reduced surface roughness. The high surface roughness is a result of tool marks and other defects during machining. The worn out tool tip and any deformations in the cutting edge leaves marks on the machined surface. The abrasive wear and fracture is more common in uncoated tools and resulted in abrasive marks on the machined surface.

The coatings acted as a thermal barrier in protecting the high temperature generated during machining from reaching substrate insert (Krain et al. 2007). There is a 2-7% reduction in surface roughness while using AlCrN inserts compared to AlTiN inserts. This is due to improved tribological properties and micromechanical characteristics of AlCrN over AlTiN coatings. The chromium oxide films protected the AlCrN coating from tool wear and resulted in longer tool life and better surface finish. The surface morphology and thermal conductivity also play a role in reducing surface roughness (Thakur et al. 2016). The AlCrN coating had a better finish than AlTiN coating and resulted in less adhesion of material particles. These above results hold good for all environments and spindle speeds.

It can be seen that as the spindle speed increases the surface finish improves. This is due to the fact that an increase in spindle speed increases the temperature in the cutting zone and thereby severe plastic deformation and softening of the machined surface (Ravi and Kumar 2011). This leads to an improvement in surface finish. Also, the BUE formation reduces with an increase in spindle speed which is the main reason for the rapid increase in flank wear. Table 4.10 presents the percentage reduction in surface roughness of machined samples using coated tools under different environment and spindle speed. The expression for calculation of percentage reduction is  $((R_{UC}-R_C)/ R_{UC}*100)$ , where  $R_{UC}$  is the surface roughness using the uncoated tool and  $R_C$  is the surface roughness using coated tool. The maximum percentage reduction in surface roughness (17.65 %) is using AlCrN coated tools during cryogenic machining at a spindle speed of 540 rpm. The surface roughness of the machined component depends on the temperature and friction developed in the machining zone. During dry machining, the side flow of chips occurs and increases the friction between workpiece and chips and deteriorate the surface finish. Generally, the use of cutting fluids reduce the cutting temperature and friction by removing the heat from the cutting zone. Due to the reduced temperature effect, the chip can become brittle and easy to break. The reduction in cutting temperature during cryogenic cooling results in minimum chip thickness thereby reducing the side flow and ploughing caused by the chips (Schoop et al. 2017).

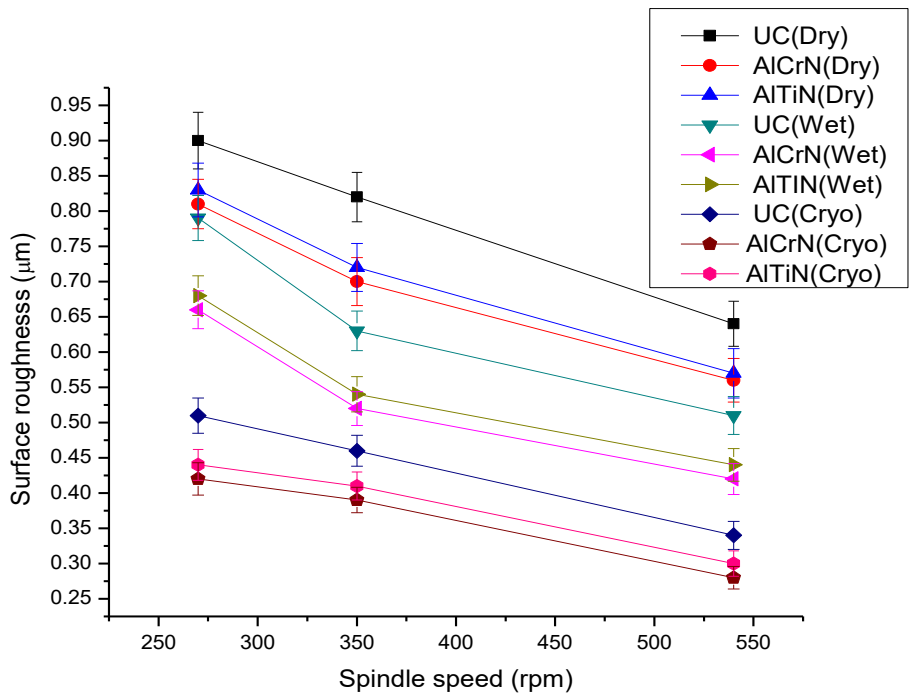


**Figure 4.31** Variation of surface roughness with spindle speed using coated and uncoated cutting tool under different environment.

**Table 4.10** Percentage reduction in surface roughness of machined sample using coated tools.

Spindle Speed	% reduction in surface roughness $((R_{UC}-R_C)/R_{UC}*100)$					
	AlTiN	AlCrN	AlTiN	AlCrN	AlTiN	AlCrN
rpm	Dry	Dry	Wet	Wet	Cryo	Cryo
270	7.78	10.00	14.36	16.32	12.87	16.83
350	12.20	14.63	14.29	15.20	10.87	17.46
540	10.94	12.50	13.73	16.65	11.76	17.65

## SUMMARY

The PVD coated tools can significantly enhance the machinability by extending tool life, better surface quality and the reduced cutting force resulting in reduced power consumption.



- The AlCrN coatings provide better machinability in comparison with AlTiN coatings. The micromechanical characteristics like hardness and plasticity index of AlCrN coatings are higher than AlTiN coatings. The aluminium chromium oxide and chromium oxide films formed due to oxidation help AlCrN to have a better wear resistance and lower thermal conductivity.
- The coated inserts showed wear resistance even at high spindle speed, and thereby reduction in chipping, crater wear and built up edge (BUE). The tool life of cutting tool improved up to 29 % during high-speed cutting while using AlCrN coated insert.
- The resultant cutting force reduced significantly using AlCrN coated inserts. The wear resistance and better tool life of coated inserts reduced the chatter and vibration of the cutting tool which resulted in a lesser cutting force during machining.
- The surface roughness of workpiece reduced significantly using coated inserts. The reduction in tool wear and cutting temperature resulted in a better surface finish.
- The cryogenic environment provides better machinability in terms of reduced tool wear, improved tool life and decreased cutting force and surface roughness.

## **4.6 CHARACTERIZATION OF TiSiN & TiAlSiN COATED TOOLS**

### **4.6.1 Microstructure and phase changes**

The microstructure of TiAlSiN & TiSiN coatings is shown in Figure 4.32. The surface morphology of coatings revealed that a homogenous and uniform coating consisting of spherically shaped clusters has been formed using a magnetron sputtering technique. The elemental composition of coatings are summarized in Table 4.11 and illustrated in Figure 4.33. The EDS analysis shows the presence of elements like Ti, Al, Si, N & O respectively. Figure 4.34 presents the XRD analysis of coatings. The XRD patterns of coatings show the presence of nanocrystalline TiAlN in TiAlSiN coatings and TiN in TiSiN coatings. The high temperature during magnetron

sputtering would have resulted in the melting of  $\text{Si}_3\text{N}_4$  phase. The XRD analysis of coatings showed the presence of TiN & substrate phase in TiSiN and TiAlN, TiN phase in TiAlSiN. The TiAlSiN structure mainly consists of amorphous  $\text{Si}_3\text{N}_4$  phase and nano-crystalline TiAlN phase. The amorphous phase cannot be seen in the XRD analysis but the presence of Silicon is evident from EDS results. The addition of aluminium and silicon into the nano-crystalline TiN has changed the morphology of TiSiN & TiAlSiN coatings from columnar to non-columnar structure (Cheng et al. 2009). The change from columnar to non-columnar structure helps in improving the mechanical properties of the coating as the columnar structure suffers from weaker bonding between the columns. The microstructure also revealed that TiAlSiN coating has a denser and uniform distribution of particles compared to TiSiN coating. The reduced intensity of TiN phase in TiSiN & TiAlSiN coating is an indication of decreased grain size (She-quan et al. 2011). Also, the broadening of TiAlN peak in TiAlSiN coating proves the grain size of TiAlSiN coating (35 nm) is much smaller compared to TiSiN coating (72 nm). The coating thickness is found to be 1-1.4  $\mu\text{m}$  for TiAlSiN coating and 1.4-1.8  $\mu\text{m}$  for TiSiN coating from the cross-section microstructure. The coating thickness and surface roughness are given in Table 4.12. The surface roughness of TiSiN coating (0.323  $\mu\text{m}$ ) is quite high compared to TiAlSiN coating (0.242  $\mu\text{m}$ ).

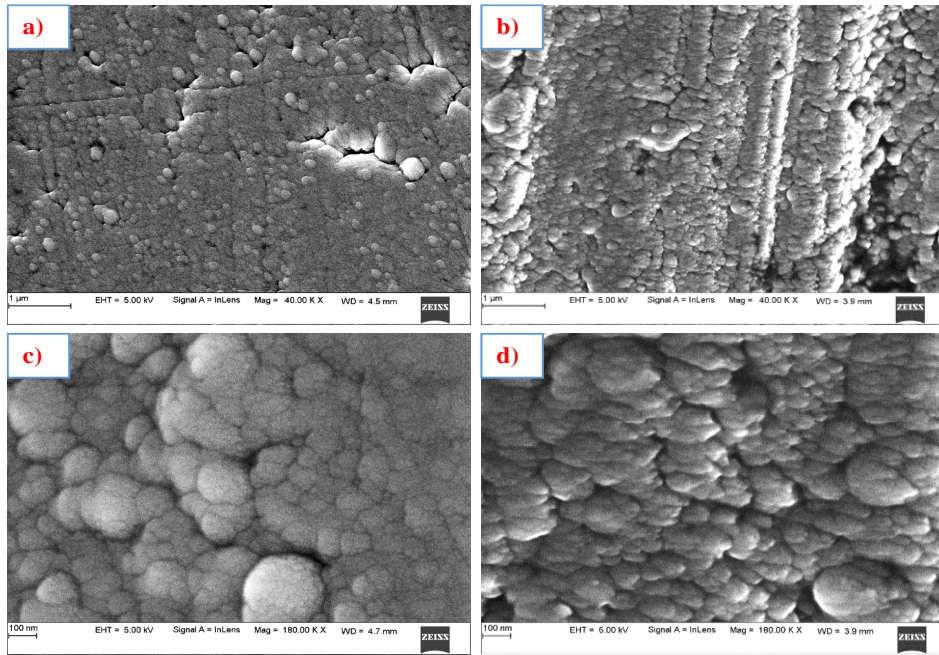


**Figure 4.32** Microstructure of coatings a) TiAlSiN at 40 K X b) TiSiN at 40 K X c) TiAlSiN at 100 K X d) TiSiN at 100 K X.

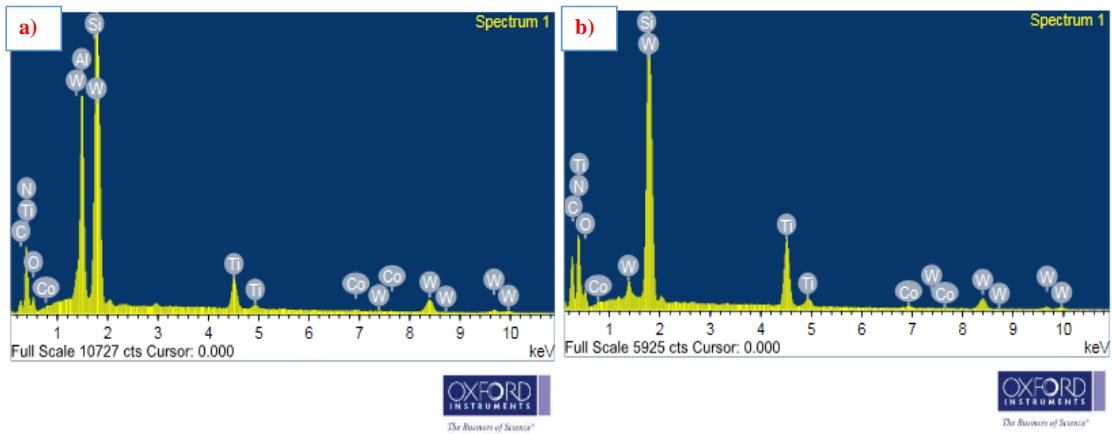


**Figure 4.33** EDS analysis of a) TiAlSiN b) TiSiN coatings.

**Table 4.11** Chemical composition of coatings from EDS analysis.

Designation	Ti (At. %)	Al (At. %)	Si (At. %)	N (At. %)	O (At. %)
TiAlSiN	4.76	13.82	3.14	59.96	18.32
TiSiN	16.58	-	4.94	67.46	11.02

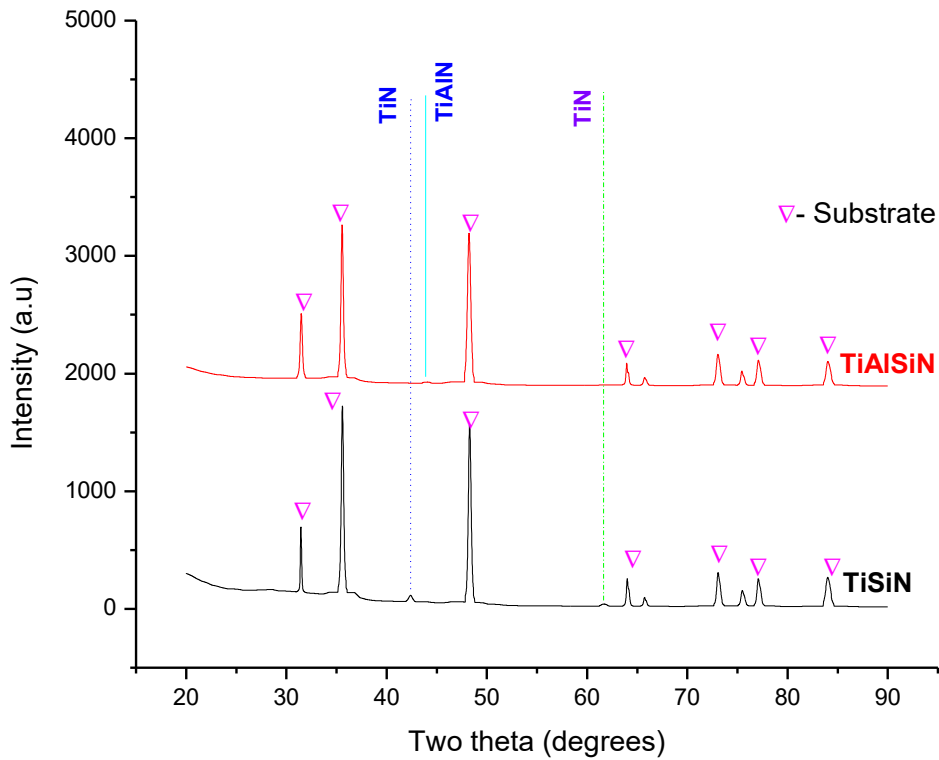


**Figure 4.34** XRD patterns of TiAlSiN & TiSiN coated WC-Co inserts.

**Table 4.12** Micro mechanical characteristics of TiAlSiN and TiSiN coatings.

Coatings	Thickness	Surface roughness	Hardness (H)	Young's modulus (E)	H/E Ratio	H <sup>3</sup> /E <sup>2</sup> Ratio	Plasticity index, [1-x(H/E)]
	μm	μm	GPa	GPa		GPa	
TiAlSiN	1.2	0.242	32 ± 2.1	380±5.6	0.084	0.227	0.975
TiSiN	1.6	0.323	28 ± 1.8	285±3.1	0.098	0.185	0.970

### 4.6.2 Raman spectroscopy

The raman spectroscopy is used to study the thermal stability of TiSiN and TiAlSiN coatings. The thermal stability of coatings is important as a cutting tool has to operate at high cutting temperature. The high cutting temperature while machining can result in the oxidation of coatings and affect the wear resistance of coatings. Figure 4.35

indicates the raman spectroscopy of TiSiN and TiAlSiN coatings. The raman spectroscopy of TiSiN shows one broad band centred approximately at 579. This band corresponds to the optic and acoustic modes in the  $100\text{ cm}^{-1}$  region. Scattering of heavy metal (Ti) ions results in the acoustic mode and scattering of light element (N) ions results in optic mode. Similarly, for TiAlSiN coating, raman spectra consist of two bands centred approximately at 220 & 560. The study by Barshilia et al. (2010) found the two bands in the raman spectra of TiAlSiN coatings represent the optic and acoustic modes. The bands between the region  $150$  and  $350\text{ cm}^{-1}$  represent the acoustic mode due to the scattering of heavy metal (Ti, Al) ions and the bands between the region  $400$  and  $650\text{ cm}^{-1}$  represent optic mode due to scattering of light metal (N) ions.

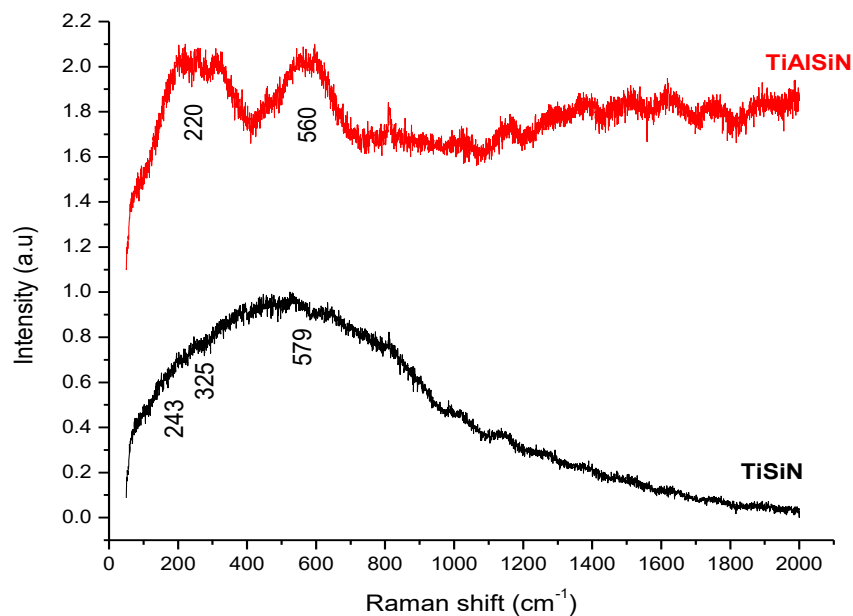


**Figure 4.35** Raman spectroscopy of TiAlSiN & TiSiN coatings.

### 4.6.3 Micromechanical characterisation

The coating thickness, surface roughness and mechanical properties of coatings are summarized in Table 4.12. The micromechanical characteristics of coatings revealed that hardness and Young's modulus is greater for TiAlSiN coating (32 GPa & 380 GPa) compared to TiSiN coating (28 GPa & 285 GPa). The increased Si percentage in TiSiN coatings formed a non-columnar structure and resulting in good mechanical

properties with better bonding between atoms. The measure of resistance to local plastic deformation is known as hardness. The hardness and toughness are the key aspects to evaluate and predict the tribological aspects for engineering applications (Ou et al. 2018). High hardness along with a good toughness is vital for the wear resistance of coatings under severe cutting conditions (Yuan et al. 2017). The hardness is directly correlated to slipping of dislocation and nucleation. The high Si content in the TiSiN reduced the grain size of the particle and plastic deformation mechanism happening in smaller grain size are grain boundary sliding and not dislocation sliding. The dislocations are generally absent in the case of TiSiN coating due to smaller grain size. The high hardness of TiSiN coating is due to the high bonding energy of Si- Ti and Si-N bonds in the grain boundary which resisted the grain sliding (Cheng et al. 2010). The strong interphase boundary between nanocrystalline TiAlN and amorphous Si<sub>3</sub>N<sub>4</sub> phase with high cohesive energy combined with grain size refinement should be the reason for the high hardness of TiAlSiN coating. In addition, the solution hardening incorporation of Al can also be the reason for higher hardness. The small grain size of TiAlSiN hinders the dislocation movement and dislocations are generally absent at very small grains resulting in high hardness. The quaternary coating (TiAlSiN) has better hardness than ternary coating (TiSiN) because the interface phase (Si<sub>3</sub>N<sub>4</sub>) retards the decomposition phase of TiAlN phase (Wang et al. 2010). Generally cutting tools requires higher values of hardness in order to avoid the drastic tool wear. Higher H/E values are obtained for TiSiN coating which is a measure of plasticity. The load-bearing capacity ( $H^3/E^2$ ) of TiAlSiN coating (0.227 GPa) is found to be higher than TiSiN coating (0.185 GPa), which indicates the plastic deformation resistance and fracture toughness is more for the former. In general tribological conditions, the higher H/E values result in lower wear. But the hardness and H/E ratio are inadequate to evaluate the performance of the coating in the severe cutting conditions like high-speed machining (Beake et al. 2009). The plasticity index is a measure of toughness and is more reliable to evaluate the actual cutting conditions. The TiAlSiN coating has higher plasticity index compared to the TiSiN coating. The plasticity index of the coating is correlated with the tool life in end milling of hardened steel (Beake et al. 2015).

## **4.7 MILLING PERFORMANCE CHARACTERISTICS OF TiSiN & TiAlSiN COATED TOOLS UNDER DRY, WET & CRYOGENIC ENVIRONMENTS**

### **4.7.1 Tool wear and tool life**

The dominant tool wears observed in the coated inserts during dry and wet milling is flank wear & chipping, not crater wear at rake face. The SEM image of flank wear during dry, wet and cryogenic milling at a spindle speed of 540 rpm is shown in Figure 4.36. The flank wear progression followed a V pattern due to the high abrasive wear while machining. The best wear performance is by TiAlSiN coated carbide tools during cryogenic end milling. This is because of the good mechanical properties of TiAlSiN coating like high hardness and toughness which helped in resisting wear. The dry environment machining involves high thermal stress due to the high heat generated. The high heat generated to deteriorate the adhesion between coating and substrate and results in peeling of the coating. The substrate is exposed after this and leads to fracture of the cutting tool. The abrasive wear is more during dry machining and a rapid progression of flank wear reduces the tool life. The tribo oxide films like  $\text{TiO}_2$ ,  $\text{SiO}_2$ ,  $\text{Al}_2\text{O}_3$  &  $\text{Al}_x\text{Si}_y\text{O}_z$  protects the TiAlSiN coating, whereas  $\text{TiO}_2$  &  $\text{SiO}_2$  protects the TiSiN coating. The presence of oxygen is evident from the EDS results (Figure 4.33) of coatings and the formation of oxide films on coatings is expected. The  $\text{TiO}_2$  &  $\text{SiO}_2$  protective layer in the TiSiN coating is comparatively weak when compared to strong oxide layers of  $\text{Al}_2\text{O}_3$  and  $\text{Al}_x\text{Si}_y\text{O}_z$  in TiAlSiN coating (Fukumoto and Ezura 2009). The alumina and silica tribo films formed on the coatings has played a vital role in increasing the wear resistance of TiAlSiN coating (Fuentes et al. 2010). The TiSiN coating and TiAlSiN coating is fractured more under dry environment than under wet & cryogenic environment. The abrasive wear is less under a wet environment as the cutting temperature dropped, better lubrication and chip removal also helped. The adhesion and built up edge formation is also less during wet machining giving a better surface finish. The micro chipping and peeling of coating are also observed in coatings under a wet environment. The chipping and adhesion of chips are comparatively less in cryogenic machining as  $\text{LN}_2$  penetrated into the tool-

chip interface and reduced the cutting temperature. The cryogenic machining reduced the tool wear of coated and uncoated tool to maximum compared to dry and wet machining. The environment has a predominant role in cutting temperature developed in the machining zone. The larger values of cutting temperature in the workpiece-tool interface cause the thermal fatigue of the tool and thereby increased tool wear, which leads to premature failure of the tool. The use of cutting fluids in the machining zone helps to remove the temperature generated which reduces the thermal fatigue and thereby tool wear. The results were in accordance with studies by Yuan et al. (Yuan et al. 2017) where TiSiN coatings had the lowest tool life. The pin hole defects affected the wear resistance and tool life of TiSiN coatings even though having good mechanical properties.

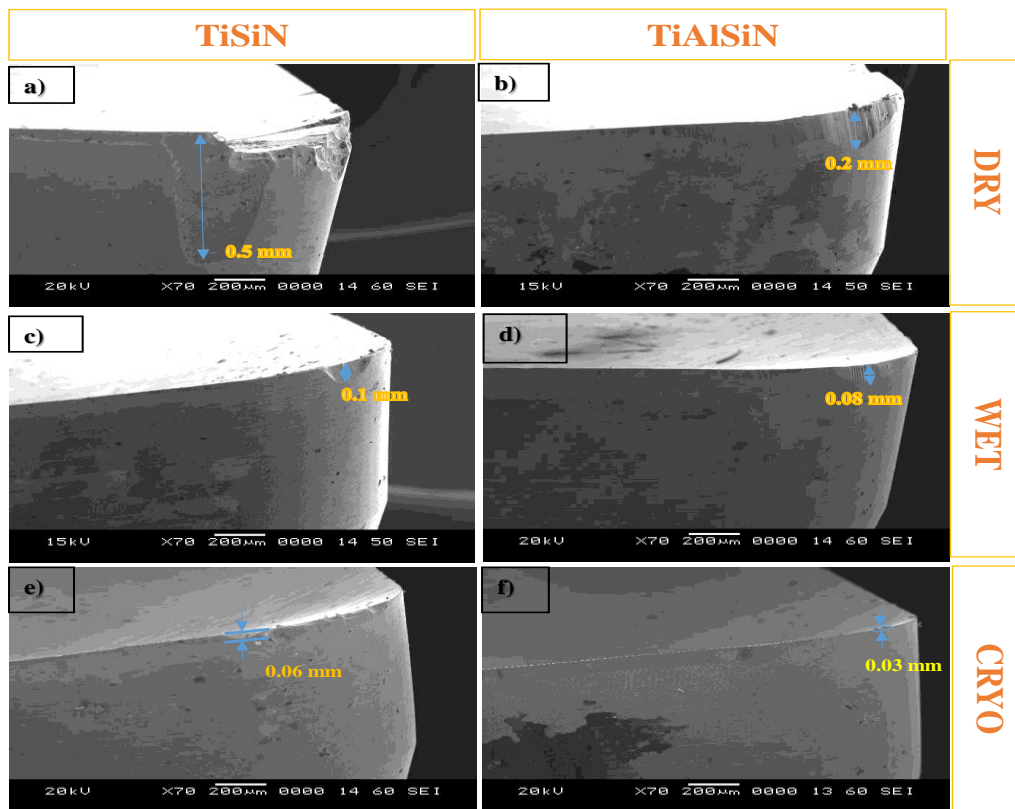


**Figure 4.36** Flank wear of coated inserts at a spindle speed of 540 rpm a) TiSiN coated insert under dry environment b) TiAlSiN coated insert under dry environment c) TiSiN coated insert under wet environment d) TiAlSiN coated insert under wet environment e) TiSiN coated insert under cryogenic environment f) TiAlSiN coated insert under cryogenic environment.



The progression of flank wear of coated and uncoated tools during machining under dry, wet and cryogenic environments at a spindle speed of 270, 350 & 540 rpm taken at an interval of 5 minutes are presented in Figure 4.37, Figure 4.38 and Figure 4.39 respectively. The tool life is estimated on the basis of maximum flank wear criteria of 0.5 mm (ISO 8688-2:1989) and the same is presented in Table 4.13. The coated tools resisted the flank wear for a long time compared to uncoated tools and extended their tool life. The cutting tools had a better flank wear resistance during lower spindle speeds and progression of flank wear increased during higher spindle speeds. Thus resulting in a better tool life during lower spindle speeds. The cutting tool is worn fast during cutting under dry machining and resulted in lesser tool life compared to wet machining. TiAlSiN coated tools had a better wear resistance compared to the TiSiN coated tool and resulted in maximum tool life of 102 minutes during wet machining at a spindle speed of 270 rpm. The formation of tribo films of  $Al_2O_3$  and  $Al_xSi_yO_z$  in TiAlSiN coating protects the cutting tool from the progression of flank wear and results in higher tool life. The wet environment reduces the cutting temperature and provides better lubrication and cooling compared to a dry environment. The reduction in cutting temperature reduces the thermal stresses and fatigue associated with insert and extends tool life. The cutting temperature is less during lower spindle speeds and reduces tool wear. It can be seen that the cryogenic environment performs superior over the other environments. This is due to the increased capacity of  $LN_2$  to remove heat generated compared to normal cutting fluids.

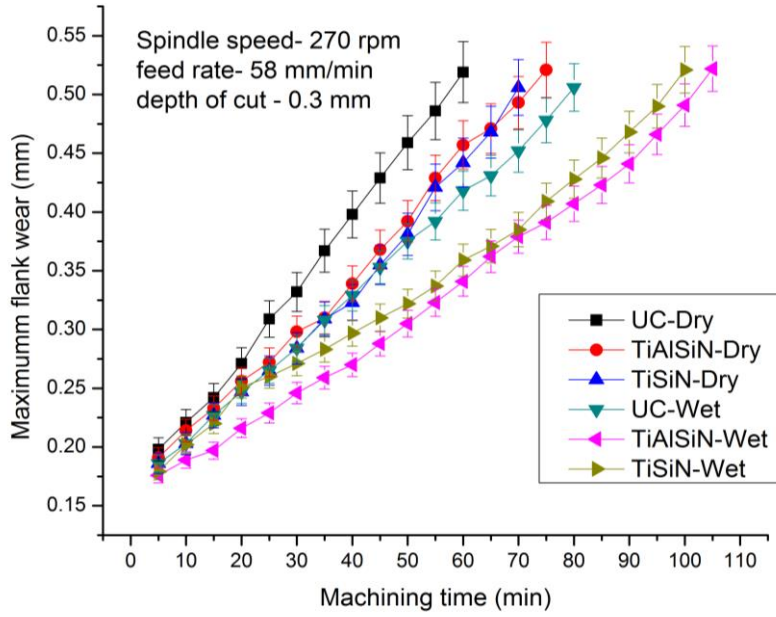


**Figure 4.37** Progression of flank wear of different cutting tool at a spindle speed of 270 rpm.

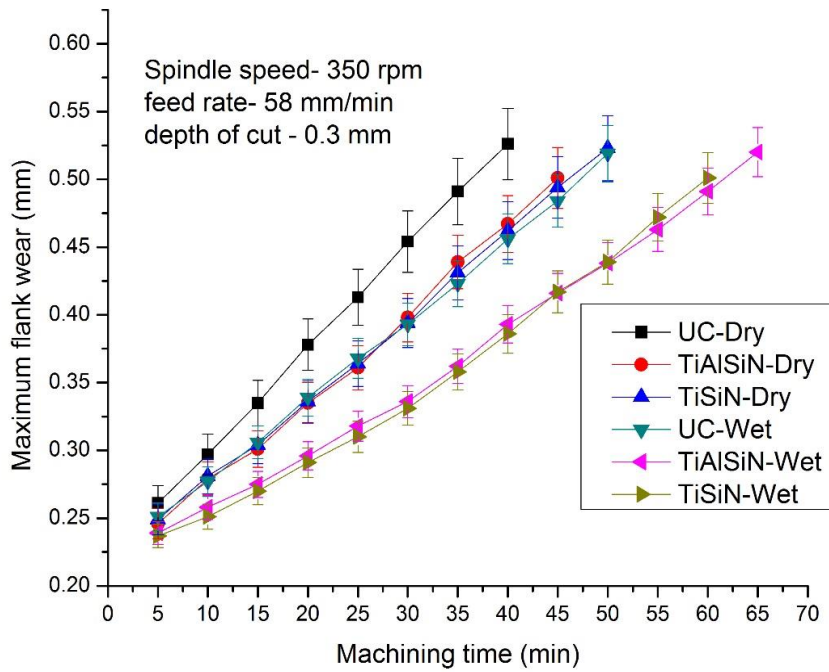


**Figure 4.38** Progression of flank wear of different cutting tool at a spindle speed of 350 rpm.

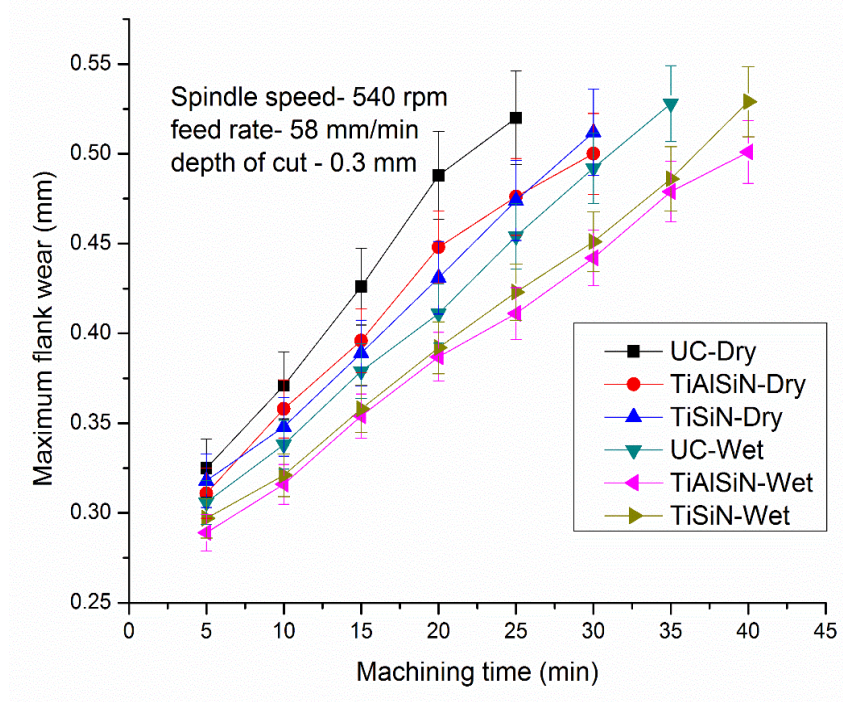


**Figure 4.39** Progression of flank wear of different cutting tool at a spindle speed of 540 rpm.

**Table 4.13** Tool life of cutting tools at different spindle speed and cutting environments.

Spindle speed	Tool life (min)								
	UC	TiAlSiN	TiSiN	UC	TiAlSiN	TiSiN	UC	TiAlSiN	TiSiN
(rpm)	Dry	Dry	Dry	Wet	Wet	Wet	Cryo	Cryo	Cryo
270	59	71	70	80	102	96	97	122	121
350	37	45	46	48	61	60	63	83	80
540	22	30	28	32	40	37	39	54	49

### 4.7.2 Cutting force

The resultant cutting force ( $F_R$ ) is used to analyse the cutting force while machining (Varghese et al. 2018b). The cutting force is directly correlated with power consumption during machining. So it is recommended to have a lower cutting force while machining to reduce the power consumption. It is also a measure of machinability index. Figure 4.40 presents the variation of resultant cutting force while

machining at a spindle speed of 270, 350 & 540 rpm using the coated carbide tool under dry wet and cryogenic environments. It is observed that TiAlSiN coated tools had lower cutting force than TiSiN coated tools under dry and wet environment. The cutting force decreased as the spindle speed increased, the chatter and vibration are more at lower spindle speed. The high hardness, Young's modulus and toughness of TiAlSiN coatings improved the wear resistance of the coating and resulted in a lower cutting force. The uniform and dense microstructure along with reduced grain size also attributed to a reduction in cutting force. The higher friction coefficient of TiSiN coatings also resulted in an increase in cutting forces (Yuan et al. 2017). The cutting force is high during machining under dry environment as the high cutting temperature increased the thermal stress and resulted in the fracture of the coating. The higher wear resistance of TiAlSiN coating helped to extend the tool life and reduce the cutting force even in the dry environment. The TiSiN coating had a higher wear rate and increased the cutting force while machining. The better lubrication and cooling effects of a cryogenic environment not only reduced the wear rate but also the cutting force. TiAlSiN coating had a better performance than TiSiN coatings and major wear mechanisms like abrasive wear, BUE formation and fracture of coatings eliminated during cryogenic machining. The tribo protective layers like alumina ( $Al_2O_3$ ) & silica ( $SiO_2$ ) also helped TiAlSiN coated tools to reduce the friction coefficient and cutting force.

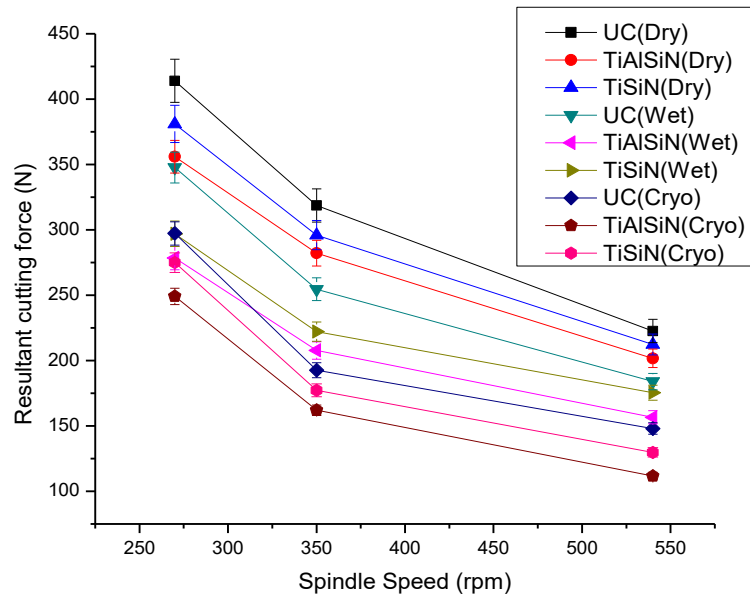


**Figure 4.40** Variation of resultant cutting force with spindle speed during dry, wet and cryogenic milling using coated carbide inserts.

### 4.7.3 Surface roughness

The surface roughness is a measure of surface integrity which affects the fatigue life of the components produced. The lower surface roughness will give a better finish and protect the component from fatigue failure. The surface roughness of maraging steel after machining at different spindle speed using TiSiN and TiAlSiN coated tools has been presented in Figure 4.41. It can be observed that the surface roughness reduced as the spindle speed increased and TiAlSiN coated tools produced a better surface finish compared to TiSiN coated tools. The wet environment helped to reduce the surface roughness of the machined surface to a large extent as seen in the figure. As the spindle speed increased, the cutting temperature also increased and resulted in the thermal softening of the workpiece. It also helped in removing the surface discontinuities and other defects along with easy chip removal. The high spindle speed also reduced the chatter and vibration of the cutting tool thereby leaving fewer tool marks on the workpiece surface. The high hardness and plasticity index of TiAlSiN coating helped to extend the wear resistance and tool life of the cutting inserts. The high wear resistance of TiAlSiN coated tool improved the surface finish

of machined workpiece compared to the TiSiN coated inserts. The fractured tool leaves more marks on the workpiece surface and it is desired to have better wear resistance for better surface finish. The alumina and silica tribo films are the reason for the wear protection of the TiAlSiN coatings and better finish of maraging steel. The cryogenic coolant helped in reducing the cutting temperature and provided better lubrication compared to the dry & wet cutting. The use of cryogenic coolant also resulted in easy chip disposal and reducing tool marks on the machined surface. The employment of coolant improved the chip breakability of the coated tool and reduced the coefficient of friction. The results were in accordance with previous works (Sivaiah and Chakradhar 2017a).

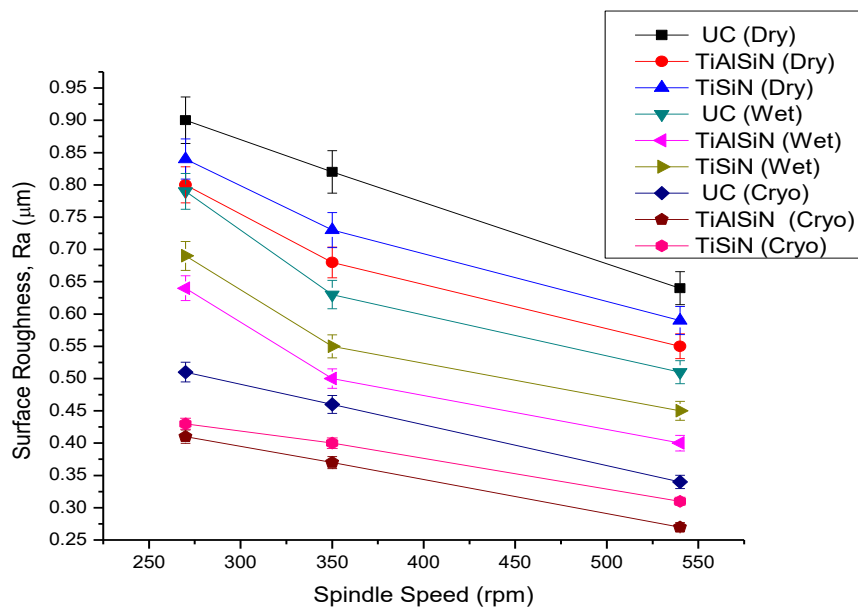


**Figure 4.41** Variation of surface roughness with spindle speed during dry, wet and cryogenic milling using coated carbide inserts.

## SUMMARY

The TiSiN & TiAlSiN coatings are well deposited on WC-Co milling inserts using PVD magnetron sputtering technique with TiSi (80/20) and TiAlSi (54/36/10) targets. The microstructure and mechanical properties of coatings were studied along with the mechanical performance of coatings during end milling of maraging steel by varying spindle speed. The following conclusions are drawn from the study:

- The microstructure revealed that coatings were uniform and densely distributed and formed a nanocrystalline structure of TiN & amorphous Si<sub>3</sub>N<sub>4</sub> phase in TiSiN coating and nanocrystalline structure of TiAlN & amorphous Si<sub>3</sub>N<sub>4</sub> phase in TiAlSiN coating.
- TiAlSiN coating had higher hardness and Young's modulus than TiSiN coating. Also, the load bearing capacity ( $H^3/E^2$  ratio) and plasticity index of the coating of TiAlSiN coating is also higher for TiSiN coating.
- The TiAlSiN coating had better wear resistance than TiSiN coating due to good mechanical properties and resulted in tool life enhancement.
- The highest tool life observed during end milling using TiAlSiN coating is 122 minutes at a spindle speed of 270 rpm under a cryogenic environment.
- The coatings performed better under cryogenic environment than the dry and wet environment. The abrasion wear, BUE formation and the fracture were more during dry machining. While adhesion wear, coating peels off and microchipping is observed more during wet machining.
- The cutting force and surface roughness is higher while machining using a TiSiN coated tool compared to TiAlSiN coated tool.





## CHAPTER 5

### 5 CONCLUSIONS AND SCOPE FOR FUTURE WORK

#### 5.1 CONCLUSIONS

The studies on end milling of maraging steel are carried out using PVD coated and cryogenically treated cemented carbide inserts under different machining environments. The cryogenic treatment is carried out at different soaking periods and analysed the characteristics as well as the machining performance. The PVD coatings were developed using cathodic arc deposition (CAD) as well as magnetron sputtering. Characterisation and machining performance of coated tools has been carried out under dry, wet and cryogenic environments. The following are some of the conclusions drawn from the experimental work.

- The cryogenic treatment can significantly enhance the machinability by extending tool life, better surface quality and the reduced cutting force resulting in reduced power consumption. The optimum soaking period of cryogenic treatment for better machinability is found to be 24 hours (CT-24).
- The grain refinement, precipitation of  $\eta$  phase carbides, more stable structure of  $\alpha$  phase, a decrease in  $\beta$  phase which resulted in an increase in compressive stress on tungsten carbide are some of the reasons to enhance the tool life after cryogenic treatment. The grain size of cryogenically treated samples reduced up to 22 % for CT-24.
- The microstructure revealed that coatings were uniform and densely distributed. The coated inserts showed wear resistance even at high spindle speed, and thereby reduction in chipping, crater wear and built up edge (BUE).
- The AlCrN coatings provide better machinability in comparison with AlTiN coatings. The micromechanical characteristics like hardness and plasticity index of AlCrN coatings are higher than AlTiN coatings. The aluminium

chromium oxide and chromium oxide films formed due to oxidation help AlCrN to have a better wear resistance and lower thermal conductivity.

- TiSiN coating formed a nanocrystalline structure of TiN & amorphous Si<sub>3</sub>N<sub>4</sub> phase and TiAlSiN coating formed a nanocrystalline structure of TiAlN & amorphous Si<sub>3</sub>N<sub>4</sub> phase. The TiAlSiN coating had better wear resistance than TiSiN coating due to good mechanical properties and resulted in tool life enhancement.
- The tool life is maximum using AlCrN coated tool (125 min) compared to cryogenic treated and other coated tools at a spindle speed of 270 rpm under cryogenic environment. AlCrN > TiAlSiN > AlTiN > TiSiN > CT-24 is the order of tool life of cutting tools.
- The cutting force is minimum when using TiAlSiN coated tool (111.7 N) compared to cryogenic treated and other coated tools at a spindle speed of 540 rpm under cryogenic environment. TiAlSiN < AlCrN < TiSiN < AlTiN < CT-24 is the order of cutting force of cutting tools.
- The surface roughness is minimum using TiAlSiN coated tool (0.27 μm) compared to cryogenic treated and other coated tools at a spindle speed of 540 rpm under cryogenic environment. TiAlSiN < AlCrN < AlTiN < TiSiN < CT-24 is the order of surface roughness of cutting tools.
- The coated and cryogenic treated tool performed better under cryogenic environment. The abrasion wear, BUE formation and the fracture were more during dry machining. While adhesion wear, coating peels off and microchipping is observed more during wet machining. The cryogenic environment provides better machinability in terms of reduced tool wear, improved tool life and decreased cutting force and surface roughness.

## **5.2 SCOPE FOR FUTURE WORK**

Although a lot of studies on machinability of maraging steel has been carried out using PVD coated and cryogenically treated cutting inserts. There is still scope for future work in this area. The following are the scope for future work in this area.

- The cryogenic treatment can be further extended to the PVD coated tools and study the characteristics and performance changes before and after the treatment.
- The cryogenic machining can be further studied by varying the flow rate and the effect of the phase of the coolant (liquid/gas) on the surface integrity of the machined surface.
- Different cryogenic coolants like helium and oxygen can be employed for machining and compared with nitrogen.
- Finite element analysis of machining under different environment to analyse cutting temperature, cutting force and residual stress can be studied.



## REFERENCES

- A. D. Shirbhate, N. V. D. and Y. M. P. (2012). "Effect of Cryogenic Treatment on Cutting Torque and Surface Finish in Drilling Operation With Aisi M2 High Speed Steel." *Int. J. Mech. Eng. Rob. Res.*, 1(2).
- Ahmed, L. S., and Kumar, M. P. (2016). "Cryogenic Drilling of Ti-6Al-4V Alloy Under Liquid Nitrogen Cooling." *Mater. Manuf. Process.*, 31(7), 951-959.
- Ahmed, L. S., and Pradeep Kumar, M. (2017). "Investigation of cryogenic cooling effect in reaming Ti-6AL-4V alloy." *Mater. Manuf. Process.*, 32(9), 970-978.
- Akhbarizadeh, A., Javadpour, S., Amini, K., and Yaghtin, A. H. (2013). "Investigating the effect of ball milling during the deep cryogenic heat treatment of the 1.2080 tool steel." *Vacuum*, 90(1), 70-74.
- Akincioglu, S., Gokkaya, H., and Uygur, I. (2015). "A review of cryogenic treatment on cutting tools." *Int. J. Adv. Manuf. Technol.*, 78(9-12), 1609-1627.
- Akincioglu, S., Gokkaya, H., and Uygur, İ. (2016). "The effects of cryogenic-treated carbide tools on tool wear and surface roughness of turning of Hastelloy C22 based on Taguchi method." *Int. J. Adv. Manuf. Technol.*, 82(1-4), 303-314.
- Alborz Shokrani, and S. T. N. (2019). "A New Cutting Tool Design for Cryogenic Machining of Ti-6Al-4V Titanium Alloy." *Materials (Basel)*, 12(477), 1-14.
- Amini, K., Akhbarizadeh, A., and Javadpour, S. (2012). "Investigating the effect of holding duration on the microstructure of 1.2080 tool steel during the deep cryogenic heat treatment." *Vacuum*, 86(10), 1534-1540.
- Amini, K., Akhbarizadeh, A., and Javadpour, S. (2014). "Investigating the effect of quench environment and deep cryogenic treatment on the wear behavior of AZ91." *Mater. Des.*, 54, 154-160.
- Aoyama, T., Kakinuma, Y., Yamashita, M., and Aoki, M. (2008). "Development of a new lean lubrication system for near dry machining process." *CIRP Ann. - Manuf. Technol.*, 57(1), 125-128.

Bailey, J. A. (1977). "Surface damage during machining of annealed 18% nickel maraging steel Part 1 - Unlubricated conditions." *Wear*, 42, 277–296.

Baldissera, P., and Delprete, C. (2008). "Deep Cryogenic Treatment: A Bibliographic Review." *Open Mech. Eng. J.*, 2(1), 1–11.

Baradie, M. a. El. (1996a). "Cutting fluids: Part I. Characterisation." *J. Mater. Process. Technol.*, 56(1–4), 786–797.

Baradie, M. a. El. (1996b). "Cutting fluids: Part II. Recycling and clean machining." *J. Mater. Process. Technol.*, 56(1–4), 798–806.

Barshilia, H. C., Ghosh, M., Shashidhara, Ramakrishna, R., and Rajam, K. S. (2010). "Deposition and characterization of TiAlSiN nanocomposite coatings prepared by reactive pulsed direct current unbalanced magnetron sputtering." *Appl. Surf. Sci.*, 256(21), 6420–6426.

Beake, B. D., Fox-Rabinovich, G. S., Veldhuis, S. C., and Goodes, S. R. (2009). "Coating optimisation for high speed machining with advanced nanomechanical test methods." *Surf. Coatings Technol.*, 203(13), 1919–1925.

Beake, B. D., Ning, L., Gey, C., Veldhuis, S. C., Komarov, A., Weaver, A., Khanna, M., and Fox-Rabinovich, G. S. (2015). "Wear performance of different PVD coatings during hard wet end milling of H13 tool steel." *Surf. Coatings Technol.*, 279, 118–125.

Beake, B. D., Smith, J. F., Gray, A., Fox-Rabinovich, G. S., Veldhuis, S. C., and Endrino, J. L. (2007). "Investigating the correlation between nano-impact fracture resistance and hardness/modulus ratio from nanoindentation at 25-500 °C and the fracture resistance and lifetime of cutting tools with Ti<sub>1-x</sub>Al<sub>x</sub>N (x = 0.5 and 0.67) PVD coatings in milling operatio." *Surf. Coatings Technol.*, 201(8), 4585–4593.

Bensely, A., Senthilkumar, D., Mohan Lal, D., Nagarajan, G., and Rajadurai, A. (2007). "Effect of cryogenic treatment on tensile behavior of case carburized steel-815M17." *Mater. Charact.*, 58(5), 485–491.

Bhukya, R., Rao, C. S. P., and Rao, G. V. (2014). "Evaluation and comparison of

- Machinability characteristics of Maraging Steel and AISI 304 Steels.” (Aimtdr), 1–7.
- Bosco, R., Beucken, J. Van Den, Leeuwenburgh, S., and Jansen, J. (2012). “Surface Engineering for Bone Implants: A Trend from Passive to Active Surfaces.” *Coatings*, 2, 95–119.
- Bouzakis, K. D., Skordaris, G., Gerardis, S., Katirtzoglou, G., Makrimallakis, S., Pappa, M., Lill, E., and M’Saoubi, R. (2009). “Ambient and elevated temperature properties of TiN, TiAlN and TiSiN PVD films and their impact on the cutting performance of coated carbide tools.” *Surf. Coatings Technol.*, 204(6–7), 1061–1065.
- Braham, T., Germain, G., Morel, A., and Benoit, F. (2015). “Influence of High-Pressure Coolant Assistance on the Machinability of the Titanium Alloy Ti555 – 3.” *Mach. Sci. Technol.*, 19(July 2015), 134–151.
- Brockhoff, T., and Walter, A. (1998). “Fluid Minimization in Cutting and Grinding.”
- Cassin, C., and Boothroyd, G. (1965). “Lubricating action of cutting fluids.” *J. Mech. Eng. Sci.*, 7(1), 67–81.
- Chen, L., Du, Y., Wang, A. J., Wang, S. Q., and Zhou, S. Z. (2009). “Effect of Al content on microstructure and mechanical properties of Ti – Al – Si – N nanocomposite coatings.” *Int. J. Refract. Met. Hard Mater.*, 27(4), 718–721.
- Cheng, Y. H., Browne, T., and Heckerman, B. (2009). “Nanocomposite TiSiN coatings deposited by large area filtered arc deposition.” *J. Vac. Sci. Technol. A Vacuum, Surfaces, Film.*, 27(1), 82.
- Cheng, Y. H., Browne, T., Heckerman, B., Jiang, J. C., Meletis, E. I., Bowman, C., and Gorokhovskiy, V. (2008). “Internal stresses in TiN/Ti multilayer coatings deposited by large area filtered arc deposition.” *J. Appl. Phys.*, 104(9).
- Cheng, Y. H., Browne, T., Heckerman, B., and Meletis, E. I. (2010). “Mechanical and tribological properties of nanocomposite TiSiN coatings.” *Surf. Coat. Technol.*, 204(14), 2123–2129.
- Chetan, Ghosh, S., and Venkateswara Rao, P. (2015). “Application of sustainable techniques in metal cutting for enhanced machinability: A review.” *J. Clean. Prod.*,

100, 17–34.

Cicek, A., Kivak, T., Uygur, I., Ekici, E., and Turgut, Y. (2012). “Performance of cryogenically treated M35 HSS drills in drilling of austenitic stainless steels.” *Int. J. Adv. Manuf. Technol.*, 60(1–4), 65–73.

Darwin, J. D., Mohan Lal, D., and Nagarajan, G. (2008). “Optimization of cryogenic treatment to maximize the wear resistance of 18% Cr martensitic stainless steel by Taguchi method.” *J. Mater. Process. Technol.*, 195(1–3), 241–247.

Das, D., Dutta, A. K., and Ray, K. K. (2009). “Optimization of the duration of cryogenic processing to maximize wear resistance of AISI D2 steel.” *Cryogenics (Guildf.)*, 49(5), 176–184.

Das, D., Dutta, A. K., Toppo, V., and Ray, K. K. (2007). “Effect of Deep Cryogenic Treatment on the Carbide Precipitation and Tribological Behavior of D2 Steel.” *Mater. Manuf. Process.*, 22(4), 474–480.

Devillez, A., Schneider, F., Dominiak, S., Dudzinski, D., and Larrouquere, D. (2007). “Cutting forces and wear in dry machining of Inconel 718 with coated carbide tools.” *Wear*, 262(7–8), 931–942.

Dhananchezian, M., Kumar, M. P., and Sornakumar, T. (2011). “Cryogenic Turning of AISI 304 Stainless Steel with Modified Tungsten Carbide Tool Inserts.” *Mater. Manuf. Process.*, 26(5), 781–785.

Dhande, S. T., Kane, V. A., Dhobe, M. M., and Gogte, C. L. (2018). “Influence of Soaking Periods Carbide in Cryogenic Treatment of Tungsten Carbide.” *Procedia Manuf.*, 20, 318–328.

Dhar, N. R., Islam, S., Kamruzzaman, M., and Paul, S. (2006a). “Wear behavior of uncoated carbide inserts under dry, wet and cryogenic cooling conditions in turning C-60 steel.” *J. Brazilian Soc. Mech. Sci. Eng.*, 28(2), 146–152.

Dhar, N. R., Kamruzzaman, M., and Ahmed, M. (2006b). “Effect of minimum quantity lubrication (MQL) on tool wear and surface roughness in turning AISI-4340 steel.” *J. Mater. Process. Technol.*, 172(2), 299–304.



- Dhar, N. R., Paul, S., and Chattopadhyay, A. B. (2001). "The influence of cryogenic cooling on tool wear, dimensional accuracy and surface finish in turning AISI 1040 and E4340C steels." *Wear*, 249(10–11), 932–942.
- Ding, Y., and Hong, S. Y. (1998). "Improvement of Chip Breaking in Machining Low Carbon Steel by Cryogenically Precooling the Workpiece." *J. Manuf. Sci. Eng.*, 120(1), 76.
- Dix, M., Wertheim, R., Schmidt, G., and Hochmuth, C. (2014). "Modeling of drilling assisted by cryogenic cooling for higher efficiency." *CIRP Ann. - Manuf. Technol.*, 63(1), 73–76.
- Endrino, J. L., Fox-Rabinovich, G. S., and Gey, C. (2006). "Hard AlTiN, AlCrN PVD coatings for machining of austenitic stainless steel." *Surf. Coatings Technol.*, 200(24), 6840–6845.
- Ezugwu, E. O. (2005). "Key improvements in the machining of difficult-to-cut aerospace superalloys." *Int. J. Mach. Tools Manuf.*, 45(12–13), 1353–1367.
- Feng, S., and Hattori, M. (2000). "Cost and Process Information Modeling for Dry Machining." *Proc. Int. Work. Environ. Conscious Manuf.*, 1–8.
- Fortunato, A., Lulaj, A., Melkote, S., Liverani, E., Ascari, A., and Umbrello, D. (2018). "Milling of maraging steel components produced by selective laser melting." *Int. J. Adv. Manuf. Technol.*, 94(5–8), 1895–1902.
- Fox-Rabinovich, G. S., Kovalev, A. I., Aguirre, M. H., Beake, B. D., Yamamoto, K., Veldhuis, S. C., Endrino, J. L., Wainstein, D. L., and Rashkovskiy, A. Y. (2009). "Design and performance of AlTiN and TiAlCrN PVD coatings for machining of hard to cut materials." *Surf. Coatings Technol.*, 204(4), 489–496.
- Fuentes, G. G., Almandoz, E., Pierrugues, R., Martínez, R., Rodríguez, R. J., Caro, J., and Vilaseca, M. (2010). "High temperature tribological characterisation of TiAlSiN coatings produced by cathodic arc evaporation." *Surf. Coatings Technol.*, 205(5), 1368–1373.
- Gill, S. S., Singh, H., Singh, R., and Singh, J. (2011a). "Flank Wear and Machining

Performance of Cryogenically Treated Tungsten Carbide Inserts.” *Mater. Manuf. Process.*, 26(11), 1430–1441.

Gill, S. S., Singh, J., Singh, H., and Singh, R. (2011b). “Investigation on wear behaviour of cryogenically treated TiAlN coated tungsten carbide inserts in turning.” *Int. J. Mach. Tools Manuf.*, 51(1), 25–33.

Gill, S. S., Singh, J., Singh, H., and Singh, R. (2012a). “Metallurgical and mechanical characteristics of cryogenically treated tungsten carbide (WC-Co).” *Int. J. Adv. Manuf. Technol.*, 58(1–4), 119–131.

Gill, S. S., Singh, J., Singh, R., and Singh, H. (2012b). “Effect of cryogenic treatment on AISI M2 high speed steel: Metallurgical and mechanical characterization.” *J. Mater. Eng. Perform.*, 21(7), 1320–1326.

Govindaraju, N., Shakeel Ahmed, L., and Pradeep Kumar, M. (2014). “Experimental Investigations on Cryogenic Cooling in the Drilling of AISI 1045 Steel.” *Mater. Manuf. Process.*, 29(11–12), 1417–1421.

Huang, X., Zhang, X., Mou, H., Zhang, X., and Ding, H. (2014). “The influence of cryogenic cooling on milling stability.” *J. Mater. Process. Technol.*, 214(12), 3169–3178.

Inspektor, A., and Salvador, P. A. (2014). “Architecture of PVD coatings for metalcutting applications: A review.” *Surf. Coatings Technol.*, 257, 138–153.

Jawahir, I. S., Attia, H., Biermann, D., Duflou, J., Klocke, F., Meyer, D., Newman, S. T., Pusavec, F., Putz, M., Rech, J., Schulze, V., and Umbrello, D. (2016). “Cryogenic manufacturing processes.” *CIRP Ann. - Manuf. Technol.*, 65(2), 713–736.

Jeleńkowski, J., Ciski, A., and Babul, T. (2010). “Effect of deep cryogenic treatment on substructure of HS6-5-2 high speed steel.” 43(1), 80–87.

Kalinga Simant Bal, B., and Maity, K. (2012). “Performance Appraisal of Cryo-Treated Tool By Performance Appraisal of Cryo-Treated Tool By Turning Operation.”

Kalsi, N. S., Sehgal, R., and Sharma, V. S. (2010). “Cryogenic Treatment of Tool

Materials: A Review.” *Mater. Manuf. Process.*, 25(10), 1077–1100.

Kalyan Kumar, K. V. B. S., and Choudhury, S. K. (2008). “Investigation of tool wear and cutting force in cryogenic machining using design of experiments.” *J. Mater. Process. Technol.*, 203(1–3), 95–101.

Kaynak, Y. (2014). “Evaluation of machining performance in cryogenic machining of Inconel 718 and comparison with dry and MQL machining.” *Int. J. Adv. Manuf. Technol.*, 72(5–8), 919–933.

Kheireddine, A. H., Ammouri, A. H., Lu, T., Dillon, O. W., Hamade, R. F., and Jawahir, I. S. (2015). “An experimental and numerical study of the effect of cryogenic cooling on the surface integrity of drilled holes in AZ31B Mg alloy.” *Int. J. Adv. Manuf. Technol.*, 78(1–4), 269–279.

Klocke, F., and Eisenblätter, G. (1998). “Dry cutting - State of research.” *VDI Berichte*, 46(1399), 159–188.

Kosaraju, S., and Chandraker, S. (2015). “Taguchi analysis on cutting force and surface roughness in turning MDN350 steel.” *Mater. Today Proc.*, 2(4–5), 3388–3393.

Krain, H. R., Sharman, A. R. C., and Ridgway, K. (2007). “Optimisation of tool life and productivity when end milling Inconel 718TM.” *J. Mater. Process. Technol.*, 189(1–3), 153–161.

Kumar. S, V., and Kumar. M, P. (2014). “Optimization of cryogenic cooled EDM process parameters using grey relational analysis.” *J. Mech. Sci. Technol.*, 28(9), 3777–3784.

Lahiri, S. (n.d.). “Robust growth for metalworking fluids.” (July 2014), 32–35.

Lawal, S. a., Choudhury, I. a., and Nukman, Y. (2012). “Application of vegetable oil-based metalworking fluids in machining ferrous metals - A review.” *Int. J. Mach. Tools Manuf.*, 52(1), 1–12.

Li, S., Xiao, M., Ye, G., Zhao, K., and Yang, M. (2018). “Effects of deep cryogenic treatment on microstructural evolution and alloy phases precipitation of a new low

carbon martensitic stainless bearing steel during aging.” *Mater. Sci. Eng. A*, 732(April), 167–177.

Liao, Y. S., and Lin, H. M. (2007). “Mechanism of minimum quantity lubrication in high-speed milling of hardened steel.” *Int. J. Mach. Tools Manuf.*, 47(11), 1660–1666.

Ma, Q., Li, L., Xu, Y., Gu, J., Wang, L., and Xu, Y. (2017). “Effect of bias voltage on TiAlSiN nanocomposite coatings deposited by HiPIMS.” *Appl. Surf. Sci.*, 392(October 2018), 826–833.

Ma, Q., Li, L., Xu, Y., Ma, X., Xu, Y., and Liu, H. (2016). “Effect of Ti content on the microstructure and mechanical properties of TiAlSiN nanocomposite coatings.” *Int. J. Refract. Met. Hard Mater.*, 59(June), 114–120.

Manivannan, R., and Kumar, M. P. (2017). “Improving the machining performance characteristics of the  $\mu$ EDM drilling process by the online cryogenic cooling approach.” *Mater. Manuf. Process.*, 33(4), 390–396.

Maranhão, C., and Davim, J. P. (2010). “Simulation Modelling Practice and Theory Finite element modelling of machining of AISI 316 steel : Numerical simulation and experimental validation.” *Simul. Model. Pract. Theory*, 18(2), 139–156.

Marksberry, P. W. (2007). “Micro-flood (MF) technology for sustainable manufacturing operations that are coolant less and occupationally friendly.” *J. Clean. Prod.*, 15(10), 958–971.

Marksberry, P. W., and Jawahir, I. S. (2008). “A comprehensive tool-wear / tool-life performance model in the evaluation of NDM ( near dry machining ) for sustainable manufacturing.” *Int. J. Mach. Tools Manuf.*, 48(7–8), 878–886.

Mo, J. L., and Zhu, M. H. (2009). “Sliding tribological behaviors of PVD CrN and AlCrN coatings against Si<sub>3</sub>N<sub>4</sub> ceramic and pure titanium.” *Wear*, 267(5–8), 874–881.

Mo, J. L., Zhu, M. H., Leyland, A., and Matthews, A. (2013). “Impact wear and abrasion resistance of CrN, AlCrN and AlTiN PVD coatings.” *Surf. Coatings Technol.*, 215, 170–177.

- Mohan Lal, D., Renganarayanan, S., and Kalanidhi, A. (2001). "Cryogenic treatment to augment wear resistance of tool and die steels." *Cryogenics (Guildf)*., 41(3), 149–155.
- Molinari, A., Pellizzari, M., Gialanella, S., Straffelini, G., and Stiasny, K. H. (2001). "Effect of deep cryogenic treatment on the mechanical properties of tool steels." *J. Mater. Process. Technol.*, 118(1–3), 350–355.
- Mukkoti, V. V., Sankaraiah, G., and Yohan, M. (2018). "Effect of cryogenic treatment of tungsten carbide tools on cutting force and power consumption in CNC milling process." *Prod. Manuf. Res.*, 6(1), 149–170.
- Munoz-Escalona, P., Shokrani, A., and Newman, S. T. (2014). "Influence of cutting environments on surface integrity and power consumption of austenitic stainless steel." *Robot. Comput. Integr. Manuf.*, 36, 1–10.
- N. Fukumoto, H. Ezura, T. S. (2009). "Synthesis and oxidation resistance of TiAlSiN and multilayer TiAlSiN/CrAlN coating." *Surf. Coatings Technol.*, 204, 902–906.
- Najiha, M. S., Rahman, M. M., and Yusoff, A. R. (2016). "Environmental impacts and hazards associated with metal working fluids and recent advances in the sustainable systems: A review." *Renew. Sustain. Energy Rev.*, 60, 1008–1031.
- Nalbant, M., and Yildiz, Y. (2011). "Effect of cryogenic cooling in milling process of AISI 304 stainless steel." *Trans. Nonferrous Met. Soc. China (English Ed.)*, 21(1), 72–79.
- Nikalje, A. M., Kumar, A., and Srinadh, K. V. S. (2013). "Influence of parameters and optimization of EDM performance measures on MDN 300 steel using Taguchi method." *Int. J. Adv. Manuf. Technol.*, 69(1–4), 41–49.
- Nohava, J., Dessarzin, P., Karvankova, P., and Morstein, M. (2015). "Characterization of tribological behavior and wear mechanisms of novel oxynitride PVD coatings designed for applications at high temperatures." *Tribol. Int.*, 81, 231–239.
- Nursel Altan Ozbek, Adem Cicek, Mahmut Gulesin, and O. O. (2016). "Application of Deep Cryogenic Treatment to Uncoated Tungsten Carbide Inserts in the Turning of

AISI 304 Stainless Steel.” *Metall. Mater. Trans. A Phys. Metall. Mater. Sci.*, 47A(6270), 6270–6280.

Ou, Y. X., Chen, H., Li, Z. Y., Lin, J., Pan, W., and Lei, M. K. (2018). “Microstructure and tribological behavior of TiAlSiN coatings deposited by deep oscillation magnetron sputtering.” *J. Am. Ceram. Soc.*, 101(11), 5166–5176.

Ozbek, N. A., Cicek, A., Gülesin, M., and Özbek, O. (2016). “Effect of cutting conditions on wear performance of cryogenically treated tungsten carbide inserts in dry turning of stainless steel.” *Tribol. Int.*, 94(December), 223–233.

Ozbek, N. A., Çiçek, A., Gülesin, M., and Özbek, O. (2014). “Investigation of the effects of cryogenic treatment applied at different holding times to cemented carbide inserts on tool wear.” *Int. J. Mach. Tools Manuf.*, 86, 34–43.

Polytechnique, C., and Lausanne, R. D. E. (2000). “PROPRIÉTÉS MÉCANIQUES À HAUTE TEMPÉRATURE DE CERMETS Ti ( C , N ) -WC-Mo-Co À GRADIENT DE COMPOSITION POUR OUTILS DE COUPE.” 2161.

Pusavec, F., Kramar, D., Krajnik, P., and Kopac, J. (2010). “Transitioning to sustainable production - Part II: Evaluation of sustainable machining technologies.” *J. Clean. Prod.*, 18(12), 1211–1221.

Pusavec, F., Lu, T., Courbon, C., Rech, J., Aljancic, U., Kopac, J., and Jawahir, I. S. (2016). “Analysis of the influence of nitrogen phase and surface heat transfer coefficient on cryogenic machining performance.” *J. Mater. Process. Technol.*, 233, 19–28.

Quint, D. T. (1996). “Technology Perspective on CVD and PVD Coated Metal-Cutting Tools.” *Int. J. Refract. Met. Hard Mater.*, 14, 7–20.

Rahman, M., Kumar, A. S., and Ling, M. S. (2003). “Effect of Chilled Air on Machining Performance in End Milling.” 787–795.

Rahman, M., Senthil Kumar, a., and Not Available, N. A. (2001). “Evaluation of Minimal of Lubricant in End Milling.” *Int. J. Adv. Manuf. Technol.*, 18(4), 235–241.

Rao, R. (2011). *Advanced Modeling and Optimization of Manufacturing Processes.*

*Media.*

Ravi, S., and Kumar, M. P. (2012). "Experimental investigation of cryogenic cooling in milling of AISI D3 tool steel." *Mater. Manuf. Process.*, 27(10), 1017–1021.

Ravi, S., and Pradeep Kumar, M. (2011). "Experimental investigations on cryogenic cooling by liquid nitrogen in the end milling of hardened steel." *Cryogenics (Guildf)*., 51(9), 509–515.

Reddy, T. V. S., Sornakumar, T., Reddy, M. V., Venkatram, R., and Senthilkumar, A. (2009). "Turning Studies of Deep Cryogenic Treated P-40 Tungsten Carbide Cutting Tool Inserts – Technical Communication." *Mach. Sci. Technol.*, 13(2), 269–281.

Sachin, B., Narendranath, S., and Chakradhar, D. (2018). "Experimental evaluation of diamond burnishing for sustainable manufacturing." *Mater. Res. Express*, 5(10).

Sanchette, F., Ducros, C., Schmitt, T., Steyer, P., and Billard, A. (2011). "Nanostructured hard coatings deposited by cathodic arc deposition: From concepts to applications." *Surf. Coatings Technol.*, 205(23–24), 5444–5453.

Santhanakumar, M., Adalarasan, R., Siddharth, S., and Velayudham, A. (2017). "An investigation on surface finish and flank wear in hard machining of solution treated and aged 18 % Ni maraging steel." *J. Brazilian Soc. Mech. Sci. Eng.*, 39(6), 2071–2084.

Schoop, J., Schoop, J., Falco, W., and Jawahir, I. S. (2017). "High speed cryogenic finish machining of Ti - 6Al4V with polycrystalline diamond tools." *J. Mater. Process. Tech.*, 250(July), 1–8.

Sharma, A. K., Tiwari, A. K., and Dixit, A. R. (2015). "Effects of minimum quantity lubrication (MQL) in machining processes using conventional and nanofluid based cutting fluids: A review." *J. Clean. Prod.*, 127, 1–18.

Shaw, M. C. (1984). *Metal Cutting Principles*. Oxford science publications, Clarendon Press.

Shaw, M. C., Pigott, J. D., and Richardson, L. P. (1951). "Effect of cutting fluid upon chip–tool interface temperature." *Trans. ASME*, 71(2), 45–56.

She-quan, W., Kang-hua, C., and Li, C. (2011). "Effect of Al and Si additions on microstructure and mechanical properties of TiN coatings." *J. Cent. South Univ. Technol.*, 18, 310–313.

Shokrani, a., Dhokia, V., and Newman, S. T. (2012). "Environmentally conscious machining of difficult-to-machine materials with regard to cutting fluids." *Int. J. Mach. Tools Manuf.*, 57, 83–101.

Shokrani, A., Dhokia, V., Muñoz-Escalona, P., and Newman, S. T. (2013). "State-of-the-art cryogenic machining and processing." *Int. J. Comput. Integr. Manuf.*, 26(7), 616–648.

Shokrani, A., Dhokia, V., and Newman, S. T. (2016a). "Investigation of the effects of cryogenic machining on surface integrity in CNC end milling of Ti-6Al-4V titanium alloy." *J. Manuf. Process.*, 21, 172–179.

Shokrani, A., Dhokia, V., and Newman, S. T. (2016b). "Comparative investigation on using cryogenic machining in CNC milling of Ti-6Al-4V titanium alloy." *Mach. Sci. Technol.*, 20(3), 475–494.

Sivaiah, P., and Chakradhar, D. (2017a). "Comparative evaluations of machining performance during turning of 17-4 PH stainless steel under cryogenic and wet machining conditions." *Mach. Sci. Technol.*, 22(1), 147–162.

Sivaiah, P., and Chakradhar, D. (2017b). "Machinability studies on 17-4 PH stainless steel under cryogenic cooling environment." *Mater. Manuf. Process.*, 32(15), 1775–1788.

Sivaiah, P., and Chakradhar, D. (2017c). "Influence of cryogenic coolant on turning performance characteristics: A comparison with wet machining." *Mater. Manuf. Process.*, 32(13), 1475–1485.

Sivalingam, V., Sun, J., Yang, B., Liu, K., and Raju, R. (2018). "Machining performance and tool wear analysis on cryogenic treated insert during end milling of Ti-6Al-4V alloy." *J. Manuf. Process.*, 36(October), 188–196.

SreeramaReddy, T. V., Sornakumar, T., VenkataramaReddy, M., and Venkatram, R.



- (2008). "Machining performance of low temperature treated P-30 tungsten carbide cutting tool inserts." *Cryogenics (Guildf)*, 48(9–10), 458–461.
- SreeramaReddy, T. V., Sornakumar, T., VenkataramaReddy, M., and Venkatram, R. (2009). "Machinability of C45 steel with deep cryogenic treated tungsten carbide cutting tool inserts." *Int. J. Refract. Met. Hard Mater.*, 27(1), 181–185.
- Thakur, A., Gangopadhyay, S., Maity, K. P., and Sahoo, S. K. (2016). "Evaluation on Effectiveness of CVD and PVD Coated Tools during Dry Machining of Incoloy 825." *Tribol. Trans.*, 59(6), 1048–1058.
- Thamizhmanii, S., Nagib, M., and Sulaiman, H. (2011). "Performance of deep cryogenically treated and non-treated PVD inserts in milling." *J. Achiev. Mater. Manuf. Eng.*, 49(2), 460–466.
- Varghese, V., Chakradhar, D., and Ramesh, M. R. (2018a). "Micro-mechanical characterization and wear performance of TiAlN / NbN PVD coated carbide inserts during End milling of AISI 304 Austenitic Stainless Steel." *Mater. Today Proc.*, 5(5), 12855–12862.
- Varghese, V., Ramesh, M. R., and Chakradhar, D. (2018b). "Experimental investigation and optimization of machining parameters for sustainable machining." *Mater. Manuf. Process.*, 33(16), 1782–1792.
- Varghese, V., Ramesh, M. R., and Chakradhar, D. (2019). "Influence of deep cryogenic treatment on performance of cemented carbide (WC-Co) inserts during dry end milling of maraging steel." *J. Manuf. Process.*, 37(October 2018), 242–250.
- Veprek, S., and Jilek, M. (2002). "Super- and ultrahard nanocomposite coatings: Generic concept for their preparation, properties and industrial applications." *Vacuum*, 67(3–4), 443–449.
- Veprek, S., and Reiprich, S. (1995). "A concept for the design of novel superhard coatings." *Thin Solid Films*, 268, 64–71.
- Veprek, S., Zhang, R. F., Veprek-Heijman, M. G. J., Sheng, S. H., and Argon, A. S. (2010). "Superhard nanocomposites: Origin of hardness enhancement, properties and

- applications.” *Surf. Coatings Technol.*, 204(12–13), 1898–1906.
- Viswanathan, U. K., Dey, G. K., and Asundi, M. K. (1993). “Precipitation hardening in 350 grade maraging steel.” *Metall. Trans. A*, 24(11), 2429–2442.
- Wang, S. Q., Chen, L., Yang, B., Chang, K. K., Du, Y., Li, J., and Gang, T. (2010). “Effect of Si addition on microstructure and mechanical properties of Ti – Al – N coating.” *RMHM*, 28(5), 593–596.
- Xavior, M. A., and Adithan, M. (2009). “Determining the influence of cutting fluids on tool wear and surface roughness during turning of AISI 304 austenitic stainless steel.” *J. Mater. Process. Technol.*, 209(2), 900–909.
- Xia, T., Kaynak, Y., Arvin, C., and Jawahir, I. S. (2016). “Cryogenic cooling-induced process performance and surface integrity in drilling CFRP composite material.” *Int. J. Adv. Manuf. Technol.*, 82(1–4), 605–616.
- Yildiz, Y., and Nalbant, M. (2008). “A review of cryogenic cooling in machining processes.” *Int. J. Mach. Tools Manuf.*, 48(9), 947–964.
- Yong, A. Y. L., Seah, K. H. W., and Rahman, M. (2007). “Performance of cryogenically treated tungsten carbide tools in milling operations.” *Int. J. Adv. Manuf. Technol.*, 32(7–8), 638–643.
- Yong, J., and Ding, C. (2011). “Effect of cryogenic treatment on WC-Co cemented carbides.” *Mater. Sci. Eng. A*, 528(3), 1735–1739.
- Yuan, Y., Qin, Z., Yu, D. H., Wang, C. Y., Sui, J., Lin, H., and Wang, Q. (2017). “Relationship of microstructure, mechanical properties and hardened steel cutting performance of TiSiN-based nanocomposite coated tool.” *J. Manuf. Process.*, 28, 399–409.

## LIST OF PUBLICATIONS AND CONFERENCES

Sl. No.	Title of the paper	Authors (in the same order as in the paper. Underline the Research Scholar's name)	Name of the Journal/ Conference, Vol., No., Pages	Month, Year of Publication	Category*
1	Experimental investigation and optimization of machining parameters for sustainable machining	<u>Vinay Varghese</u> , M. R. Ramesh, D. Chakradhar	Materials and Manufacturing Processes (SCIE), Vol 33, 1782-1792.	May 2018	1
2	Influence of deep cryogenic treatment on performance of cemented carbide (WC-Co) inserts during dry end milling of maraging steel	<u>Vinay Varghese</u> , M. R. Ramesh, D. Chakradhar	Journal of Manufacturing Processes (SCIE), Vol 37, 242-250.	January-2019	1
3	Investigation on the performance of AlCrN and AlTiN coated cemented carbide inserts during end milling of maraging steel under dry, wet and cryogenic environments	<u>Vinay Varghese</u> , Akhil K., M. R. Ramesh, D. Chakradhar	Journal of Manufacturing Processes (SCIE), Vol 43, 136-144.	May 2019	1
4	Experimental investigation of cryogenic end milling on maraging steel using cryogenically treated tungsten carbide-cobalt inserts	<u>Vinay Varghese</u> , M. R. Ramesh, D. Chakradhar	Journal of Advanced Manufacturing Technology (SCIE), 1-19	September 2019	1
5	Characterisation and performance evaluation of TiSiN & TiAlSiN coatings by RF magnetron sputtering deposition during end milling of maraging steel	<u>Vinay Varghese</u> , M. R. Ramesh, D. Chakradhar	Material Research Express (SCIE)	Revision submitted	1

6	Micro-mechanical characterization and wear performance of TiAlN/NbN PVD coated carbide inserts during end milling of AISI 304 Austenitic Stainless Steel	<b><u>Vinay Varghese,</u></b> M. R. Ramesh, D. Chakradhar	Materials Today Proceedings (Scopus), Vol 5, Issue 5, 12855-12862.	June 2018	3
7	Machining performance of AlCrN and AlTiN coated cemented carbide inserts during the dry end milling of maraging steel	<b><u>Vinay Varghese,</u></b> M. R. Ramesh, D. Chakradhar	8 <sup>th</sup> International Engineering Symposium, Kumamoto University, Japan.	March 2019	3

\* Category: 1: Journal paper, full paper reviewed                      4: Conference/Symposium paper, abstract reviewed  
2: Journal paper, Abstract reviewed                                      5: Others (including papers in Workshops, NITK Research Bulletins, Short notes etc.)  
3: Conference/Symposium paper, full paper reviewed  
(If the paper has been accepted for publication but yet to be published, the supporting documents must be attached.)

Vinay Varghese	Dr. Ramesh M R	Dr. D. Chakradhar
Research Scholar	Research Guide	Research Guide
Name & Signature, with Date	Name & Signature, with Date	Name & Signature, with Date

## BIO-DATA

Name: Vinay Varghese

Father's Name: Varghese V.J

Date of Birth: 22-01-1990

Nationality: Indian

Marital Status: Single

Address:

Permanent Address

15/306, Vallanatt (H)

Kumbalangi P.O

Cochin-682007

Dist: Ernakulam, Kerala, India

**Mobile Number:** +918792194091

Educational Qualification:

Present Address

Department of Mechanical Engineering

National Institute of Technology Karnataka

Surathkal-575025, Srinivasanagar,

Mangalore, Karnataka, India.

**E-mail id:** vinujavs@gmail.com

Qualification	College/school	University/Board	Year of Passing	Percentage
Ph.D. Mechanical Engineering	National Institute of Technology Karnataka	NITK, Surathkal		
M. Tech CAD/CAM	Vellore Institute of Technology, Chennai Campus	VIT University	2014	7.93 CGPA
B. Tech. Mechanical Engineering	Marian Engineering College, Trivandrum	Kerala University	2011	6.03 CGPA
Plus Two	St. Sebastian's HSS, Palluruthy, Cochin	Kerala State Board	2007	76.8
SSLC	C.C.P.L.M.A.I.H.S, Cochin	Kerala State Board	2005	80.2

I declare that the above information is true and correct to best of my knowledge.

(VINAY VARGHESE)